การพัฒนาไมโครไบโอเซ็นเซอร์เชิงเคมีไฟฟ้าเพื่อใช้ตรวจวัดสารบ่งชี้ทางชีวภาพ

นางสาวกุลวดี ปิ่นวัฒนะ

DEVELOPMENT OF ELECTROCHEMICAL MICROBIOSENSOR FOR
DETECTION OF BIOMARKERS

Miss Kulwadee Pinwattana

A Dissertation Submitted in Partial Fulfillment of the Requirements

for the Degree of Doctor of Philosophy Program in Chemistry

Department of Chemistry

Faculty of Science

Chulalongkorn University

Academic Year 2010

Thesis Title   DEVELOPMENT OF ELECTROCHEMICAL

MICROBIOSENSOR FOR DETECTION OF

BIOMARKERS

By   Miss Kulwadee Pinwattana

Field of Study   Chemistry

Thesis Advisor   Asscociate Professor Orawon Chailapakul, Ph.D.

Accepted by the Faculty of Science, Chulalongkorn University in Partial Fulfillment of the Requirements for the Doctoral Degree

……………………………………… Dean of the Faculty of Science

(Professor Supot Hannongbua, Dr.rer.nat.)

THESIS COMMITTEE

……………………………………… Chairman

(Assistant Professor Warinthorn Chavasiri, Ph.D.)

……………………………………… Thesis Advisor

(Associate Professor Orawon Chailapakul, Ph.D.)

……………………………………… Examiner

(Associate Professor Nattaya Ngamrojanavanich, Ph.D.)

……………………………………… Examiner

(Assistant Professor Narong Praphairaksit, Ph.D.)

……………………………………. External Examiner

(Anchana Preechaworapun, Ph.D.)

กุลวดี ปิ่นวัฒนะ : การพัฒนาไมโครไบโอเซ็นเซอร์เชิงเคมีไฟฟ้าเพื่อใช้ตรวจวัดสารบ่งชี้ทางชีวภาพ. (DEVELOPMENT OF ELECTROCHEMICAL MICROBIOSENSOR FOR DETECTION OF BIOMARKERS) อ. ที่ปรึกษาวิทยานิพนธ์หลัก : รศ. ดร. อรวรรณ ชัยลภากุล, 104 หน้า.

งานวิจัยนี้แบ่งออกเป็นสองส่วน ส่วนแรกคือ การพัฒนาเซ็นเซอร์เชิงเคมีไฟฟ้าสำหรับวิเคราะห์หาปริมาณคอเลสเตอรอลด้วยขั้วไฟฟ้าที่มีขนาดระดับไมโครเมตร ขั้วไฟฟ้าขนาดเล็ก ซึ่งสร้างขึ้นมาจากคาร์บอนไฟเบอร์ที่มีขนาดเส้นผ่านศูนย์กลาง 7 ไมโครเมตรและเส้นลวดแพลทินัมที่มีขนาดเส้นผ่านศูนย์กลางขนาด 25 ไมโครเมตร อนุภาคทองขนาดนาโนเมตรถูกทำให้ติดกับผิวหน้าขั้วไฟฟ้าในสารละลายกรดคลอโรออริก โดยขั้นตอนเดียวด้วยเทคนิคไซคลิกโวลแทมเมตรี ตรวจสอบคุณลักษณะอนุภาคทองที่ติดอยู่ผิวหน้าขั้วไฟฟ้าด้วยสแกนนิงอิเล็กตรอนไมโครสโกปีและเทคนิคไซคลิกโวลแทมเมตรี สำหรับเซ็นเซอร์เชิงเคมีไฟฟ้านั้นสามารถแบ่งออกเป็นสองแบบคือ ไมโครเซ็นเซอร์และไมโครไบโอเซ็นเซอร์ สำหรับเซ็นเซอร์เชิงเคมีไฟฟ้านั้นสามารถแบ่งออกเป็นสองแบบคือ ไมโครเซ็นเซอร์และไมโครไบโอเซ็นเซอร์ สำหรับไมโครเซ็นเซอร์ ขั้วไฟฟ้าคาร์บอนไฟเบอร์ที่มีอนุภาคทองถูกนำมาใช้วิเคราะห์หาคอเลสเตอรอลในสารละลายฟอสเฟตบัฟเฟอร์ที่มีคอเลสเตอรอลออกซิเดสอยู่ด้วย จากการวิเคราะห์ด้วยเทคนิคโครโนแอมเปอโรเมตรีหาคอเลสเตอรอลแสดงช่วงความเป็นเส้นตรงที่ 50-500 ไมโครโมลาร์และค่าขีดจำกัดต่ำสุดของการวิเคราะห์เท่ากับ 10 ไมโครโมลาร์ สำหรับไมโครไบโอเซ็นเซอร์ คอเลสเตอรอลออกซิเดสถูกตรึงไว้ที่อนุภาคทองที่เกาะบนผิวขั้วไฟฟ้าแพลทินัม โดยใช้ 1-เอทิล-3-(3-ไดเมทิลอะมิโนโพรพิล)คาร์โบไดอิไมด์/เอ็น-ไฮดรอกซีซัลโฟซักซินิไมด์เป็นตัวเชื่อม ภายใต้ภาวะที่เหมาะสมกระแสไฟฟ้าจากโครโนแอมเปอโรเมตรีมีความสัมพันธ์เป็นเส้นตรงกับความเข้มข้นที่เพิ่มขึ้นของคอเลสเตอรอลในช่วง 0.001-7 มิลลิโมลาร์ สัญญาณการตรวจวัดของไมโครเซ็นเซอร์และไมโครไบโอเซ็นเซอร์เท่ากับ 10 วินาที และ นอกจากนี้ไมโครไบโอเซ็นเซอร์ยังประสบความสำเร็จในการนำมาประยุกต์ใช้ในตัวอย่างจริงซีรัมของวัว สำหรับส่วนที่สองของงานวิจัยได้พัฒนาเทคนิคทางเคมีไฟฟ้าร่วมกับอิมมูโนแอสเสย์และควอนตัมดอทของแคดเมียมเซลิไนด์/ซิงค์ซัลไฟด์เพื่อวิเคราะห์หาฟอสโพริลเลตโบวีนซีรัมอัลบูมิน โดยใช้ควอนตัมดอทที่ถูกติดฉลากด้วยแอนติบอดีของแอนติฟอสโฟเซอรีนเป็นตัวขยายสัญญาณเคมีไฟฟ้าจากแซนวิชอิมมูโนแอสเสย์ ในวิธีการนี้ฟอสโพริลเลตโบวีนซีรัมอัลบูมินถูกเติมลงในไมโครเพลทที่มีแอนติบอดีของโบวีนซีรัมอัลบูมินอยู่และควอทตัมดอทที่ถูกติดฉลากจะถูกเติมลงในไมโครเพลท เพื่อให้เกิดการจับกันแบบจำเพาะของอิมมูโนแอสเสย์โดยสมบูรณ์ และสุดท้ายควอนตัมดอทที่ติดอยู่จะถูกวิเคราะห์ด้วยเทคนิคสทริปปิง กระแสไฟฟ้าที่ได้มีความเป็นเส้นตรงของฟอสโพริลเลตโบวีนซีรัมอัลบูมิน ในช่วง 0.5-500 นาโนกรัมต่อมิลลิลิตรที่มีขีดต่ำสุดของการตรวจวัดเท่ากับ 0.5 นาโนกรัมต่อมิลลิลิตร

ภาควิชา...................เคมี.............ลายมือชื่อนิสิต...

สาขาวิชา.................เคมี............ลายมือชื่อ อ.ที่ปรึกษาวิทยานิพนธ์หลัก...........................

ปีการศึกษา.............2553...........

4973805923 : MAJOR CHEMISTRY
KEYWORDS : MICROSENSOR / MICROBIOSENSOR / ELECTROCHEMICAL IMMUNOASSAY / QUANTUM DOT / CHOLESTEROL / PHOSPHORYLATED PROTEIN

KULWADEE PINWATTANA : DEVELOPMENT OF ELECTROCHEMICAL MICROBIOSENSOR FOR DETECTION OF BIOMARKERS. ADVISOR : ASSOC. PROF. ORAWON CHAILAPAKUL, 104 pp.

This research is divided into two parts, the first part is the development of the electrochemical sensor for the determination of cholesterol using microelectrodes. Microelectrodes were fabricated from a 7 μm diameter carbon fiber (CF) and a 25 μm diameter platinum wire (Pt). Gold nanoparticles (AuNPs) were electrochemically deposited on the microelectrode surface in $HAuCl_4$ solution using one step by cyclic voltammetry. The deposited AuNPs on the microelectrode surfaces were characterized by scanning electron microscopy and cyclic voltammetry. For the microsensor, an AuNPs/CF microelectrode was used to detect cholesterol in the phosphate buffer solution containing cholesterol oxidase. Chronoamperometric measurements of cholesterol showed the linear response in the range of 50 to 500 μM with the detection limit of 10 μM. For the electrochemical sensor, it was separated into two types: microsensor and microbiosensor. For the microbiosensor, cholesterol oxidase was covalently immobilized on the AuNPs/Pt microelectrode surface using 1-ethyl-3-(3-dimethyl aminopropyl) carbodiimide (EDC)/N-hydroxysulfosuccinimide (NHS) as a cross-linker. Under the optimal conditions, chronoamperometric current was linearly increased with the increase of the logarithm of cholesterol concentrations in the range from 0.001 to 7 mM. The response time of the microsensor and microbiosensor is 10 seconds. In addition, the microbiosensor was successfully applied to a real sample of bovine serum. In the second part, CdSe/ZnS quantum dot (QD) based electrochemical immunoassay was used to detect the phosphorylated bovine serum albumin (BSA-OP) as a protein biomarker. The QDs were used as labels for amplifying electrochemical signals and were conjugated with a secondary anti-phosphoserine antibody in a sandwich immunoassay. In this assay, the BSA-OP was added to the primary BSA antibody coated polystyrene microwell, and then the QD labeled anti-phosphoserine antibody was added for completing immunorecognition. Finally, the bound QD was detected by electrochemical stripping analysis. The voltammetric response was linear over the range of 0.5 to 500 ng mL^{-1} of BSA-OP, with a detection limit of 0.5 ng mL^{-1}.

Department : ......Chemistry...... Student's Signature ....

Field of Study : ......Chemistry...... Advisor's Signature ....

Academic Year : ......2010......

ACKNOWLEDGEMENTS

CONTENTS

LIST OF TABLES

LIST OF FIGURES

FIGURE   **PAGE**

FIGURE **PAGE**

FIGURE   **PAGE**

FIGURE   **PAGE**

ABBREVIATIONS

A	electrode area
Ab	antibody
Ag	antigen
anti-BSA	monoclonal anti-bovine serum albumin
ASV	anodic stripping voltammetry
AuNPs	gold nanoparticles
BSA-OP	phosphorylated bovine serum albumin
CF	carbon fiber
ChOx	cholesterol oxidase
cm	centimeter
D	diffusion coefficient
dL	deciliter
E	enzyme
E^{0}	standard potential
EDC	1-Ethyl-3-(3-dimethyl aminopropyl) carbodimide
ELISA	enzyme-linked immunosorbent assay
E_{p}	peak potential
$E_{p,a}$	anodic peak potential
$E_{p,c}$	cathodic peak potential
$i_{p,a}$	anodic peak current
$i_{p,c}$	cathodic peak current

K	equilibrium constant
M	molar
μm	micromolar
mg	milligram
mL	milliliter
mM	millimolar
mV	millivolte
nA	nanoampere
NHS	*N*-hydroxysulfosuccinimide
nm	nanometer
O	oxidized form
P	product
PBS	phosphate buffer saline
PEG	polyethylene glycol
pM	picomolar
Pt	platinum
QDs	quantum dots
R	reduce form
S	substrate
SPE	screen printed electrode
SWV	square wave voltammetry
TEM	transmission electron microscopy
V	volt

CHAPTER I

INTRODUCTION

1.1   Introduction

In recent years, the biosensors are powerful analysis for detection, diagnosis, and application in clinical work, food analysis, environmental monitoring, agriculture, water-quality control, and safety. The combination of a biological sensing element, such as an enzyme, antibody-antigen, nucleic acid, cells, and protein receptor, with a physical transducer, which together relates the concentration of an analyte to a quantitative signal, is very attractive. Many biosensors for biomarkers have been developed with various transducers. In general, several techniques of biosensor have been reported including spectrophotometry, surface plasmon resonance, quartz crystal microbalance, and electrochemistry. However, electrochemical techniques have numerous advantages: for example, they are relatively inexpensive, inherently simple, applicable to optically opaque media, and suitable for miniaturizable instrumentation with low power requirements. Thus, electrochemical techniques have been widely used for the development of biosensors.

Various nanoparticles, including metal nanoparticles (gold and silver) and oxide nanoparticles (zinc and iron) are receiving a great deal of attention as alternative matrices for enzyme immobilization and to improve stability and sensitivity of biosensors. Particularly, gold nanoparticles (AuNPs) are one of the most popular nanoparticles used as enhancing interfacial platform for developing an electrochemical biosensor. Besides this, AuNPs provide high surface areas for higher enzyme loading and a biocompatible microenvironment help the enzyme to retain its bioactivity.

Cholesterol and its fatty acid esters are essential constituents of mammalian cell membrane. They are precursors of other biological materials, such as bile acid and steroid hormones. However, the accumulation of cholesterol and an excess of cholesterol-containing food cause serious coronary heart diseases because the

accumulated cholesterol on the walls of arteries favors the atherosclerotic plaque formation and blocks the blood flow. According to the world health organization, cardiovascular disease causes approximately 17.5 million deaths in the world each year. One of the highest risk factors for health disease is high cholesterol in blood. Therefore, the determination of cholesterol has profound clinical applications in the diagnosis and prevention of heart diseases. The normal level of total cholesterol in a healthy person's blood should be less than 5.17 mM (<200 mg/dL). The borderline high is defined as 5.17-6.18 mM (200-239 mg/dL), and the high value is defined as above 6.21 mM ($\geq$ 240 mg/dL). In addition, quality control in the food industry is another application for determination of cholesterol. This has led to an increased interest in the development of various biosensors for the monitoring of cholesterol in food and serum samples.

The advantage of microelectrodes over the classical macroelectrode has an extremely high sensitivity due to high signal to noise ratio, enhanced mass transport, and reduced ohmic drop. Especially, the use of microelectrodes provides the opportunity for an in vivo biosensor application. In this work, an electrochemical biosensor using a carbon fiber (CF) microelectrode was developed to detect cholesterol. AuNPs were electrochemically deposited on a CF microelectrode. The cholesterol measurement was carried out in the solution containing cholesterol oxidase (ChOx). Cholesterol can generate hydrogen peroxide by ChOx. The enhanced response of hydrogen peroxide at AuNPs deposited on the CF microelectrode was obtained from the electrochemical sensor. In addition, a platinum (Pt) microelectrode was fabricated for cholesterol biosensor. Following the electrodeposition of AuNPs, ChOx molecules were covalently immobilized on the surface of the AuNPs on the Pt microelectrode. The Pt microelectrode can efficiently catalyze the electrochemical oxidation of enzymatically generated hydrogen peroxide.

Regarding the electrochemical immunoassay, immunoassay is based on the use of an antibody that reacts specifically with the antigen of the analyte to be measured, including radioimmunoassay, fluorescence-based immunoassay, chemiluminescence immunoassay, enzyme-linked immunosorbent assay, and electrochemical immunoassay.

The quantification of immunoassay is commonly achieved by measuring the specific activity of the label.   A larger number of labels, such as various nanoparticles (gold and silica), quantum dots (QDs), and apoferritin nanoparticles, have been developed with the great nanotechnological advances for labeling of immunoassay. In particular, to enhance the sensitivities, biosensors and bioassays using electrochemical stripping analysis based on QDs have shown great potential for the detection of trace biomolecules. Especially, QDs have been widely used for labeling and biosensing of electrochemical immunoassays because of their unique advantages such as nanometer size similar to proteins and versatility in surface modification with various biomolecules (peptides, oligonucleotides, and proteins)

Protein phosphorylation is one of the most important and most thoroughly investigated post-translational modifications in living organisms.   Because of its fundamental role in the regulation of cellular functions, such as cell division, signal transduction, and cell differentiation, much effort has been focused on the development of detection methodologies for the different substrates. The phosphorylation process has been demonstrated to involve some 518 protein kinases and 100 phosphoprotein phosphatases in the human genome. Approximately thirty percent of all proteins in eukaryotic cells are supposed to be phosphorylated at any given time. Recently, many human diseases have been recognized to be associated with the abnormal phosphorylation of cellular protein and protein phosphorylation is also associated with the pathways of cancer.   Therefore, the analysis of protein phosphorylation has increasingly become the focus of attention in the field of proteomics due to its highly dynamic nature and low stoichiometry.

For this work, the application of QDs in the electrochemical detection of phosphorylated proteins was demonstrated.   Phosphorylated bovine serum albumin (BSA-OP) was chosen as the model analyte because of the potential biohazards of using phosphorylated human serum albumin.   A sandwich-type immunoassay format was employed by the primary antibody immobilized on the surface of a 96-well microplate. After the captured analyte, the secondary antibody conjugated to QDs labels will

recognize the analyte. The released metal ions from QDs labels were determined by electrochemical stripping analysis.

1.2   Objectives of the research

There are two targets for this research.

1. To develop the electrochemical microbiosensor with AuNPs for cholesterol determination with low limit of detection, and a fast analysis time.
2. To improve the sensitivity of the electrochemical immunosensor using CdSe/ZnS QDs labeling for the determination of phosphorylated BSA.

CHAPTER II

THEORY AND LITERATURE SURVEY

2.1 Biosensors

A biosensor, which is an analytical device, is composed of two main parts. The first is the biological recognition system, which employs a biological material to specifically interact with an analyte to convert information from a biological response into a chemical or physical output signal. The second is a transducer, which translates the physicochemical event into a recognizable physical signal. The main regions of a typical biosensor are shown in Figure 2.1.
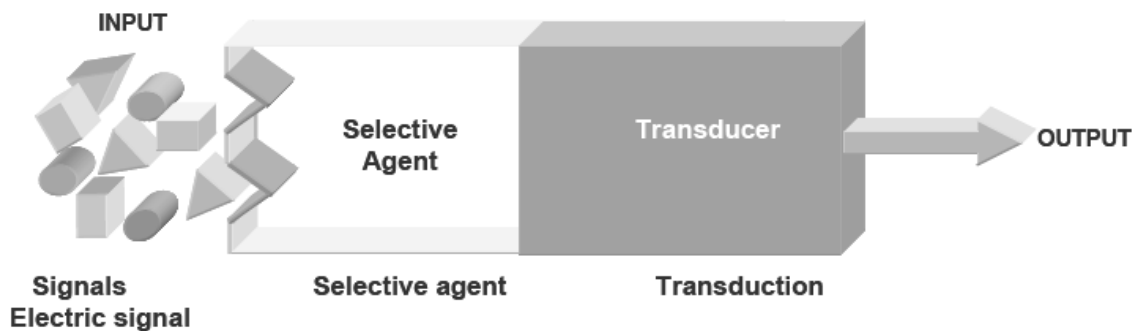
Figure 2.1 Schematic diagram of all the components of a biosensor.

Biosensors use a biological recognition system with a suitable transducer. Physicochemical change is produced by specific interactions between the biorecognition system and an analyte and is measured by the transducer, such as electrochemical, optical, piezoelectric, and acoustic transducer. The amount of generated signal from the transducer is directly proportional to the concentration of the analyte, allowing for both quantitative and qualitative measurements. A general scheme of the biosensor device is shown in figure 2.2. The transducer of the biosensor can take many formations depending upon the parameters.
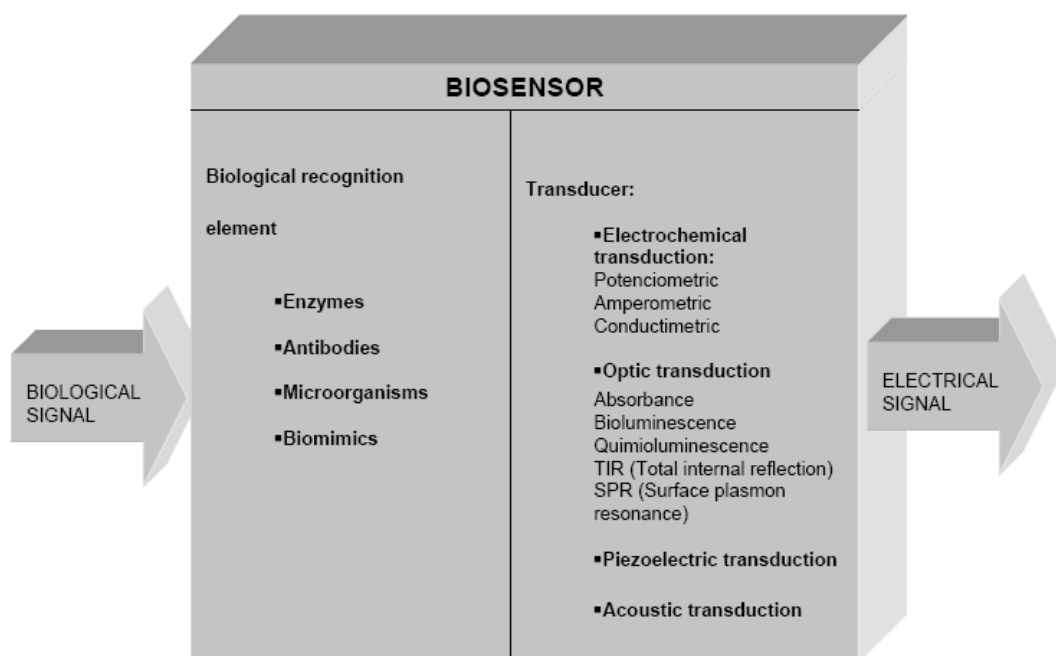
Figure 2.2 Schematic of biological recognitions and transducers for biosensor

Biosensors are typically classified into a variety of basic groups according to the method of signal transduction, or according to the biorecognition principle. The main transduction of the biosensors can be classified according to the physicochemical properties.

An optical biosensor is based on various technologies of optical phenomena, which are the result of interaction of an analyte with the receptor. This group may be further divided into various types of optical properties, such as absorbance, reflectance, luminescence, fluorescence, refractive index, and light scattering.

Electrochemical biosensor transforms the effect of the electrochemical interaction between an analyte and electrode into a signal using biological recognition. The most typical applications of electrochemical transducer are divided into three parts, which is amperometric, potentiometric, and impedimetric transducers.

Mass sensitive biosensor transforms the mass change at a specially modified surface into a change of a property of the support material and the mass change is caused

by accumulation of the analyte. For instance, piezoelectric devices involve the measurement of the frequency change of the quartz oscillator plate caused by adsorption of a mass of the analyte at the oscillator. Surface acoustic wave devices are based on the modification of the propagation velocity of a generated acoustic wave affected by the deposition of a determined mass of the analyte.

Among these various types of transducers of biosensors, the electrochemical transducers are a class of the most widespread, numerous, and successfully commercialized devices, because of the simplicity of construction and cost for biosensor applications. Electrochemical transducers are often used for the listed types of measurement in table 2.1.

Table 2.1 Type of the electrochemical measurement techniques and receptors used in biosensors

Analytes	Receptor	Measurement technique
Ions	Biological ionophores, enzymes	Potentiometric, voltammetric
Dissolved gases, vapors, odors	Enzymes, antibody	Amperometric, potentiometric, impedance
Substrates	Enzymes, whole cells, membrane receptor, plant or animal tissus	Amperometric, potentiometric, conductometric
Antibody/antigen	Antibody/antigen, oligonucleotide duplex, aptamer, enzyme labeled	Amperometric, potentiometric, impedance
Various proteins and low molecular weight substrates	Specific ligands, protein receptors, enzyme labeled	Amperometric, potentiometric, impedance

2.2   Enzyme biosensors

In 1962, the birth of biosensors was pioneered by Clark and Lyons to develop a glucose biosensor, which was based on the use of glucose oxidase with electrochemical detection.   Since then, this basic concept has been widely extended in biosensors development.   Enzyme biosensors have attracted much attention due to the potential applications in many areas, such as health care, food safety, and environmental monitoring.   Biosensor applications are most widely used in health care, for example monitoring blood glucose levels and cholesterol levels.   Moreover, the reliable detection of urea has shown that there is a potential applications for using the biosensor application with patients at home or in the hospital.   Industrial applications for enzyme biosensors include monitoring fermentation broths or food processing procedures.

Enzyme biosensor is an analytical device that combines an enzyme with a transducer to produce a signal proportionate to the concentration of analyte.   Enzymes are a kind of protein that catalyzes a chemical reaction.   In enzymatic reactions, substrates are molecules at the beginning of the process and they are converted into different molecules.   Almost all reactions need enzymes to occur at a significant rate and enzymes are selective for their substrates only a few reactions.   For enzyme biosensors, the essential part for construction is the biorecognition element immobilized on the surface of the transducer.   Consequently, immobilization of enzymes is an important and crucial point of biosensor construction.

2.2.1   Enzyme reaction

In general, enzymes provide speed, specific, and regulatory control to reactions in the body.   Enzymes are usually proteins that act as catalysts and enzyme catalyzed reactions have three basic steps:

(1) Binding of substrate: $\mathbf{E} + \mathbf{S} \leftrightarrow \mathbf{ES}$

(2) Conversion of bound substrate to bound product: $\mathbf{ES} \leftrightarrow \mathbf{EP}$

(3) Release of product: $\mathbf{EP} \leftrightarrow \mathbf{E} + \mathbf{P}$
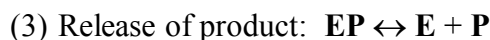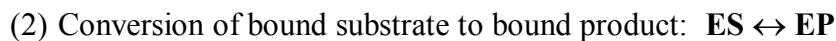
An enzyme binds the substrates of the reaction it catalyzes and brings them together at the right direction. Then, the enzyme participates in the breaking of bonds required for product formation, releases the products, and returns to its original structure. Each enzyme commonly catalyzes a specific biochemical reaction. To catalyze a reaction, the enzyme forms an enzyme-substrate complex in its active catalytic site (Figure 2.3). The active site is regularly a cleft or crevice in the enzyme formed. Within the active site, cofactors and functional groups from the polypeptide chain participate in transforming the bound substrate molecules into products.
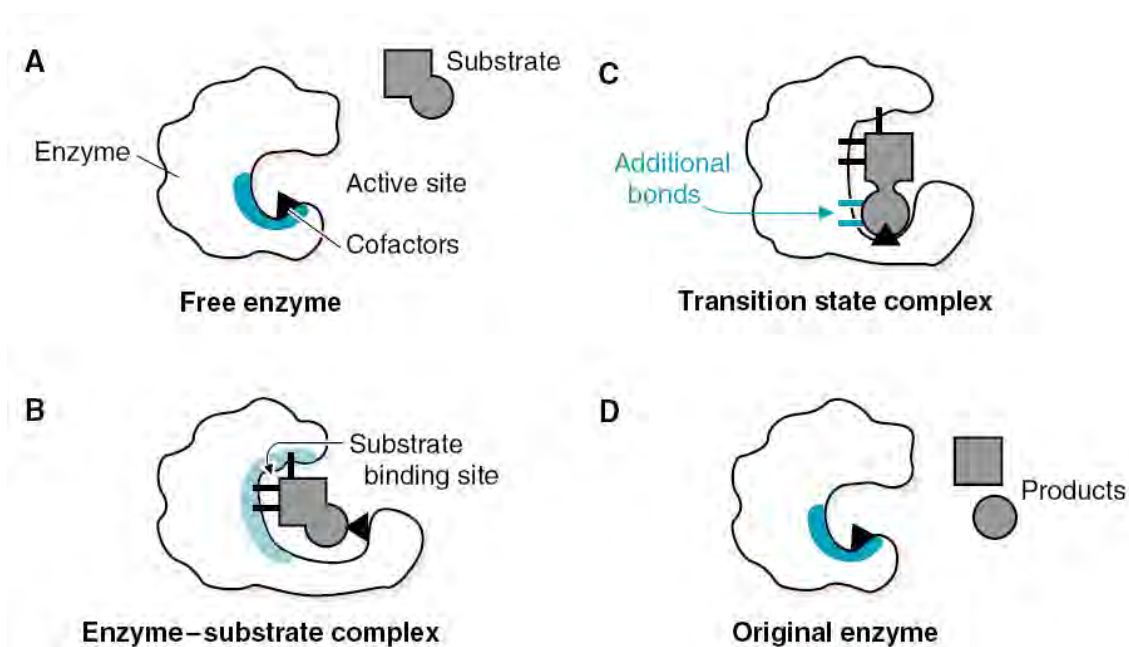
Figure 2.3 Reaction in the enzyme active site.

Enzymes have a wide variety of reaction pathways and enzyme names, which has been systematically classified by the Enzyme Commission of the International Union of Biochemists and Molecular Biologists. Many reactions of enzymes are similar and occur frequently in different pathways. The basic reaction types are divided into six major groups according to the type of catalyzed reaction in table 2.2.

Table 2.2 International classification of enzymes

Number	Class	Type of reaction catalyzed
1	Oxidoreductases	Transfer of electrons (hydride ions or H atoms)
2	Transferases	Group transfer reactions
3	Hydrolases	Hydrolysis reactions (transfer of functional groups to water)
4	Lyases	Addition of groups to double bonds, or formation of double bonds by removal of groups
5	Isomerases	Transfer of groups within molecules to yield isomeric forms
6	Ligases	Formation of C-C, C-S, C-O, and C-N bonds by condensation reactions coupled to ATP cleavage

The enzymatic catalysis of reactions is important to living systems. Under biologically suitable conditions, most biological molecules are quite stable in the neutral pH, mild temperature, with aqueous environment inside cells.

2.2.2 Methods for enzyme immobilization

In order to make an enzyme biosensor, the method used to attach the enzyme is the key step. This step is known as enzyme immobilization and is governed by various interactions between enzymes and material interface. The choice of immobilization method depends on many factors, for example the nature of the biological element, the type of transducer, and the physicochemical properties of the analyte. Various methods have been employed including physical adsorption, covalent binding, physical entrapment, self assembly, and affinity methods. The common approaches of several enzyme immobilization methods are shown in figure 2.4.
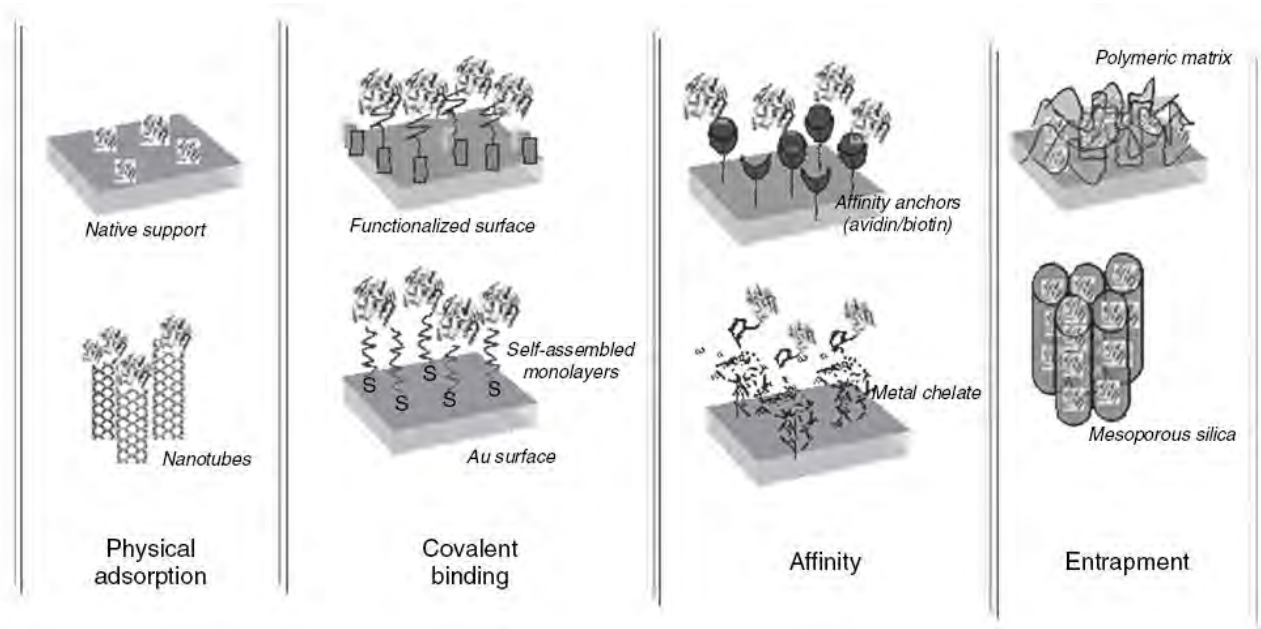
Figure 2.4 Schematic representations of various enzyme immobilization methods.

Nanostructured materials were first used as support matrices to attach enzymes. This is accomplished almost exclusively through physical adsorption via the weak bonds, for instance van der Waals forces, ionic binding or hydrophobic interactions. In addition, more current methods involve the use of physical entrapment, covalent, and affinity based methods. There are four regular methods for enzyme immobilization and they are briefly described as shown below:

- **Physical adsorption**

Usually, physical adsorption is the simplest, inexpensive, fastest and least denaturing immobilization method. The process consists of the simple deposition of the enzyme onto the support or electrode material. It does not implicate additional reagents, sequential steps or enzyme modifications that could affect its activity. On the other hand, due to the fact that the binding forces involved are weak, the enzyme immobilized in this method is vulnerable to pH, temperature, solvent and ionic strength changes. This immobilized method does not provide increased enzyme activity and storage stability.

- **Covalent binding**

In this method, the attachment of an enzyme by covalent linkage consists of two steps. In the first step, the activation of the material was activated to provide useful chemical reactivity for subsequent binding of the biomolecule. In general, this is performed with bifunctional groups, such as glutaraldehyde, carbodiimide/succinimide, self-assembled monolayers or multilayers (SAM), and aminopropyltriethoxysilanes. The second step consists of the enzyme to an activated material. The chemistry involved in the immobilization procedure depends upon the kind of material used and its surface characteristics. Typically, this method has been effectively developed for noble metals and carbon-based materials. This process has some advantages, such as the increased stability of the enzyme due to the strong chemical binding, but the immobilized enzyme has relatively low activity due to the fact that the procedure can involve groups that are essential for its activity.

- **Affinity immobilization**

This method can ensure controlled spatial orientation, without loss of enzyme activity during the immobilization process. The current trend is to create bioaffinity bonds between an activated material of support and a specific group of the protein sequence. As the groups of the native enzyme are not present, they can be engineered at a specific position, which does not affect the activity or the folding of the protein. Specific examples of affinity interactions consist of cellulose-cellulose binding domain bearing enzymes, polyclonal/monoclonal antibodies for specific enzymes, and lectins-glycoenzymes bearing suitable oligosaccharides. This process is usually reversible facilitating the reuse of a support matrix and provides stable enzyme attachment. Conversely, enzymes immobilization onto nanostructures using bioaffinity bonds is still relatively unexplored and represents an important research direction.

- **Entrapment**

The most convenient method of enzyme immobilization is physical entrapment in an inert material, such as photopolymerized monomers and sol gel matrices. This method has some advantages over the other processes, for instance mild conditions, less step fabrication, low cost, and high stability of encapsulated enzyme. The limitations of this method are diffusion barriers of the transport of substrate or product resulting in long response times, difficulties in controlling the pores dimensions, and possible enzyme leaching. In some examples, the activity of the enzyme can be affected by the physical and chemical properties of the immobilization matrix.

2.3   Immunoassay

Immunoassay is one important analytical method, which represents a group of every useful analytical method for quantification of the extremely low concentrations of analytes. In this respect, immunoassay relies on antibody-antigen interactions that provide a promising means of analysis owing to their specificity and sensitivity. In 1945, the concept of immunoassay was first described by Landsteiner and stated that antibodies could bind selectively to small molecules when they were conjugated to a larger carrier molecule. This concept was explored by Yalow and Berson in the late 1950s, and resulted in immunoassay, which was applied to insulin monitoring in humans. This work was pioneered to set the stage for the rapid advancement of immunochemical methods for clinical analysis.

Antibodies are produced in living organisms (excluding plants) via the immune response to an immunogen, which may be defined as any agent capable of eliciting an immune response. A schematic representation of the immune response is shown in Figure 2.5.
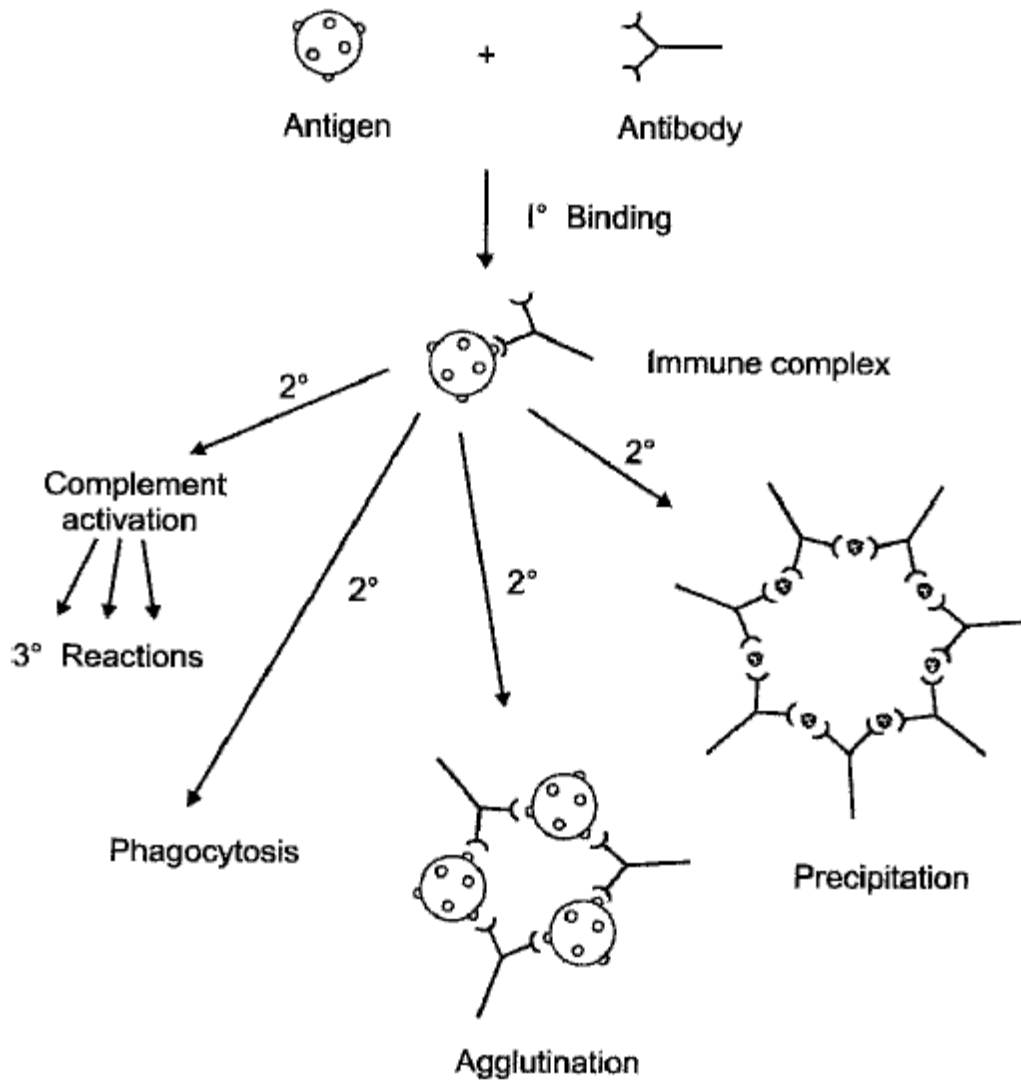
Figure 2.5 Simplified representation of the immune response.

2.3.1 The antibody-antigen interaction

Immunoassays are analytical systems that use the remarkable specificity provided by the molecular recognition of an antigen by antibodies. Antibodies are a family of glycoprotein known as immunoglobulins (Ig). They are five distinct classes of glycoproteins (IgA, IgG, IgM, IgD, and IgE) with IgG being the most abundant class and most often used in immunoanalytical techniques.
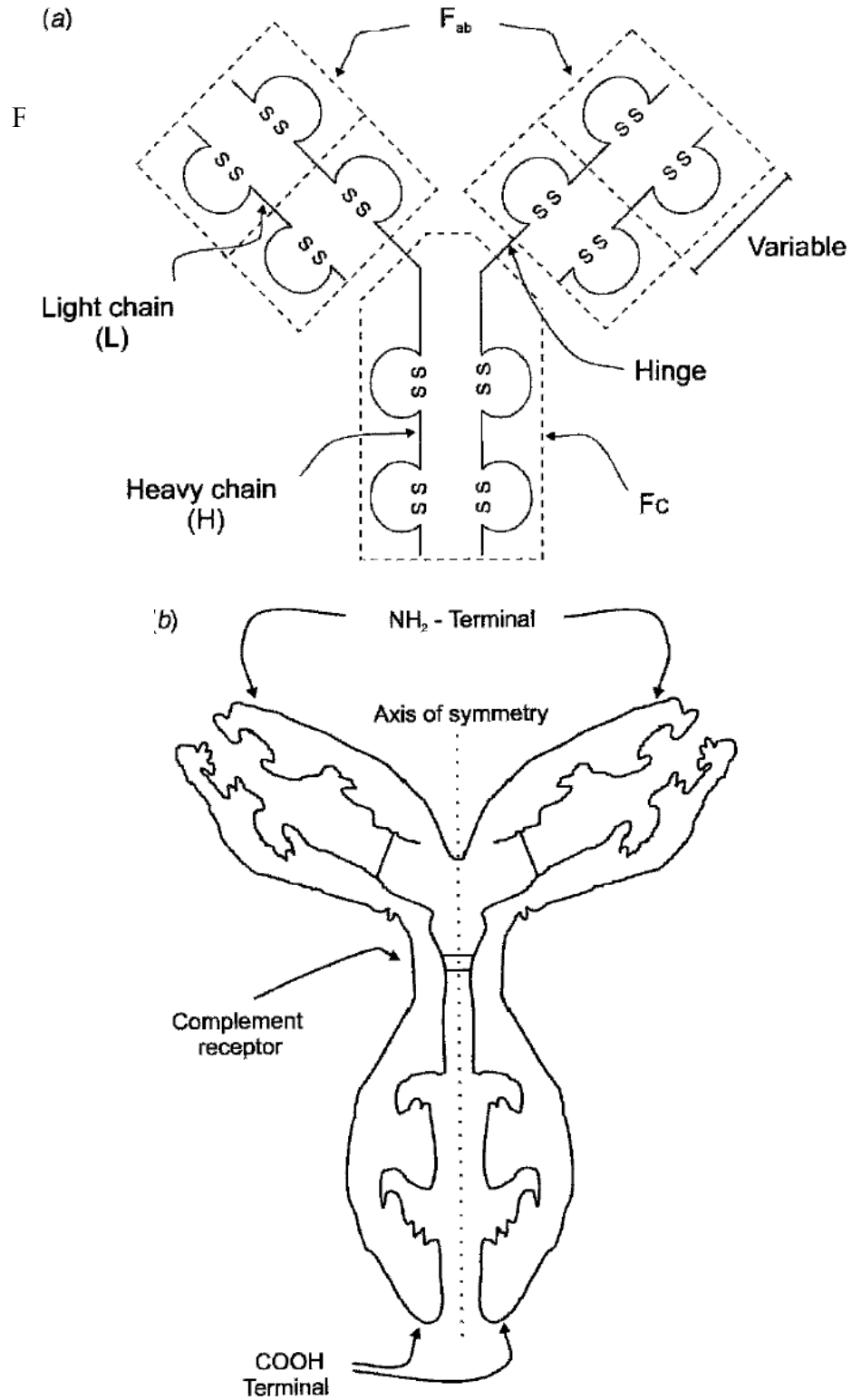
Figure 2.6 Structural diagrams representing antibody molecules.

All immunoglobulin have a number of structural features in common as shown in figure 2.6. They have two "light" polypeptide chains, each with an approximate molecular weight of 25,000 Dalton (Da), and two "heavy" polypeptide chains of 50,000 Da each. These four chains are bound together in a single antibody molecule with disulfide bonds, and form a Y-shape with a central axis of symmetry. In general, the antibody molecule may be divided into two main fragments, the antigen-binding fragment (Fab) and the non-antigen binding fragment (Fc). For the antigen-binding fragment, the N-terminal ends of the light polypeptide chains (L) occur near the top of the "Y" structure. These are the antigen-binding fragments of the antibody, which have been cleaved and used in immunoassays based on primary antigen-antibody interactions in the same approach. It is the amino acid sequence of these N terminal ends which can determine the specific antigen-binding properties of the molecule.

The antigen-binding site of an antibody has a structure, which allows a complementary fit with structural elements and functional groups on the antigen. The part of the antigen that interacts specifically with the antigen-binding site on the antibody is called epitope. Antigens may be classified according to their binding characteristics of the total number of sites and the number of different types. There are four classes of antigens:

- Only a single epitope on the surface that is capable of binding to an antibody: unideterminate and univalent.

- Two or more epitopes of the same kind on one antigen molecule: unideterminate and multivalent.

- Many epitopes of different kinds, but only one kind on one antigen molecule: multideterminate and univalent. Most protein antigens fall into this type.

- Many epitopes of different kinds, and more than one kind per antigen molecule: multideterminate and multivalent such as polymerized proteins and whole cells.

The binding affinity between an antibody (Ab) and an antigen (Ag) can usually be described by the equilibrium expression:

$$Ag + Ab \longrightarrow AgAb \qquad (1)$$

And $\qquad K = [AgAb] / [Ag] [Ab] \qquad mol^{-1}$ \qquad (2)

Where K is the equilibrium constant for the interaction and Ab-Ag is the immunocomplex formed between Ab and its specific Ag. Therefore, these features make many antibodies ideal biological recognition components in immunoassays.

2.3.2 Immunoassay formats

Immunoassays are the quantitative methods of analysis. The antibodies are the primary binding agents for the antigen of interest. The K value in equation (2) dictates the equilibrium and the binding between an antibody and its antigen in a particular system. The results of an immunoassay are thus often the analysis of the binding between an antibody and its antigen and the differentiation between bound and unbound antigen. In other terms, all immunoassays depend on measuring the partial occupancy of the recognition sites. Nevertheless, a measurement can rely on either the assessment of occupied sites or on measuring unoccupied sites. This leads to the development of either a competitive or a non-competitive immunoassay format.

2.3.2.1 Competitive immunoassay systems

In a competitive immunoassay, the sample analyte is mixed with labeled analyte, which both compete for a limited number of antibody-binding sites. This is schematically depicted in figure 2.7a.
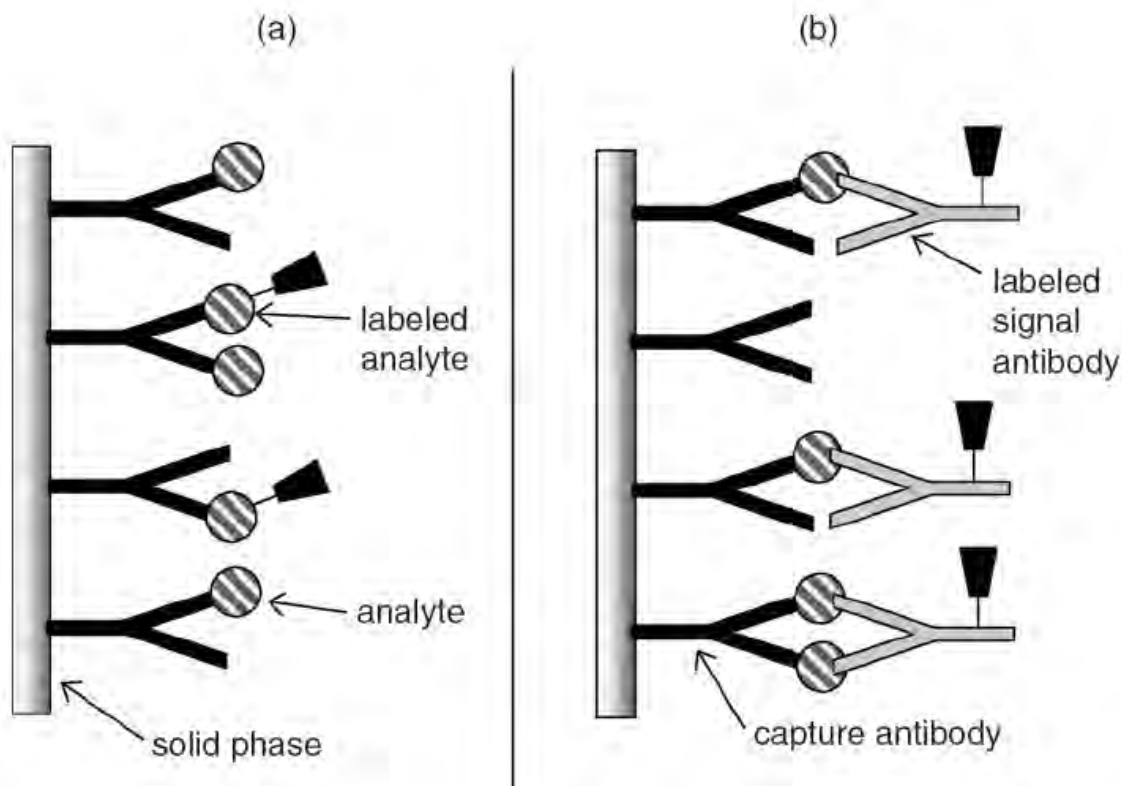
Figure 2.7 Schematic representation of (a) competitive and (b) non-competitive immunoassay formats.

Quantitative analysis can be accomplished by determining the amount of labeled analytes that interacted at the binding sites. With a fixed number of antibody sites, a smaller signal is expected when the ratio between the quantities of sample to labeled analyte is large. On other hand, a large signal is obtained when there is a small quantity ratio. Therefore, the signal produced by the bound labeled analyte is regularly inversely proportional to the amount of sample analyte. The standard curve of a competitive binding assay has a negative slope in figure 2.8.

Most of competitive immunoassays may be used to determine small chemical substances. There are many examples of competitive immunoassays for detecting clinical important analytes.
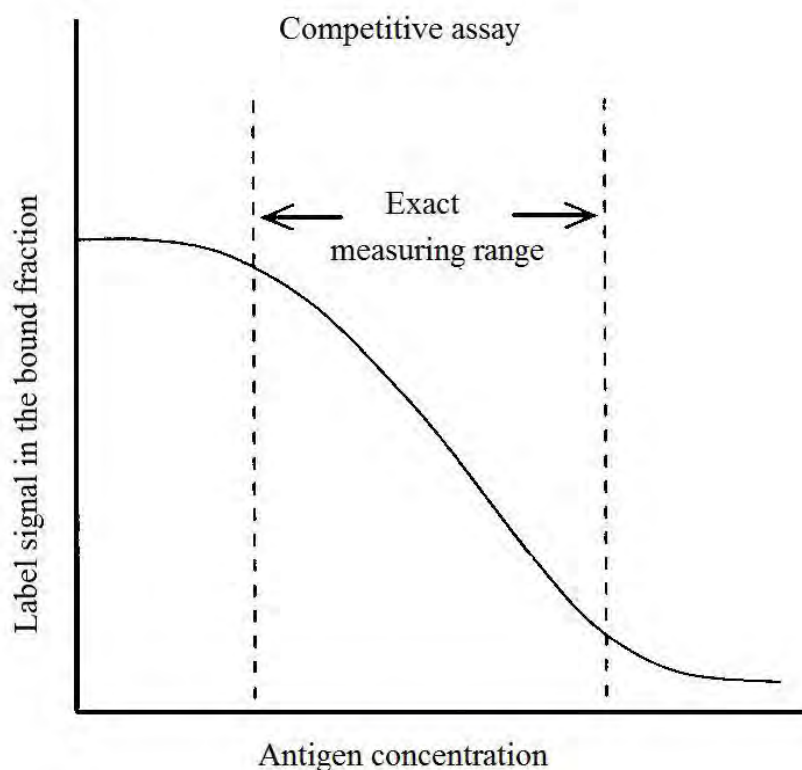
Figure 2.8 Typical standard curves of a competitive immunoassay.

2.3.2.2 Non-competitive immunoassay systems

For a non-competitive immunoassay or sandwich immunoassay, the sample analyte is captured by an excess of a captured antibody as primary antibody, separating it from the bulk sample. The captured analyte is then exposed to an excess of secondary antibody or signal antibody, which will only bind to the existing captured antibody-analyte complex. As shown in figure 2.7b, this structure is now a classic two site immunoassay complex. The analyte is sandwiched between two antibodies. In this method, the signal antibody is often conjugated to either an enzyme label or an electroactive label that produces a signal proportional to the amount of bound analyte. In an ideal non-competitive immunoassay, no signal would be produced in the absence of any analyte because there are no suitable sites available for binding to the signal antibody. Nevertheless, this is not the case due to non specific interactions between the signal antibody and other components of the immunoassay in practice. Consequently, it

is always desirable to use a blocking agent to reduce these non specific interactions. Non specific adsorption also needs to be considered as determining the quantity of signal antibody. Although this immunoassay format often offers superior specificity, it can only be used for the quantification of analytes with two antibodies that can be simultaneously recognized. The typical standard curves of a non-competitive immunoassay are shown in figure 2.9.
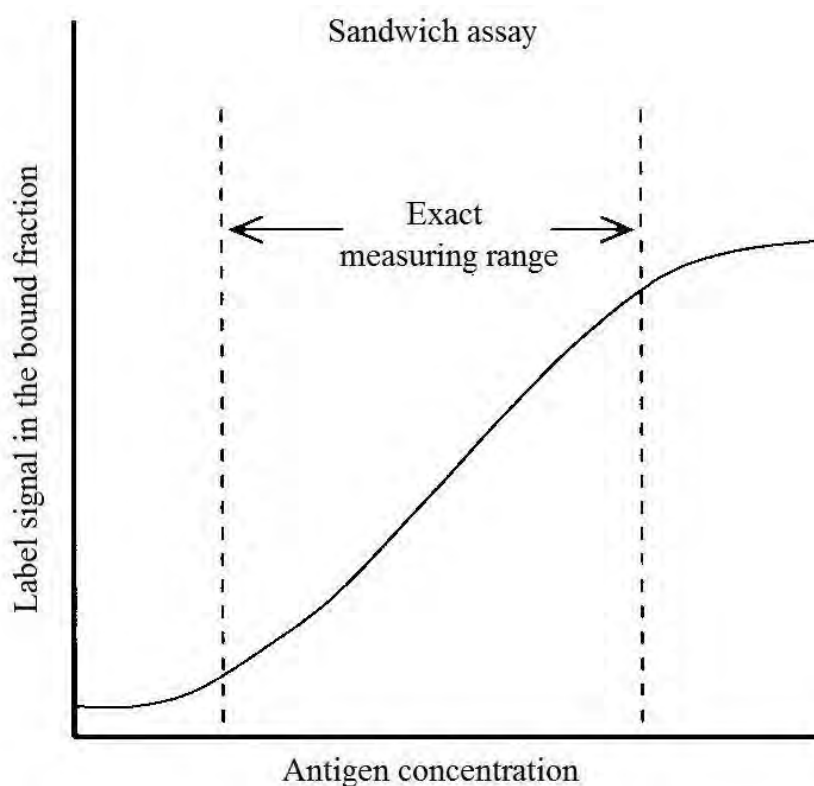
Figure 2.9 Typical standard curves of a non-competitive or sandwich immunoassay.

2.4   Nanoparticles for biosensors

The appearance of nanotechnology is opening new prospects for the application of nanoparticles in biosensors. Figure 2.10 gives relative sizes of nanomaterials and biological molecules. In particular, nanoparticles are generally refer to the materials with dimensions ranging from 1 to 100 nm and are a great interest in the world of nanoscience because of their unique physical and chemical properties.
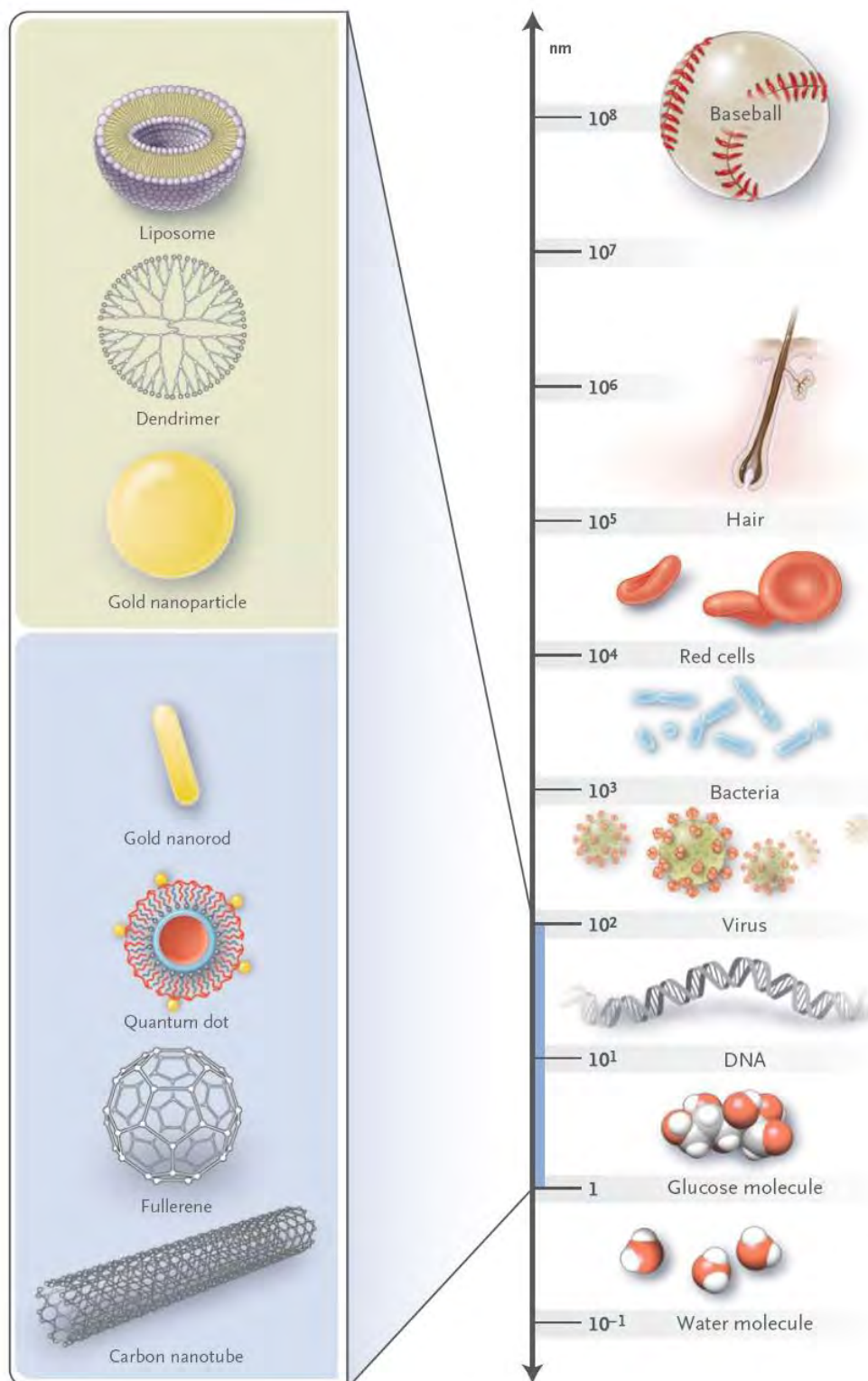
Figure 2.10 Relative sizes of nanomaterials and biological molecules.

These properties offer excellent probability for chemical and biological sensing. Nanoparticles with different compositions and dimensions have been widely used in recent years as versatile and sensitive tracers for the electronic and optical transducers. Gold nanoparticles and semiconductor quantum dot nanoparticles are particularly attractive for numerous bioanalytical applications. The power and scope of nanoparticles can be well enhanced by coupling them with biological recognition reactions and electrical processes.

The applications of nanoparticles in biosensors can be divided into two categories according to their functions:

1) Nanoparticles-modified transducers for bioanalytical applications.

2) Biomolecule-nanoparticle conjugates as labels for biosensing and bioassay.

2.4.1   Gold nanoparticles

Gold nanoparticles are the most intensively studied and applied metal nanoparticles in biosensors owing to their stable physical and chemical properties, useful catalytic activities, and small dimensional size. Gold nanoparticles could provide a stable immobilization for biomolecules retaining their bioactivity. Furthermore, electron transfer between redox biomolecules and electron surfaces is facilitated, which is induced by many factors, such as the high surface to volume ratio, high surface energy, and the functioning as electron conducting pathways between prosthetic groups and the electrode surface from the gold nanoparticles. Gold nanoparticles are generally synthesized by chemical method and electrodeposition.

The electrodes are normally modified by gold in different strategies to improve the performance of the biosensor. The electrode surface could be roughened by gold nanoparticles to increase the interaction of enzyme with the electrode.

2.4.2   Quantum dots

QDs, which are spherical nanometer scale crystals of semiconductor materials, take advantage of the quantum confinement effect, giving these nanoparticles unique optical and electronic properties. They can be made of nearly each semiconductor metal, such as CdS, CdSe, CdTe. The prototypical QD is cadmium selenium (CdSe) as shown in figure 2.11. QDs range between 2 and 10 nm in diameter. Generally, QDs have been coated with an additional semiconductor shell, such as ZnS, to improve the optical properties of the material. This core shell material is further coated with a polymer shell, which allows the materials to be conjugated to biological molecules.

QDs are rendered water soluble using several synthesis methods, such as water soluble ligands, silanization, organic dendrons, cysteines, dihydrolipolic acid, encapsulation with block-copolymer micelles, with amphiphilic polymers, amphiphilic polymers conjugated with poly(ethylene glycol), and surface coating with phytochelatin-related peptides. In addition, QDs can be conjugated to biological molecules, such as proteins, oligonucleids, and small molecules, which are used to direct binding of the QDs to areas of interest for biolabeling and biosensing.
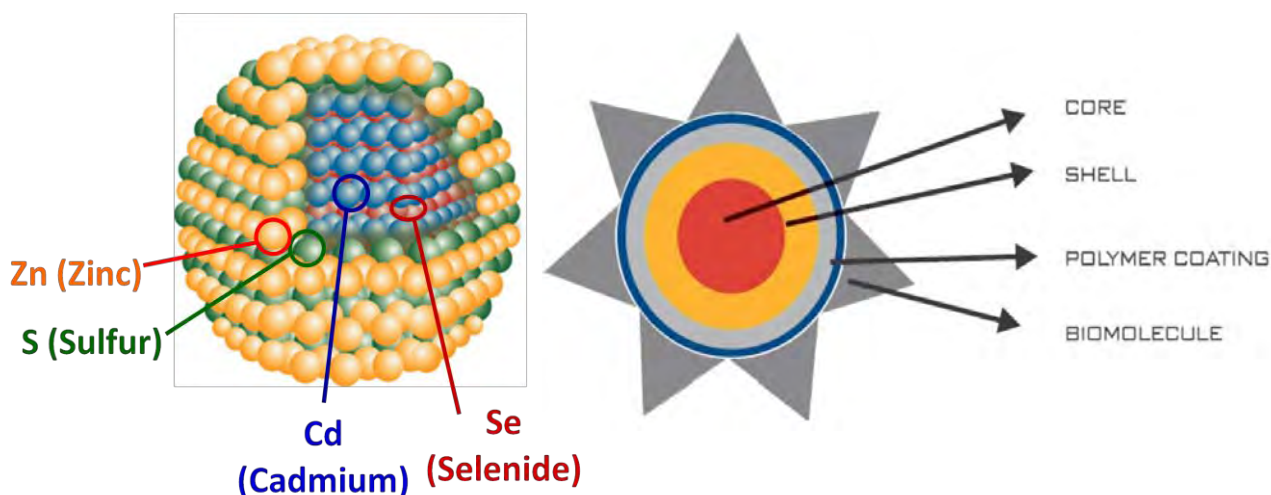
Figure 2.11 Schematic representation of a CdSe/ZnS quantum dot.

2.5 Biomarkers

Biomarkers are a molecular biological, or physical characteristic that can be used to identify risk for humans and environmental, to make a diagnosis, to indicate disease, to guide treatment and monitor clinical response.

The interest in biomarkers has increased in the past two decades. Especially in the area of clinical research, biomarkers can be used to affect patient care. Biomarkers can be used to determine disease risk factors allowing the doctor to recommend more intensive monitoring of a patient.

2.5.1 Cholesterol

Cholesterol and its fatty acid esters are an important lipids. Figure 2.12 displays the structure of cholesterol. They are one of the main constituents of mammalian cell membrane and are precursors of other biological materials, such as bile acid and steroid hormones. Dietary cholesterol is absorbed from the jejunum and is esterified with fatty acids and incorporated into the triglyceride core of chylomicrons. They are secreted into the intestinal lymphatic and reach the blood circulation.
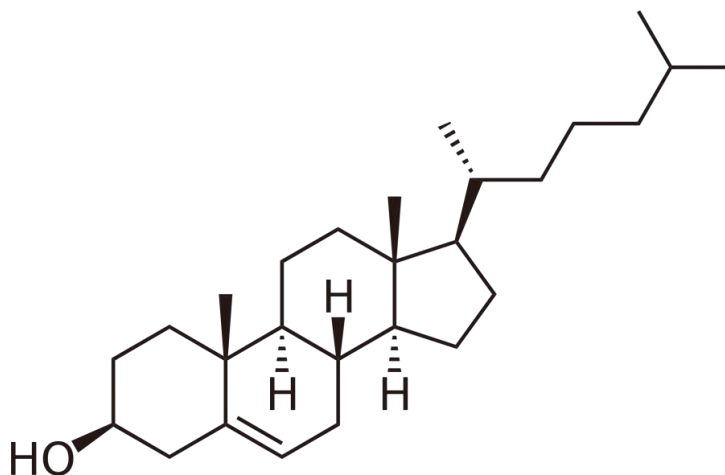
Figure 2.12 Cholesterol structure.

Some of the cholesterol in blood is derived from the food, but for the most part, cholesterol is manufactured in the liver. Consequently, if the diet had no cholesterol, the liver would manufacture more cholesterol to compensate. Some surplus cholesterol is excreted in the bile. Cholesterol is present in foods of animal origin, such as eggs, milk, butter, cheese, and meats. At the high cholesterol level in blood, the accumulation of cholesterol in causes serious coronary heart diseases, cerebral thrombosis, and arteriosclerosis because the accumulated cholesterol on the walls of arteries favors the atherosclerotic plaque formation and blocks the blood flow.

The high cholesterol in blood is one of the highest risk factors for health disease. Therefore, the level of total cholesterol is an important factor in the diagnosis and prevention of heart diseases. Table 2.3 displays the level of total cholesterol and total cholesterol category in blood.

Table 2.3 The level of total cholesterol and total cholesterol category in blood.

Total cholesterol level	Total cholesterol category
Less than 200 mg/dL	Desirable
200–239 mg/dL	Borderline high
240 mg/dL and above	High

2.5.2   Phosphorylated protein

In the early 19th century, it was recognized that phosphates could bind to proteins. Most of phosphorylated proteins were found in milk (caseins) and egg yolk (phosvitin) and were simply considered a biological method of providing phosphorus as a nutrient.

In the 1950s, phosphorylated protein began to emerge as a key regulator of cellular life. An initialing parameter of this emergence occurred in 1954, when enzyme activity was noticed that transferred a phosphate onto another protein and this biological reaction is called phosphorylation as shown in figure 2.13. The protein responsible was a liver enzyme, which catalyzed the phosphorylation of casein and became known as a protein kinase. This is the first of its kind to be discovered.
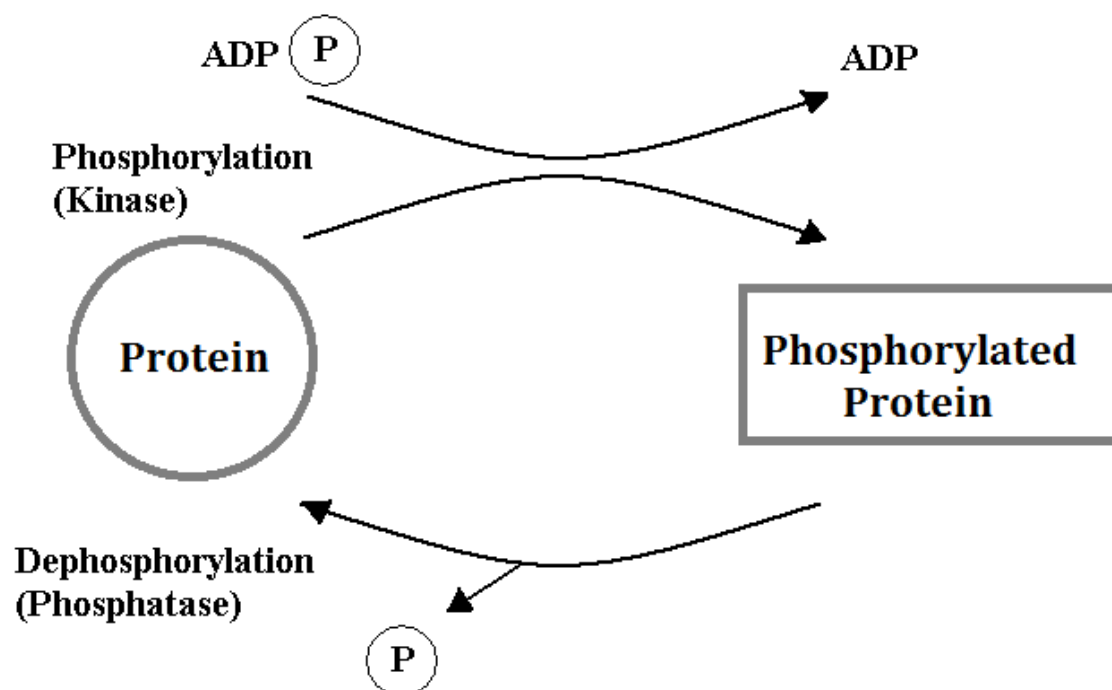
Figure 2.13 Schematic presentation of reversible protein phosphorylation.

A year later, the role of phosphoryltation became more attractive as Fischer and Krebs showed that an enzyme involved in glycogen metabolism was regulated by the addition or removal of a phosphate group. In 1992, Fischer and Krebs received the Nobel Prize in medicine for their pioneering efforts.

Nowadays, this phosphorylation process has an essential role in eukaryotic cell life, as demonstrated by the occurrence of 518 protein kinases and 100 phosphoprotein phosphatases in human genome. Phosphorylated protein is one third of the proteins present in a typical mammalian cell by phosphorylation process. In fact, it has been

estimated that approximately one-third of all proteins in eukaryotic cells are phosphorylated at any given time. There are more than 100,000 predicted phosphorylation sites in mammalian proteomes.

Phosphorylation plays key roles in diverse processes, such as cellular proliferation, differentiation, motility, metabolism, and gene expression, while abnormal phosphorylation contributes to a very large number of human diseases, including cancer, development abnormality, diabetes, inflammation, and neurological disorders. For the aforementioned reasons, the analysis of protein phosphorylation has increasingly becomes the focus of attention in the field of proteomics.

2.6 Electrochemical Method

In 1922, Jaroslay Heyrovsky discovered polarography, which is a branch of electrochemistry, and he received the 1959 Nobel Prize in chemistry. In the 1960s and 1970s, significant advances were made in all areas of voltammetry, which enhanced the sensitivity and expanded the range of analytical methods. The coincidence of these advances with the advent of low cost operational amplifiers also facilitated the rapid commercial development of relatively inexpensive instrumentation.

The typical characteristic of all voltammetric methods involves the application of a potential to an electrode in electrochemical cell. In many instances the applied potential is varied or the current is monitored over a period of time. Therefore, all voltammetric methods can be described as function of potential, current, and time, as shown in figure 2.14. They are considered active methods because the applied potential forces a change in the concentration of an electroactive species at the electrode surface by electrochemically reducing or oxidizing it.

Waveform	Type of voltammetry
	Linear-scan voltammetry
	Differential voltammetry
	Square-wave voltammetry
	Cyclic voltammetry
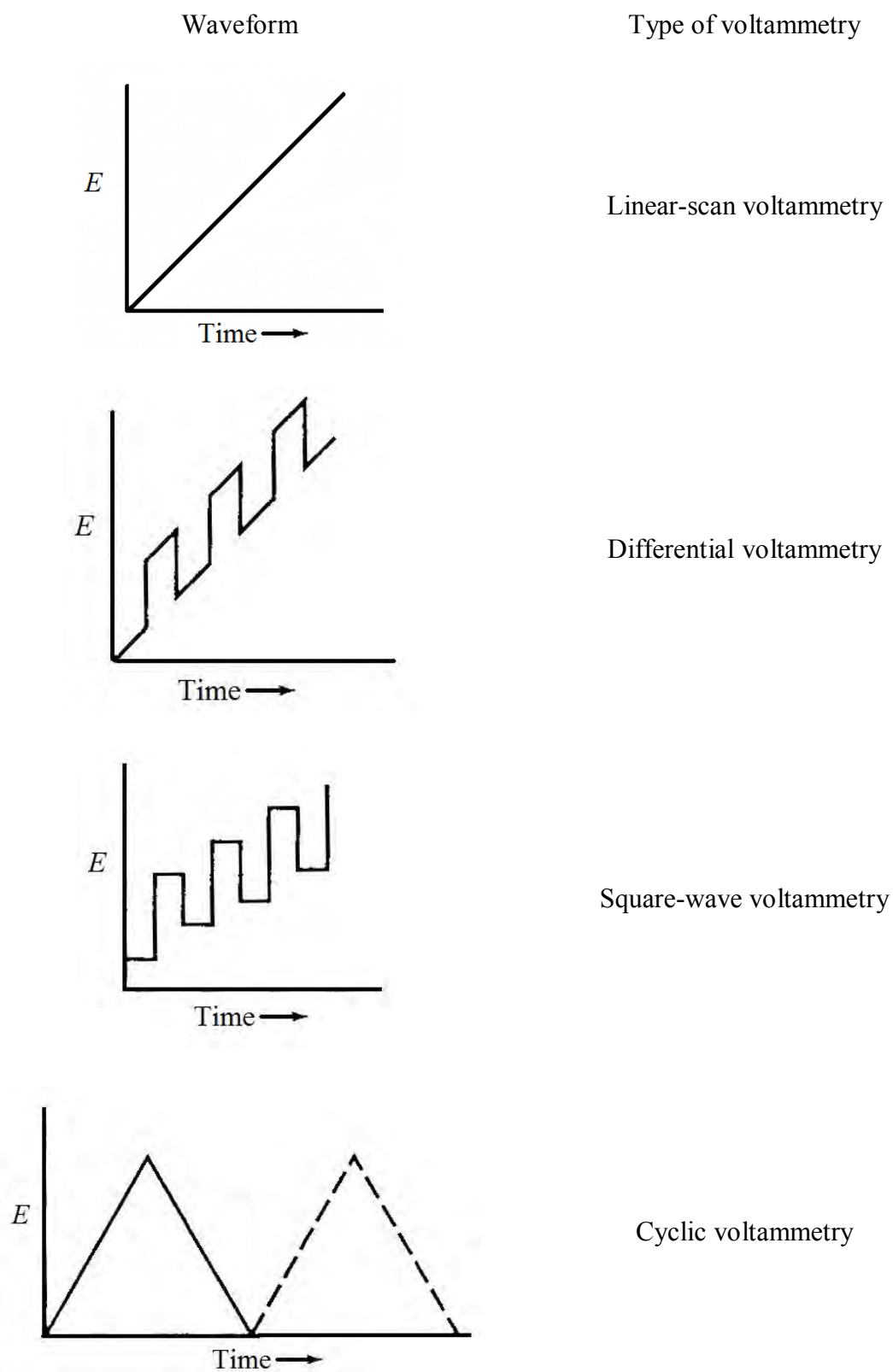
Figure 2.14 The electrochemical waveform used in voltammetry.

The analytical advantages of the several methods include excellent sensitivity with a very large useful linear concentration range for inorganic and organic species, a large number of useful solvents and electrolytes, a wide range of temperatures, rapid analysis times, and simultaneous determination of various analytes. Moreover, electrochemical methods also comprise the ability to determine kinetic and mechanistic parameters, the ability to reasonably estimate the values of unknown parameters, and the ease with which different potential wave forms can be generated.

In this part some electrochemical methods used in this thesis including cyclic voltammetry, anodic stripping voltammetry, and chronoamperometry, which are described respectively.

2.6.1 Cyclic voltammetry

Cyclic voltammetry has become an important and widely used electroanalytical method. It is rarely used for quantitative determinations, but it is generally used for the study of redox processes to understand the reaction of intermediates, and to obtain the stability of reaction products. Cyclic voltammetry is a completed voltage scan (y axis) versus time (x axis) in forward and backward directions, as shown in figure 2.14. For example, the initial scan could be in the negative direction to the switching potential. At that point the scan would be reversed and run in the positive direction, depending on the analysis. This method provides information about the properties and characteristics of the electrochemical process and also gives insight into any complicating side processes, for instance pre- and post-electron-transfer reactions as well as kinetic considerations.

For the period of the potential sweep, the potentiostat measures the current resulting from the applied potential. This resulting plot is called cyclic voltammogram, as shown in figure 2.15. The voltammogram illustrates the shape of a reversible cyclic voltammogram during a single potential cycle. It is assumed that only the oxidized form (O) is present initially. Consequently, a negative-going potential scan is selected for the first half cycle, starting from a value where no reduction occurs.
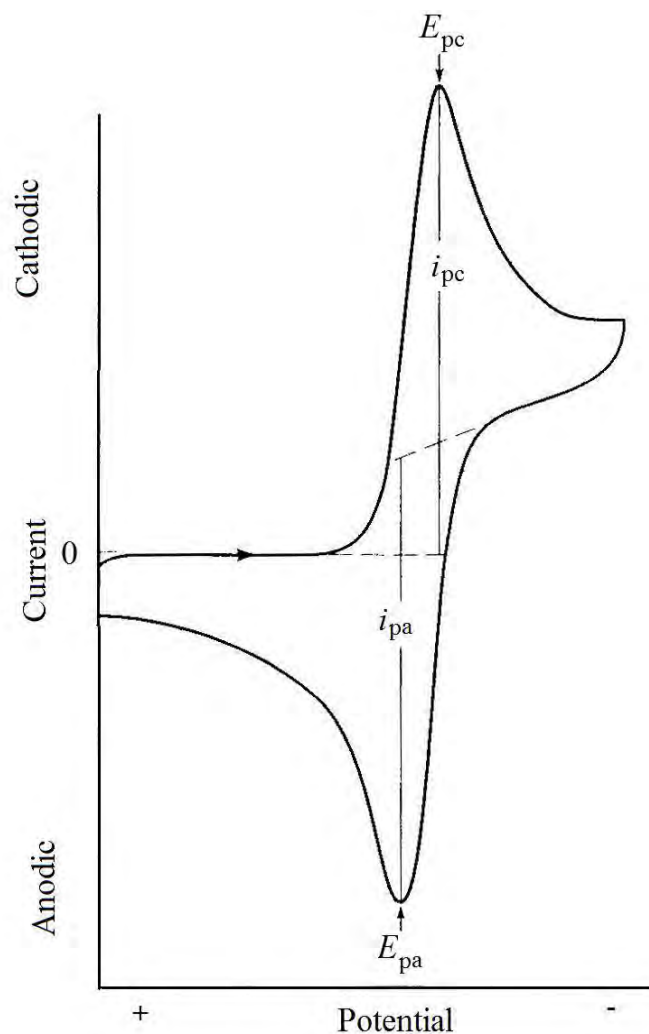
Figure 2.15 Typical reversible cyclic voltammogram with the initial sweep direction towards more negative potential.

While the applied potential approaches the characteristic E^0 for the redox process, a cathodic current begins to increase, until a peak is reached. During reverse scan, R (reduce form) molecules, which were generated in the forward half cycle and accumulated near the electrode surface, are reoxidized back to O as shown in the anodic peak results.

The voltammogram is characterized by a peak potential, E_p, at which the current reaches its maximum value and that value is called the peak current, i_p. The $i_{p,a}$ and $E_{p,a}$ are anodic peak current and anodic peak potential , respectively. The $i_{p,c}$ and $E_{p,c}$ are

cathodic peak current and cathodic peak potential, respectively. The current peaks are commonly measured by extrapolating the preceding baseline current. The peak current for a reversible couple is given by the Randles-Sevcik equation:

$$i_p = (2.69 \times 10^5) n^{3/2} A C D^{1/2} v^{1/2} \quad \text{at 25 °C} \tag{3}$$

where i_p is in A, A (electrode area) is in cm^2, D (diffusion coefficient) is in $cm^2\ s^{-1}$, C (concentration of electroactive species) is in $mol\ cm^{-3}$, and v (scan rate) is in $V\ s^{-1}$.

The ratio of the reverse-to-forward peak currents, $i_{p,a}/i_{p,c}$, is unity for a simple reversible couple. As will be discussed in the following sections, this peak ratio can be strongly affected by chemical reaction coupled to the redox process. The peak potential (E_p) is related to the formal potential of the redox process. The formal potential for a reversible couple is centered between $E_{p,a}$ and $E_{p,c}$:

$$E^0 = \frac{E_{p,a} + E_{p,c}}{2} \tag{4}$$

The separation between the peak potential for a reversible couple is given by:

$$\Delta E_p = E_{p,a} - E_{p,c} = 0.059/n \quad V \tag{5}$$

2.6.2   Square wave voltammetry

Square wave voltammetry is a great amplitude differential method in which a waveform composed of a symmetrical square wave, is superimposed on a base staircase potential. This potential is applied to the working electrode. The current is sampled twice during each square wave cycle, once at the end of the forward pulse and and once at the end of the reverse pulse. While the square wave modulation amplitude is very large, the reverse pulses cause the reverse reaction of the product. The difference

between the two measurements is plotted versus the base staircase potential. A feature plot of the theoretical forward, reverse, and different currents is given in figure 2.16. The resulting voltammogram is symmetrical concerning the half wave potential, and the peak current is proportional to the concentration.
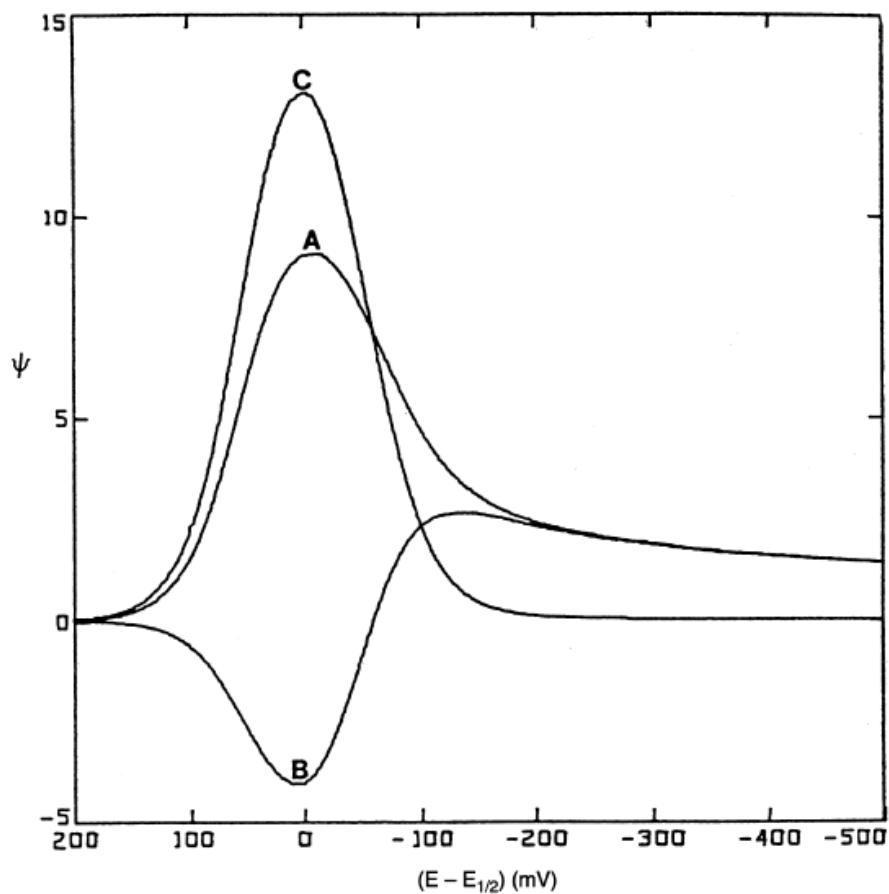
Figure 2.16 Square wave voltammograms for reversible electron transfer. Curve A: forward current. Curve B: reverse current. Curve C: net current.

2.6.3   Anodic stripping voltammetry

Anodic stripping voltammetry (ASV) is the most widely used type of stripping analysis. In this instance, the metals are preconcentrated by electrodeposition into a small-volume mercury electrode (a thin mercury film or a hanging mercury drop). The

preconcentration is done by cathodic deposition at a suitable time and potential. The metal ions reach the mercury electrode by diffusion and convection and they are reduced and concentrated as amalgams:

$$M^{n+} + ne^- + Hg \quad \rightarrow \quad M(Hg) \tag{6}$$
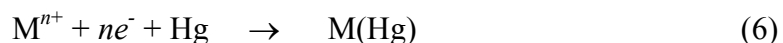
Figure 2.17 displays the potential-time sequence used in ASV, along with the resulting stripping voltammogram. The voltammetric peak reflects the time-dependent concentration gradient of the metal in the mercury electrode for the period of the potential scan. The resulting peak depends upon several parameters of the deposition and stripping steps, in addition to the characteristics of the metal ion and the electrode geometry. Therefore, peak potentials can identify a kind of metal in the sample.
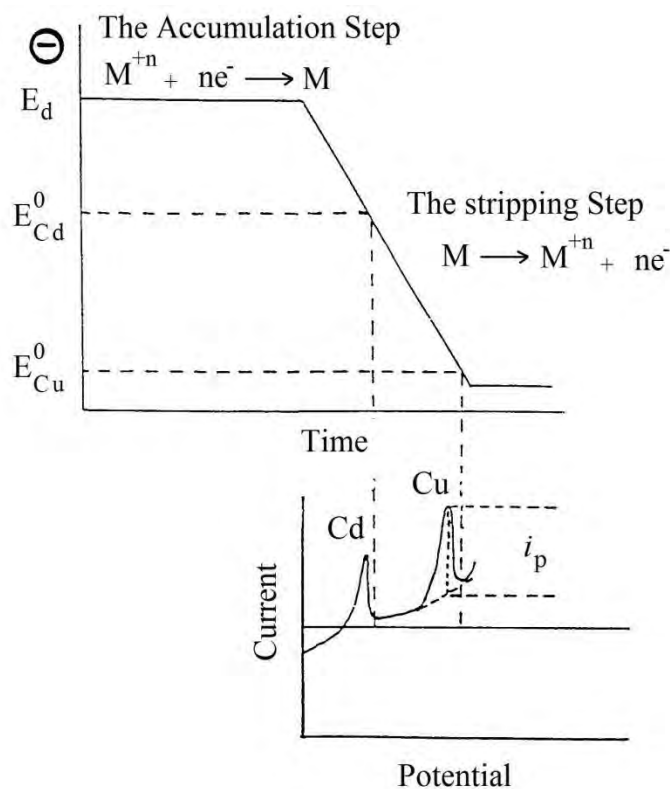
Figure 2.17 Anodic stripping voltammetry: the potential-time waveform (top), along with the resulting voltammogram (bottom).

2.6.4 Chronoamperometry

Chronoamperometry is an electrochemical method for the measurement of current when a fixed potential is applied on a working electrode. A stationary working electrode and unstirred solution are used. This involves stepping the potential of the working electrode from a value at which no faradaic reaction occurs, while the surface concentration of the electroactive species is effectively zero, as shown in figure 2.18A. The resulting current-time dependence is monitored. When mass transport under these conditions is only by diffusion, the current-time curve reflects the change in the concentration gradient in the close area of the surface. Figure 2.18B shows a gradual expansion of the diffusion layer associated with the depletion of the reactant and then the slope of the concentration profile is decreased as time progresses. Thus, the current declines with time (figure 2.18C), as given by the Cottrell equation:

$$i(t) = \frac{nFACD^{1/2}}{\pi^{1/2}t^{1/2}} = kt^{-1/2} \qquad (7)$$

Chronoamperometry is frequently used for measuring the diffusion coefficient of electroactive species or the surface area of the working electrode. Analytical applications of chronoamperometry rely on pulsing the potential of the working electrode repetitively at fixed intervals. Chronoamperometry is very popular in the biosensor field because of a better signal to noise.
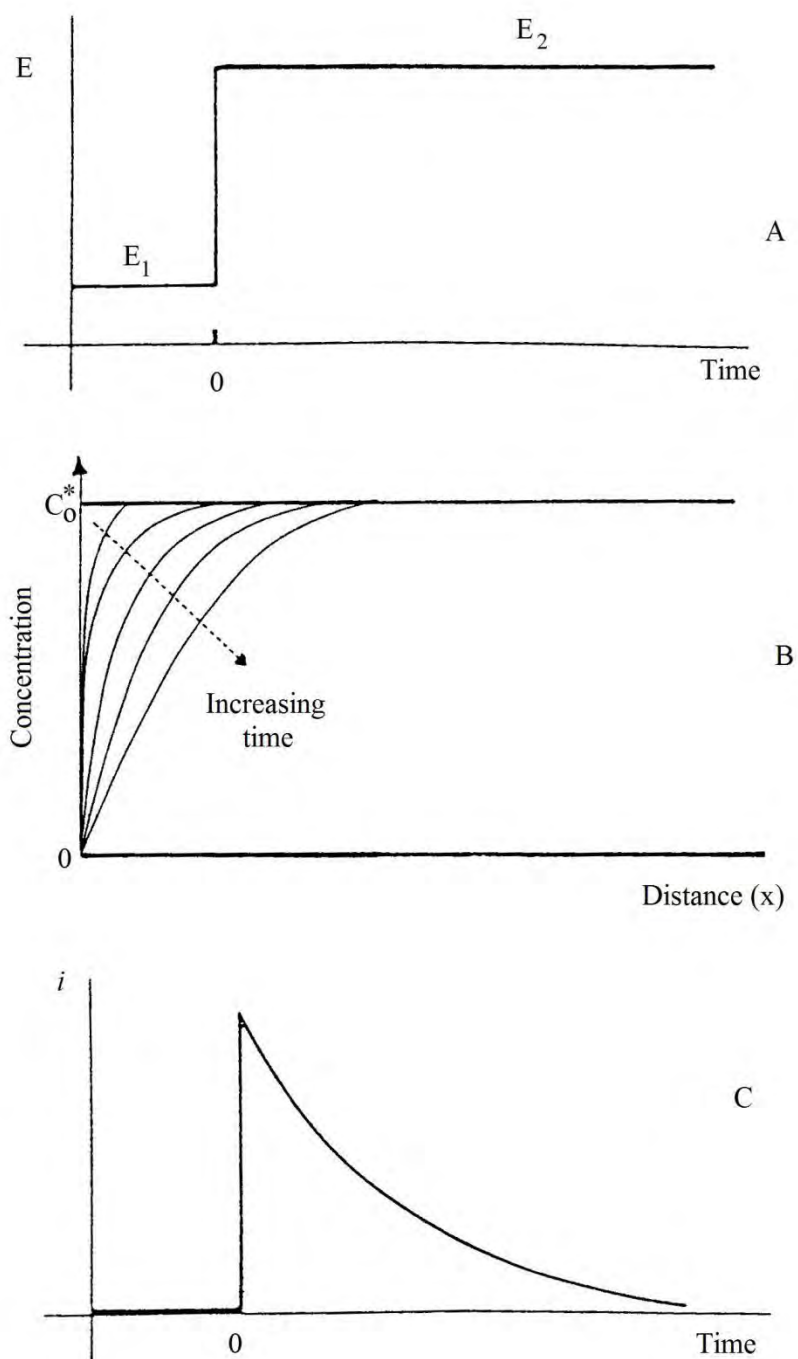
Figure 2.18 Chronoamperometric experiment: (A) potential-time waveform; (B) change of concentration profiles with time; (C) the resulting current-time response.

2.7   Working electrodes

The performance of the voltammetric method is strongly influenced by the material of the working electrode. The working electrode should provide high signal-to-noise characteristic, in addition to reproducible response.   Therefore, its selection depends mainly on two factors: the redox behavior of the electroactives species and the background current over the potential region required for the measurement. Additional considerations include the potential, electrical conductivity, surface reproducibility, mechanical properties, cost, availability, and toxicity. A variety of material has been applied as working electrodes for electroanalysis. The most popular materials are those found in carbon and noble metals, such as platinum and gold.

2.7.1   Screen printed carbon electrodes

Screen printing technology is a method often used in the fabrication of electrodes for the development of disposable electrochemical biosensors. A screen printed electrode is a planar device based on multiple layers of a graphite-powder-based ink printed on a polyimide, plastic, and epoxy or alumina ceramic substrates.   The advantages of designable techniques, adapted from microelectronics, have made screen printing technology. This technology is one of the most important techniques for fabrication of disposable biosensors in the market of handheld instruments. The main advantages of the screen printed electrode consist of simplicity, versatility, modest cost, portability, ease of operation, reliability, small size, and mass production capabilities, which lead to its development in a variety of applications in the electroanalytical field.

2.7.2   Carbon fiber electrodes

The growing interest in microelectrodes has led to widespread use of carbon fibers in electroanalysis. Such materials are produced, mainly in association with the preparation of high strength composites, by high-temperature pyrolysis of polymer textiles or via catalytic chemical vapor deposition. Different carbon fiber microstructures are available, depending upon the manufacturing process. They can be classified into

three broad categories, namely, low-, medium-, and high-modulus types. The last type is most suitable for electrochemical experiments because of its efficient graphite-like structure and low porosity. The most electroanalytical applications rely on fibers of 5-20 μm diameter, which provide the desired radial diffusion. Such fibers are usually mounted at the tip of a pulled glass capillary with epoxy adhesive, and are used in cylindrical or disk configurations. The main advantage of carbon fiber microelectrodes is their small size (5-30 μm diameter for commercially available fibers), which are a very attractive in various microenvironments.

2.7.3   Metal electrodes

As a wide choice of noble metals is available, platinum and gold are the most widely used metallic electrodes. Such electrodes present very favorable electron-transfer kinetics and a large anodic potential range. In contrast, the low hydrogen overvoltage at these electrodes limits the cathodic potential window region, depending upon the pH. Other metals, for example copper, nickel, or silver have been used as electrode materials in connection with specific applications, such as the determination of amino acids or carbohydrates in alkaline medium using copper and nickel and the determination of cyanide or sulfur compounds using silver.

2.7.4   Microelectrodes

Miniaturization is a growing development in the field of analytical chemistry. The miniaturization of working electrodes not only has obvious practical advantages, but also started some fundamentally new possibilities. The term "microelectrode" is reserved here for electrodes with at least one dimension not greater than 25 μm. It is now typical that a microelectrode has dimensions of tens of micrometers or less, down to submicrometer range. Microelectrodes of a variety of geometries have been prepared and used, as shown in figure 2.19.
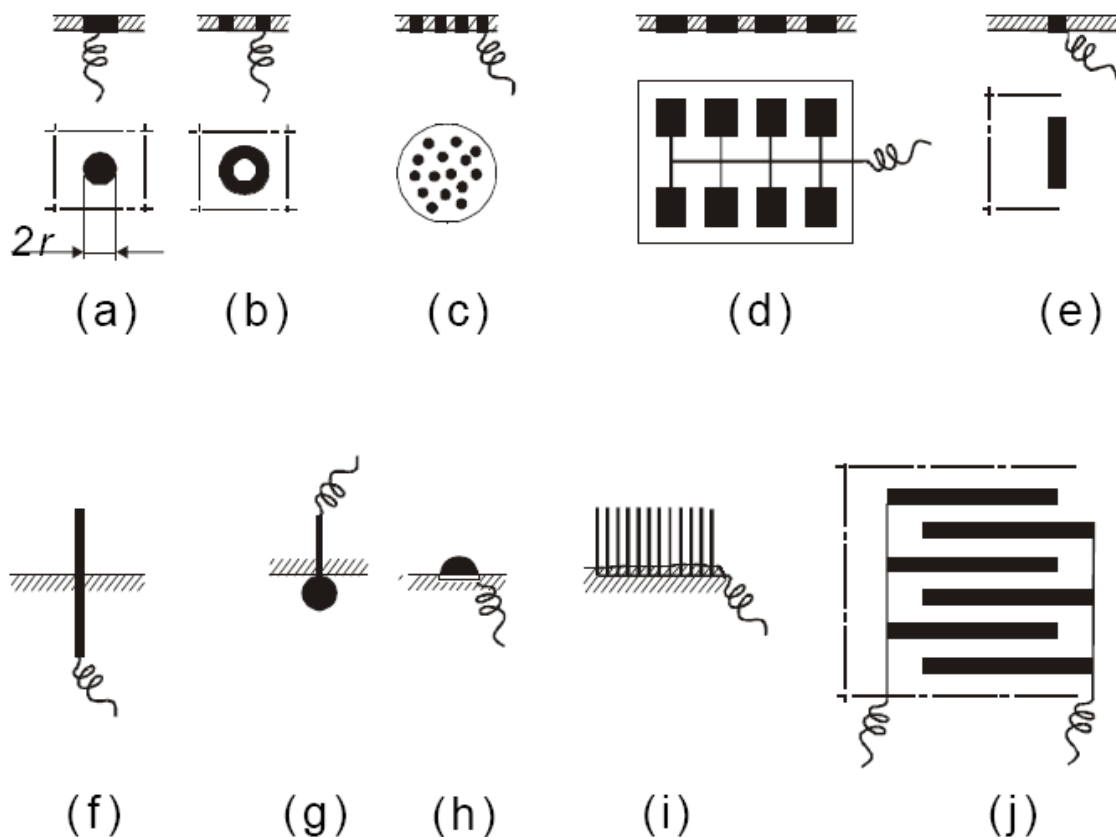
Figure 2.19 The geometries of microelectrodes and microelectrode arrays: (a) microdisk, (b) microring; (c) microdisk array; (d) lithographically produced microband array; (e) microband; (f) single fiber; (g) microsphere; (h) microhemisphere; (i) fiber array; (j) interdigitated array.

If the geometric dimensions of a working electrode become increasingly smaller then the behavior of the electrode begins to depart from that of a large electrode, which can be approximated by an electrode of infinite dimension. These differences are caused by changing conditions of the mass transport from the bulk of solution toward the electrode. Microelectrodes have several important practical implications, for example a decreased ohmic drop of potential, IR, fast establishment of a steady-state signal, a current increase due to enhanced mass transport at the electrode boundary, and increased signal-to-noise ratio. These properties make sufficiently small electrodes advantageous in many areas of electroanalytical chemistry. The application of small-size electrodes was further enhanced by increasing demands from analytical chemistry and biochemistry.

2.8   Literature review

2.8.1   Microsensor and microbiosensor

Miniaturization of electrodes gives rise to new challenges for microsensors or microbiosensor. Microelectrodes have revolutionized the field of analytical electrochemistry, leading to novel methodologies, making new time, and space scales accessible to experimentation. For microsensor and microbiosensor, microelectrode induces an electrochemical reaction, and the resulting current is proportional to a electroactive species. For biological applications, the microelectrode as a probe is dramatically improved when combined with biological recognition element. Enzymes are frequently chosen as the recognition element due to their remarkable specificity.

In 2005, Devadoss et al. reported that platinum microelectrodes are modified with a lipid bilayer membrane incorporating ChOx. The electrode surface modifications are presented along with characterization studies of electrode response to cholesterol solution and to cholesterol contained in the lipid bilayer membrane of vesicles. Amperometric responses obtained at an oxidase-modified electrode for exposure to cholesterol content and the signals indicated a correlation with cholesterol concentration (1.6-12.5 μM). Direct contact between the electrode and a vesicle lipid bilayer membrane showed a response that correlated with vesicle membrane cholesterol content.

In 2007, Masson et al. prepared the glucose microbiosensors by covalent attachment of glucose oxidase at a gold microelectrode surface. They studied that self-assembled monolayers of the *N*-hydroxysuccinimide ester of 16-mercaptohexadecanoic acid (NHS-MHA) at gold microelectrodes enable spontaneous covalent linking of glucose oxidase to the gold surface of microelectrodes. This microbiosensor was calibrated in the range of 1-10 mM with the detection limit of 60 μM.

In 2007, Biloivan et al. fabricated bi-enzyme microbiosemsor for protein detection. The microbiosensor based on all-solid-state microelectrodes with a polypyrrole solid internal contact and immobilized trypsin and carboxypeptidase B was

developed. The result of protein detection showed that quantitative proteins determination can be performed with the microbiosensor in the concentration range of 1-60 μg mL^{-1} and the detection limit of different protein concentration determination can be achieved as 1-2 μg^{-1} in buffer solution.

In 2010, Ali et al. fabricated a a potentiometric glucose biosensor as microsensor by immobilization of glucose oxidase nanowires. Zinc oxide nanowires with diameter of 250-300 nm and length of approximately 1.2 μm were grown on the surface of silver wires with a diameter of 250 μm. Glucose oxidase was electrostatically immobilized on the surface of the nanowires. The response was found to be linear over a relatively wide logarithmic concentration range (0.5-1000 μM).

In 2011, Salazar et al. described an amperometric glucose microbiosensor based on a prussian blue modified carbon fiber electrode with diameter of 10 μm. The electrocatalytic properties of the prussian blue film enabled detection of an enzymatic by H_2O_2 at a very low potential. These microbiosensors displayed a good glucose sensitivity (~12 nA μM^{-1} cm^{-2}) and exploratory pharmacological and electrical stimulations reported that these devices have sufficient sensitivity and stability to monitor multiphasic and reversible changes in brain glucose levels *in vivo*.

This work focuses on the development of microsensor and microbiosensor using modified microelectrode as working electrode for electrochemical detection. Electrochemical microsensor based on gold nanoparticles (AuNps) deposited on carbon fiber microelectrode was developed for detection of cholesterol. For microbiosensor, the modified electrode was fabricated by electrodepositing AuNPs on platinum microelectrode. ChOx has been covalently immobilized on AuNPs using a cross-linker.

2.8.2 Electrochemical immunoassay

Currently, the immunoassay based on a specific recognition of the antigen and antibody has been successfully employed. Electrochemical techniques have numerous advantages for their use in biosensor development, including inexpensive, inherent

simplicity, applicable to optically opaque media, and miniaturizable instrumentation with low power requirements. Thus, the combination the specificity of immunological recognition and electrochemical detection can achieve a way out for detection of analytes with high sensitivity and specificity. Furthermore, a larger number of labels, such as various nanoparticles (gold, silica), quantum dots (QDs), (CdS, PbS, and ZnS) and apoferritin nanoparticles were successfully developed for labeling.

In 2007, Wu et al. described a QD based electrochemical immunoassay to detect a protein biomarker, interleukin-1α (IL-1α). QD conjugated with anti-IL-1α antibody was used as a label in an immunorecognition event and QD labels were attached to the magnetic-bead surface through the antibody-antigen immunocomplex. Electrochemical stripping analysis of the captured QDs was used to quantify the concentration of IL-1α after an acid-dissolution step. The response is highly linear over the range of 0.5–50 ng mL^{-1} IL-1 α, and the limit of detection is estimated to be 0.3 ng mL^{-1} (18 pM).

In 2008, Luo et al. reported a novel electrochemical immunoassay based on the unique features of agarose beads and the special amplified properties of biometallization. in a homogeneously dispersed medium. The immunochemical recognition event between human immunoglobulin G (IgG) and goat anti-human IgG antibody is chosen as the model. The logarithm of the anodic stripping peak current depended linearly on the logarithm of the concentration of human IgG in the range from 1 to 1000 ng mL^{-1} with a detection limit of 0.5 ng mL^{-1}.

In 2009, Yang et al. presented a sensitive aptamer-based sandwich-type sensor to detect human thrombin using QDs as electrochemical label. QDs were labeled to the secondary aptamer and were determined by the square wave stripping voltammetric analysis. The peak currents were linear versus thrombin concentration from 1 nM to 25 nM with a detection limit of 1 pM.

In order to enhance the sensitivities, biosensors and bioassays using electrochemical stripping analysis based on QDs have shown great potential for detection of trace biomolecules. Especially, QDs have been widely used for labeling and

biosensing of the electrochemical immunoassay techniques because of their unique advantages such as nanometer size similar to proteins and versatility in surface modification with various biomolecules (peptides, oligonucleotides, and proteins). This work firstly reported the determination of phosphorylated bovine serum albumin (phosphorylated BSA) using QDs as electrochemical labels.

In this research, we report on an electrochemical immunoassay approach for the quantification of BSA-OP, using QDs as electrochemical labels. The serine site of BSA was phosphorylated and BSA-OP was chosen as the model phosphoprotein in this work.

CHAPTER III

Experimental

The information about the instruments, chemicals, materials, preparation and modification of electrodes are explained thoroughly in this chapter.

3.1 Instruments

3.1.1 Electrochemical measurement

The instruments for the electrochemical measurement are listed in table 3.1.

Table 3.1 List of instruments for the electrochemical measurement.

Instruments	Suppliers
Autolab PGSTAT30 potentiostat with a GPES 4.9 software package for the determination of cholesterol	Eco Chemie B. V., The Netherlands
μAutolab type III potentiostat with a GPES 4.9 software package for the determination of cadmium	Eco Chemie B. V., The Netherlands
Ag/AgCl reference electrode	BAS, Japan
Conventional three-electrode electrochemical cell	1 ,1.5 and 3 mL, Home made
Platinum wire for counter electrode	Goodfellow, USA
Platinum microelectrode (disk; 25 μm)	Home made
Carbon fiber microelectrode (disk; 7 μm)	Home made
Disposable screen printed electrode for the determination of cadmium	Alderon Biosciences, Inc., USA
744 pH meter	Metrohm, Switzerland

3.1.2 Immunoassay

The instruments for immunoassay measurement are listed in table 3.2.

Table 3.2 List of instruments for the electrochemical measurement.

Instruments	Suppliers
C24 Incubator shaker	New Brunswick Scientific, USA
Orbital shaker	VWR Scientific Products, USA
Benchtop eppendorf centrifuge 5415D	Eppendorf, Germany
96 well microplates	Corning, USA
Microplate reader	TECAN, Switzerland

3.1.3 Characterization of QD-anti-phosphoserine conjugates and microelectrodes

All instruments for characterization in this work are shown in table 3.3.

Table 3.3 List of instruments for characterization.

Instruments	Suppliers
Scanning electron microscope (JSM-5410LV)	JEOL, Japan
High-resolution transmission electron microscope (JEOL 2010 HR TEM)	JEOL, Japan

3.1.4 Microelectrode preparations

The instruments for fabrication of carbon fiber and platinum microelectrodes are listed in Table 3.4.

Table 3.4 List of instruments for microelectrode preparations.

Instruments	Suppliers
Carbon fiber with a 7 μm diameter	Goodfellow, England
Platinum wire with a 25 μm diameter	Goodfellow, England
Micropipette tip	200 μL
Microscope	Olympus, Japan
Electrical wire	Bangkok cable

3.1.5 Preparation of QD-anti-phosphoserine conjugates

The instruments for labeling are listed in Table 3.5.

Table 3.5 List of instruments for QD-anti-phosphoserine conjugates.

Instruments	Suppliers
Centrifugation tube	
Desalting column (NAP^{TM}-5)	Qdot$^®$655 antibody conjugation kit,
Ultrafiltration device	Molecular Probes, Inc., USA
Column (for separation media)	

3.2 Chemicals

3.2.1 Microlectrode preparations

The chemicals involved in the fabrication of platinum and carbon fiber microelectrode are listed in table 3.6.

Table 3.6 List of chemicals for the microelectrode preparation.

Chemicals	Suppliers
Epoxy	Royal adhesives & sealants, USA
High purity silver paint	SPI supplies, USA
Methanol	Merck

3.2.2 Electrochemical measurement of cholesterol

The chemicals used in this work are listed in table 3.7. All materials were prepared by Milli-Q water from a Millipore Milli-Q system.

Table 3.7 List of chemicals for electrochemical measurement of cholesterol.

Chemicals	Suppliers
Cholesterol ≥99%	Sigma
30% Hydrogen peroxide (H_2O_2)	Merck
Triton X-100 for molecular biology	Sigma
2-propanol	Merck
Potassium dihydrogen phosphate (KH_2PO_4)	Merck
Dipotassium hydrogen phosphate (K_2HPO_4)	Merck

3.2.3 Electrochemical measurement of cadmium in QDs

The chemicals for the detection of cadmium in QDs used in this work are listed in table 3.8.

Table 3.8 List of chemicals for electrochemical measurement of cadmium in QDs.

Chemicals	Suppliers
Hydrochloric acid (HCl)	Sigma-Aldrich
Sodium acetate (CH$_3$CO$_2$Na)	Aldrich
Acid acid (CH$_3$CO$_2$H	Aldrich
Mercury for atomic absorption standard solution (Hg)	Aldrich

3.2.4   Immobilization of cholesterol oxidase

The chemicals for immobilization used in this work are listed in table 3.9.

Table 3.9 List of chemicals for immobilization of cholesterol oxidase.

Chemicals	Suppliers
Cholesterol oxidase from *Streptomyces* sp.	Sigma
Gold standard solution (HAuCl$_4$)	Merck
L-cysteine	Fluka
1-Ethyl-3-(3-dimethyl aminopropyl) carbodimide (EDC)	Sigma
N-hydroxysulfosuccinimide (NHS)	Sigma
Potassium dihydrogen phosphate (KH$_2$PO$_4$)	Merck
Dipotassium hydrogen phosphate (K$_2$HPO$_4$)	Merck
Sodium chloride (NaCl)	Merck

3.2.5 Immunoassay

The chemicals for immunoassay used in this work are listed in table 3.10.

Table 3.10 List of chemicals for the immunoassay.

Chemicals	Suppliers
Phosphoserine-bovine serum albumin (BSA-OP)	Sigma-Aldrich
Bovine serum albumin (BSA)	Sigma-Aldrich
Anti-phosphoserine antibody	Abcam, Inc.
Monoclonal anti-bovine serum albumin (anti-BSA)	Rockland Immunochemicals, Inc.
γ-globulins	Sigma-Aldrich
Cadmium chloride ($CdCl_2$)	Sigma-Aldrich
Phosphate buffer saline (PBS 0.01 M)	Sigma-Aldrich
Tween 20	Sigma-Aldrich
Polyethylene glycol-6000 (PEG)	Fluka

3.2.6 Preparation of QD-anti-phosphoserine conjugates

The chemicals for labeling used in this work are listed in table 3.11.

Table 3.11 List of chemicals for QD-anti-phosphoserine conjugates.

Chemicals	Suppliers
QD nanocrystals (CdSe/ZnS)	
Succinimidyl-4-(*N*-maleimidomethyl) cyclohexane-1-carboxylate (SMCC)	Molecular Probes, Inc.
Dithiothreitol (DTT)	

Chemicals	Suppliers
Dye-labeled markers	
β-mercaptoethanol	Molecular Probes, Inc.
Separation media	
Exchange buffer	

3.3 Chemicals preparations

3.3.1 Electrochemical measurement of cholesterol

3.3.1.1 10 mM stock solution of cholesterol

Stock solution of 10 mM cholesterol was prepared by dissolving 19.33 mg of cholesterol in solution containing 1 mL of Triton X-100 and 0.4 mL of 2-propanol. The solution was gently stirred with magnetic bar at 60°C to obtain a clear solution. After that, the solution was made up to 5 mL with Milli-Q water and was stored at 4°C.

3.3.1.2 100 mM phosphate buffer solution, pH 7.4

The phosphate buffer solution was prepared by mixing 1 M of K_2HPO_4 and 1 M of KH_2PO_4, as shown in table 3.12.

Table 3.12 Preparation of 0.1 M phosphate buffer.

Desired pH	Volume of 1 M K_2HPO_4	Volume of 1 M KH_2PO_4 (mL)
5.8	8.5	91.5
6.0	13.2	86.8
6.2	19.2	80.8
6.4	27.8	72.2

Desired pH	Volume of 1 M K$_2$HPO$_4$	Volume of 1 M KH$_2$PO$_4$ (mL)
6.6	38.1	61.9
6.8	49.7	50.3
7.0	61.5	38.5
7.2	71.7	28.3
7.4	80.2	19.8
7.6	86.6	13.4
7.8	90.8	9.2
8.0	94.0	6.0

3.3.1.3 0.1 M H$_2$O$_2$

The standard solution of 100 mM H$_2$O$_2$ was prepared by pipetting 15 µL of 30% H$_2$O$_2$ in 1,485 µL of Milli-Q water.

3.3.1.4 Serum sample

To validate our method, a labeled concentration of cholesterol in adult bovine serum was used to represent the real serum sample. A serum sample solution was prepared by dissolving 75 mg of adult bovine serum powder in 1 mL of 0.1 mM PBS, pH 7.4.

3.3.2 Electrochemical measurement of cadmium in QDs

3.3.2.1 1 M HCl

8.3 mL of concentrated HCl was diluted to 100 mL by Milli-Q water.

3.3.2.2   0.1 M Acetate buffer with 10 ppm Hg

0.1 M acetic acid (2.8 mL of glacial acetic acid and 6.8 g of sodium acetate) and 2.5 mL of 1000 ppm Hg standard solution were prepared. The solution was mixed and adjusted to 250 mL with Milli-Q water.

3.3.3   Immobilization of cholesterol oxidase

3.3.3.1   1 mM Gold solution

The solution of 1 mM gold solution was prepared by pipetting 200 μL of $H(AuCl_4)$ in 800 μL of phosphate buffer solution.

3.3.3.2   10 mM L-cysteine

17.6 mg of L-cysteine was weighed, and dissolved in 10 mL of Milli-Q water.

3.3.3.3   Mixture of 50 mM EDC and 20 mM NHS

9.6 mg of EDC and 4.3 mg of NHS were weighed. The solution was mixed and adjusted to 1 mL with 100 mM phosphate buffer saline.

3.3.3.4   Phosphate buffer saline

90 mg of NaCl was weighed, and adjusted to 10 mL with 100 mM phosphate buffer solution.

3.3.4   Immunoassay

3.3.4.1   Anti-BSA antibody solution

The solution was prepared by pipetting 1 μL of anti-BSA antibody in 200 μL of Milli-Q water and was stored at $4^°C$.

3.3.4.2 BSA-OP solution

The solution of the desired concentration was diluted with 0.5% globulin in 0.01 M of PBS and was stored at 4°C.

3.3.4.3 QD-anti-phosphoserine conjugates solution

The solution was prepared by pipetting 1 μL of QD-anti-phosphoserine conjugates solution in 200 μL of 3% globulin in 0.01 M of PBS. The solution was stored at 4°C.

3.3.4.4 Blocking buffer

This solution is 2% (w/v) PEG and 3% (w/v) globulin in 0.01 M PBS. Firstly, 0.75 g of globulin was diluted with 25 mL of 100 mM PBS. Then, 500 μL of PEG was diluted with 25 mL of 3% (w/v) globulin in 0.01 M PBS. The solution was stored at 4°C and was freshly prepared before use.

3.3.4.5 Washing buffer

The washing buffer was prepared by pipetting 0.5 mL of Tween20 and was diluted to 1,000 mL of phosphate buffer saline, pH 7.4, containing 0.138 M NaCl, and 0.003 M KCl.

3.4 Electrochemical measurement of cholesterol

3.4.1 Carbon fiber microsensor

3.4.2.1 Preparation of carbon fiber microelectrode

A single carbon fiber was first attached to the end of a copper wire (electrical wire) with a conductive silver paint, as shown in figure 3.1. When the silver paint was allowed to dry, the carbon fiber was inserted into a micropipette tip. The copper wire

attached to a carbon fiber was fixed to a micropipette tip using a fast drying epoxy resin and was cured at a temperature of 60°C for 2 hours.

3.4.2.2 Electrodeposition of AuNPs on carbon fiber microelectrode

Prior to electrodeposition, the carbon fiber microelectrode was polished with 0.3 and 0.05 μm of aqueous alumina slurries and then sonicated in ethanol and Milli-Q water, respectively. The electrodeposition was carried out in a three-electrode cell, consisting of Ag/AgCl as a reference electrode, platinum wire as a counter electrode, and a carbon fiber microelectrode as a working electrode. The electrodeposition of AuNPs was made in cyclic voltammetry. AuNPs were electrochemically deposited onto the surface of carbon fiber microelectrode by cycling the potentials between -0.6 to 1.2 V (2 cycles) with scan rate of 100 mV s^{-1} in 0.1 M HCl/KCl solution containing 10 ppm of HAuCl$_4$, as shown in figure 3.1.
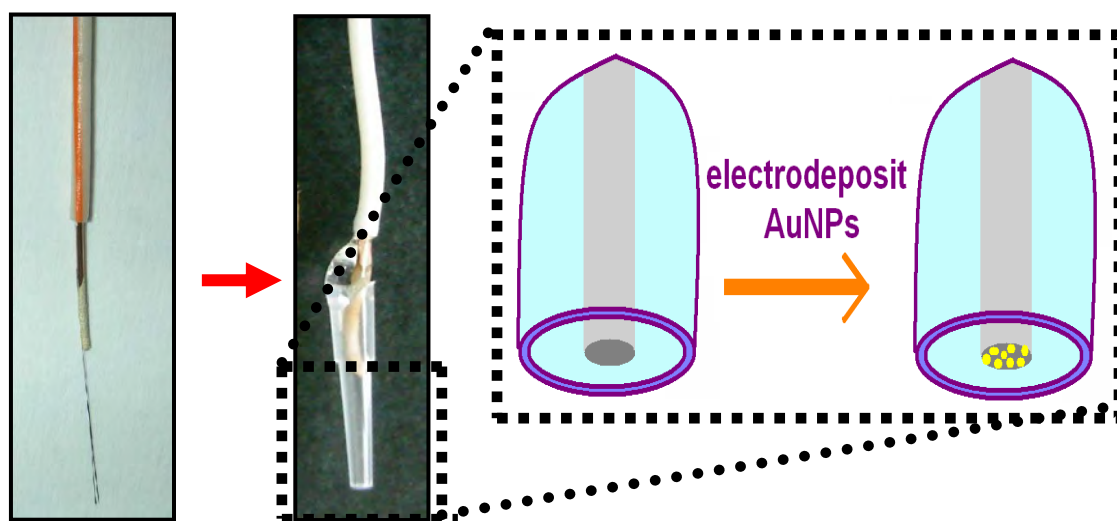
Figure 3.1 Schematic presentations of the preparation of a microelectrode and electrodeposition of AuNPs.

3.4.2   Platinum microbiosensor

3.4.2.1   Preparation of platinum microelectrode

A platinum wire was first attached to the end of a copper wire (electrical wire) with a conductive silver paint. When the silver paint was allowed to dry, the platinum wire was inserted into a micropipette tip. The copper wire attached to a platinum wire was fixed to a micropipette tip using a fast drying epoxy resin and was cured at a temperature of 60°C for 2 hours.

3.4.2.2   Electrodeposition of AuNPs on platinum microelectrode

Prior to electrodeposition, the platinum microelectrode was polished with 0.3 and 0.05 µm of aqueous alumina slurries and then sonicated in ethanol and Milli-Q water, respectively. The electrodeposition was carried out in a three-electrode cell, consisting of Ag/AgCl as a reference electrode, platinum wire as a counter electrode, and a platinum microelectrode as a working electrode. The electrodeposition of AuNPs was made in cyclic voltammetry. AuNPs were electrochemically deposited onto the surface of platinum microelectrode by cycling the potentials between -0.1 to -0.9 V (20 cycles) with scan rate of 100 mV s^{-1} in 0.1 M PBS solution containing 1 mM of HAuCl$_4$.

3.4.2.3   Immobilization of cholesterol oxidase on platinum microelectrode

The AuNPs/Pt microelectrode was immersed in 10 mM of L-cysteine at room temperature for 6 hours. After that, the AuNPs/Pt microelectrode was washed with Milli-Q water to remove any unattached excess of L-cysteine and was immersed in solution containing 50 mM of EDC and 20 mM of NHS at 4°C for 2 hours. The modified microelectrode was rinsed with Milli-Q water and was finally immersed in cholesterol oxidase at 4°C for 6 hours. The microbiosensor was rinsed with Milli-Q water and was stored at 4°C when not in use.

3.4.3 Electrochemical detection of cholesterol

Electrochemical measurement was carried out in a three-electrode cell, consisting of Ag/AgCl as a reference electrode, platinum wire as a counter electrode, and a modified microelectrode as a working electrode, as shown in figure 3.2. Chronoamperometric response was investigated in 0.1 M of PBS as electrolyte. Cholesterol was determined at 0.4 V in open atmosphere to detect oxidation current of H_2O_2. After enzymatic reaction for the occurrence of H_2O_2, a suitable potential was applied by the potentiostat. The electrochemical measurement was controlled by a computer system using the GPES 4.9 software. The temperatures of experiments were maintained at $25^{\circ}C$.
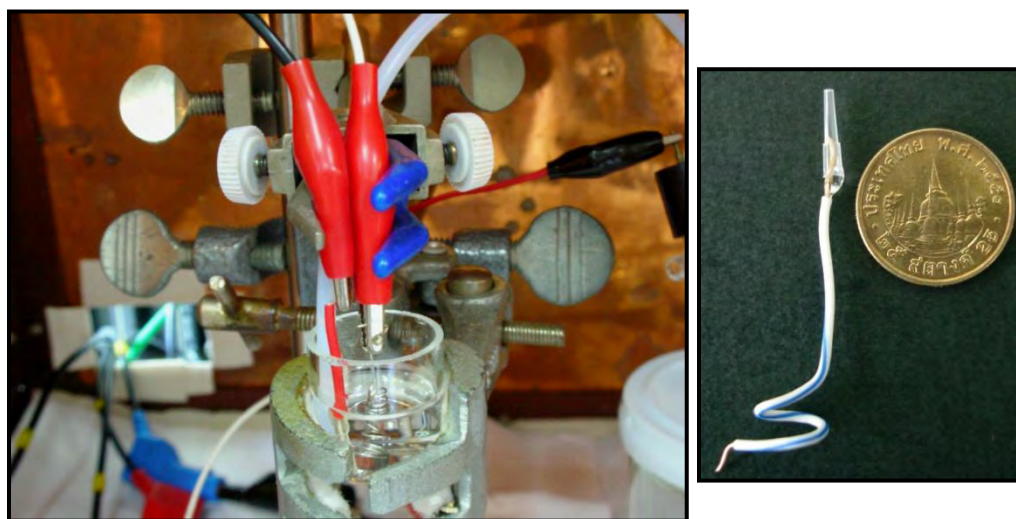
Figure 3.2 The electrochemical cell for the detection of cholesterol.

3.5 Electrochemical measurement of BSA-OP

3.5.1 Preparation of QD-anti-phosphoserine conjugates

The QD-anti-phosphoserine conjugates were prepared with the Qdot®655 antibody conjugation kit following the manufacturer's protocol. The QDs were coated with a layer of polymer by the manufacturer. This process involved six steps :

(A) QD nanocrystals in dimethylsulfoxide solution were activated with hetero-bifunctional crosslinker (10 mM of SMCC) at room temperature for 1 hour, and then excess any SMCC was removed via a NAP-5 desalting column with the exchange buffer provided in the kit as the elution solvent. Approximately 500 µL of the QDs with maleimide-nanocrystal surfaces were collected.

(B) 300 µL of 0.5 mg mL^{-1} anti-phosphoserine antibody was reduced with 20 mM DTT at room temperature for 0.5 hour to expose free sulfhydryl groups.

(C) Anti-phosphoserine antibody was then labeled with the dye-labeled marker and purified with the NAP-5 desalting column, collecting approximately 500 to 600 µL of the colored fraction.

(D) The activated QD nanocrystals and reduced antibodies were then mixed and allowed to conjugate (sulfur-maleimide bond formation) at room temperature for 1 hour.

(E) The reaction was quenched by the addition of β-mercaptoethanol and concentrated to a final volume of 20 µL via ultrafiltration (7000 rpm for approximately 10-15 minutes on a benchtop Eppendorf centrifuge) using the 0.5 mL concentrator supplied in the kit.

(F) Finally, the QD-anti-phosphoserine conjugates were purified by Superdex 200 gel chromatography with PBS as the eluent buffer. The initial dark brown-colored eluent was collected in the dead space of the column (~200 µL), and then stored at 4°C before use.

The QD-anti-phosphoserine conjugates were further characterized with TEM. The sample was prepared by dispersing 5 µL of 200 fold diluted QD-anti-phosphoserine solution on the surface of the carbonate support film of a TEM grid, and allowing it to dry at room temperature.

3.5.2 Immunoassay procedure

This procedure is divided into six steps:

(A) The anti-BSA antibody solution was added into a 96-well microplate and incubated overnight at 4°C with gentle shaking.

(B) After the solution was removed, the wells were washed four times with washing buffer followed by the addition of 250 µL of blocking buffer and incubated at 37° C for 2 hours with gentle shaking to block the remaining active sites.

(C) The plates were then washed, followed by the addition of 50 µL of BSA-OP of the desired concentration into the wells and incubated at 37°C for 1 hour with gentle shaking.

(D) The wells were then washed four times, as mentioned above, prior to the addition of 50 µL of the QD-anti-phosphoserine conjugates solution and incubated at 37°C for 1 hour with gentle shaking in order to obtain the sandwich immunoreactions.

(E) The completed microplate was washed four more times. Finally, to release cadmium ions from the captured QDs, 20 µL of 1 M HCl was added into each well, and then the solution was mixed with 50 µL of acetate buffer with 10 ppm of Hg.

(F) The resulting solution was quantified by square wave voltammetry.

3.5.3 Electrochemical detection of BSA-OP

Square wave voltammetric (SWV) measurements were performed with a screen printed electrode (SPE), consisting of a carbon working electrode, a carbon counter electrode, and a Ag/AgCl reference electrode. Each SPE was first pretreated electrochemically by cyclic voltammetric scanning 10 times at a potential range of 0 - 1.5 volt (V) in 0.05 M PBS. After washing and drying with an airstream, 50 µL of sample solution was dropped onto the sensing area of the SPE. The cadmium solution was measured with SWV using an in situ plated mercury film on the SPE. The SWV

parameters used were a conditioning potential of 0.6 V for 60 second (s), deposition potential of -1.2 V for 120 s, equilibration time of 10 s, amplitude of 25 mV, step potential of 4 mV, and a frequency of 15 Hertz (Hz). A baseline correction of the resulting voltammogram was performed using the GPES 4.9 software.

CHAPTER IV

RESULTS AND DISCUSSION

In this chapter, the detail was separated into three parts. The first and second part are the results and discussion from using microsensor and microbiosensor for the determination of cholesterol. The results were obtained from cyclic voltammetry and chronoamperometry. Electrochemical immunoassay based QD labels for the determination of phosphorylated bovine serum albumin was described in the third part. The results were obtained from stripping voltammetry.

4.1 Electrochemical detection of cholesterol using microsensor

The enzymatic reaction for the cholesterol detection is ChOx as a receptor which can be described in the figure 4.1.
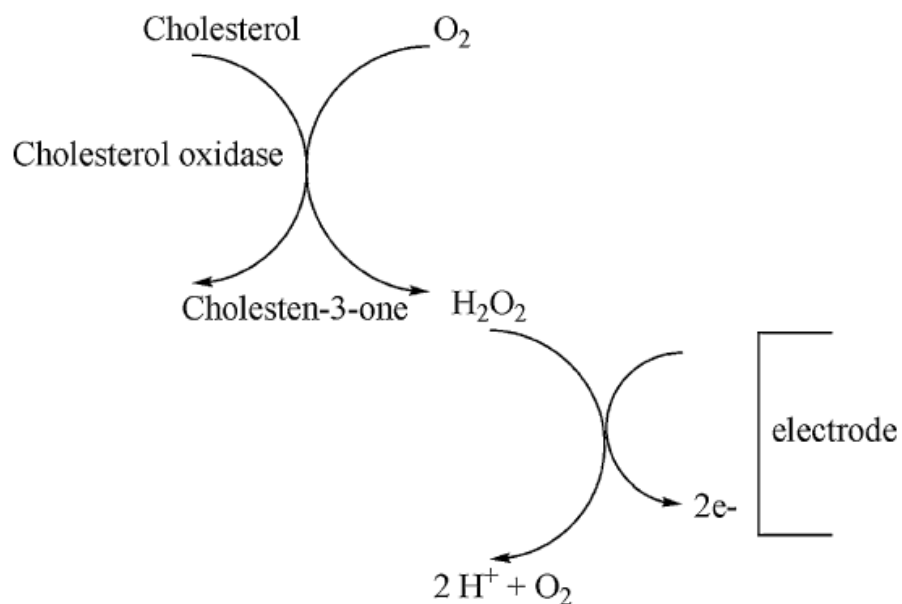
Figure 4.1 Schematic presentations of the mechanism of electrochemical cholesterol microsensor.

The cholesterol is catalyzed by ChOx in the presence of oxygen and at the same time, the product of the enzymatic reaction is hydrogen peroxide. The hydrogen peroxide is an electroactive substance, so hydrogen peroxide can be detected at the suitable potential applied to the electrode.

4.1.1 Electrochemical behavior of the carbon fiber microelectrode

After preparation of carbon fiber (CF) microelectrode, the first step is the determination of $K_4[Fe(CN)_6]$ for testing at the bare CF microelectrode. A cyclic voltammogram of $K_4[Fe(CN)_6]$ is shown in figure 4.2 and the voltammogram shows a well-defined reversible of electroactive species.
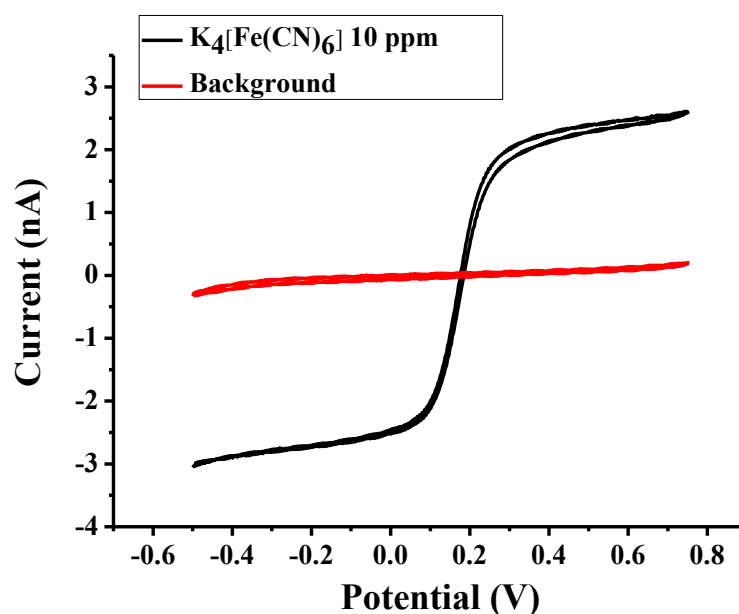
Figure 4.2 Cyclic voltammograms of 10 ppm of $K_4[Fe(CN)_6]$ in 0.05 M phosphate buffer solution, pH 7.4.

4.1.2   Characterization of AuNPs on a carbon fiber microelectrode

AuNPs were electrodeposited on a CF microelectrode from 0.1 M of HCl/KCl solution containing 10 ppm of $HAuCl_4$ by cyclic voltammetry. The scan rate of 100 mV s^{-1} was applied between -0.6 to 1.2 V as shown in figure 4.3.
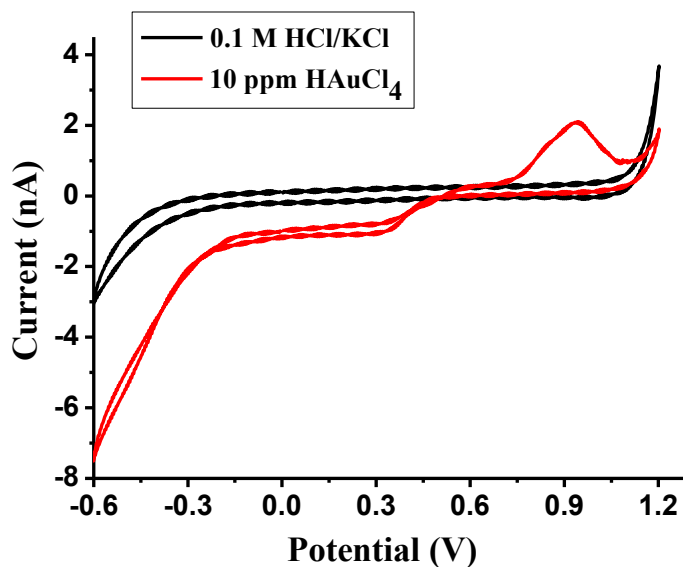
Figure 4.3 Cyclic voltammograms of 10 ppm of $HAuCl_4$ in 0.1 M HCl/KCl.

Figure 4.3 shows cyclic voltammogram of 10 ppm of $HAuCl_4$ solution at CF microelectrode. This result indicated that AuNPs were deposited on the surface of microelectrode. Moreover, scanning electron microscopy (SEM) was used for characterizing the AuNPs on a CF microelectrode surface. As shown in figure 4.4, SEM images indicate that AuNPs were deposited on the microelectrode surface. The electrodeposited-AuNPs were well distributed on the surface with a sizes ranging from 80-150 nm.
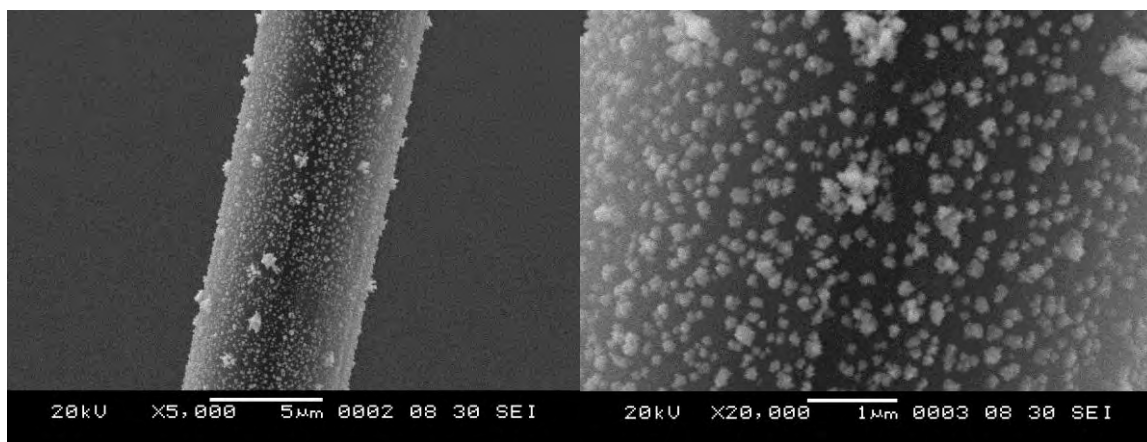
Figure 4.4 Scanning electron microscope images of AuNPs at the carbon fiber microelectrode after the electrodeposition by cyclic voltammetry.

To optimize the condition of electroanalysis, H_2O_2 is a suitable electroactive reactant because it is a product of enzymatic reaction.

By comparing between a bare CF microelectrode (figure 4.5A) and an AuNPs/CF microelectrode (figure 4.5B), cyclic voltammograms for the determination of H_2O_2 show that AuNPs/CF microelectrode can improve the sensitivity because AuNPs have the ability to enhance the electrode conductivity and facilitate the electron transfer.

For the SEM images and cyclic voltammograms, the results indicated that AuNPs deposited on a CF microelectrode can improve an electrochemical signal of H_2O_2, so AuNPs/CF was chosen for microsensor to detect H_2O_2.
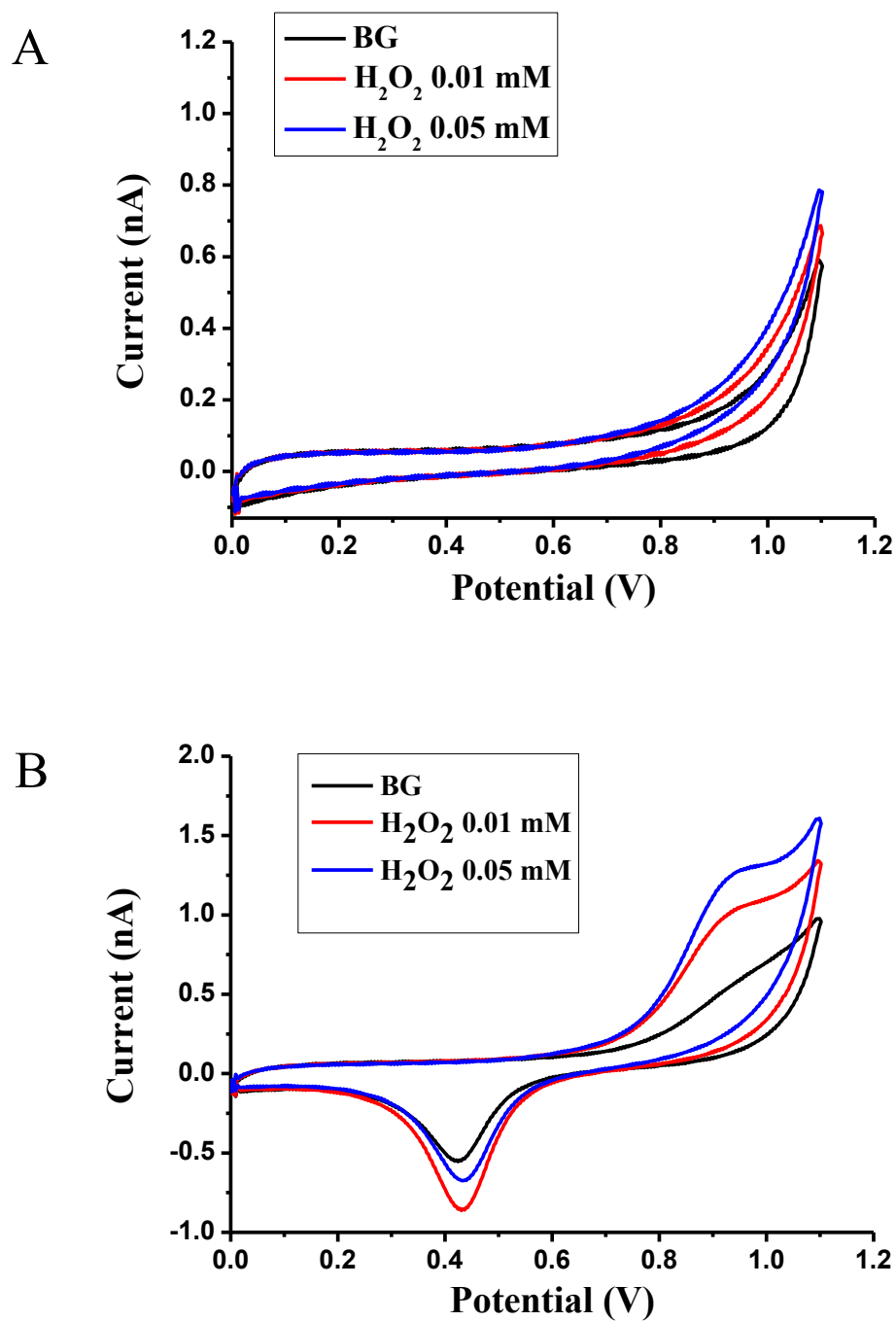
Figure 4.5 Cyclic voltammograms of 0, 0.01, and 0.05 mM H_2O_2 in 0.05 M phosphate buffer solution at a bare CF microelectrode (A) and an AuNPs/CF microelectrode (B).

4.1.3   Electrochemical detection of cholesterol

4.1.3.1   The effect of detection potential of microsensor

The detection potential is an important influence over the microsensor response because the detection potential contributes to the sensitivity of the electroanalysis. In this research, the steady state response to 0.05 mM of H_2O_2 in 0.05 M PBS was measured at several potentials.

As shown in figure 4.6, the signal to background ratio were considered because the background current also increased. From the results, a detection potential of 0.5 V was chosen.
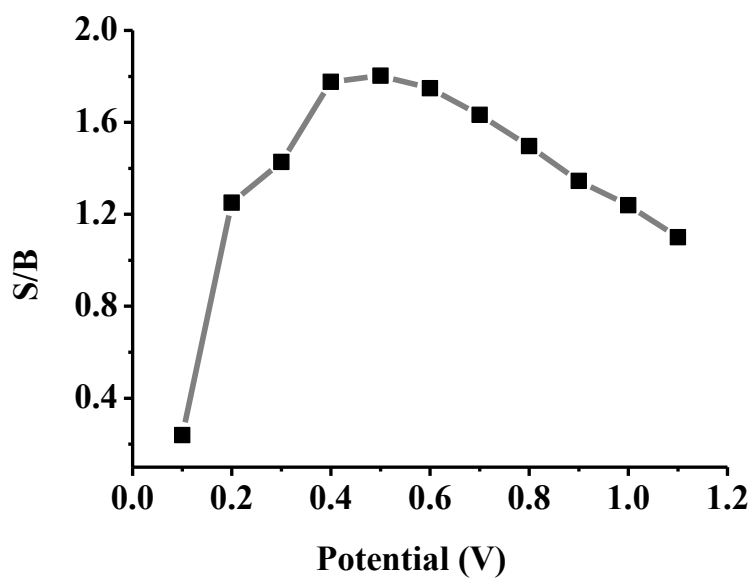
Figure 4.6 The effect of detection potential on the signal to background ratio of H_2O_2 0.05 mM and background at AuNPs/CF microelectrode.

4.1.3.2   The calibration curve of H₂O₂ and cholesterol of microsensor

The calibration curve of H_2O_2 obtained from the amperometric response is shown in figure 4.7.   Under optimum conditions, the current is linearly proportional to H_2O_2 concentration in the range of 0.01 to 1.5 mM in 0.05 M phosphate buffer solution, pH 7.4, with a correlation coefficient of 0.9947.   The detection limit was 4 μM based on the criterion of a signal to background ratio of 3.   The response time of detection is 10 s.

y = 0.673x + 0.3356
R² = 0.9947
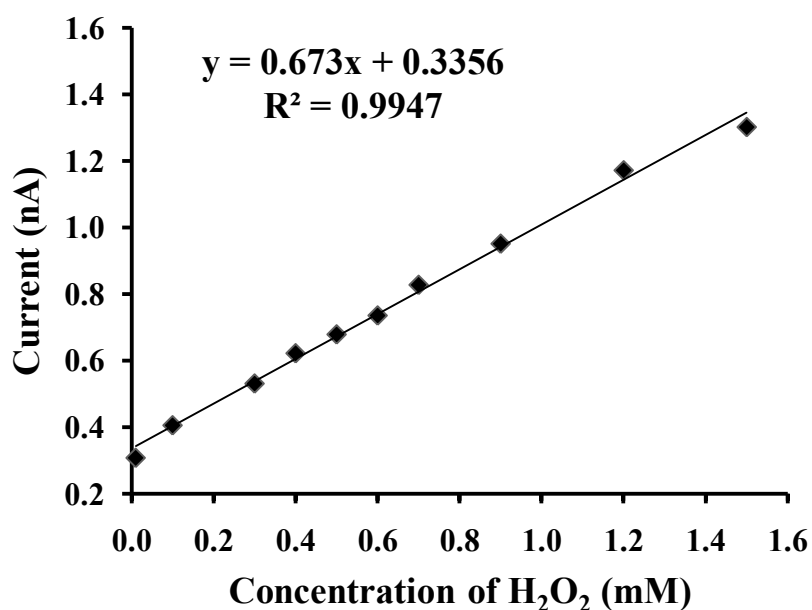
Figure 4.7 Calibration curve of H_2O_2 determination (0.01 to 1.5 mM) using AuNPs/CF microelectrode.

For cholesterol detection, ChOx was added to the solution containing cholesterol in 0.05 mM phosphate buffer solution.   The solution was stirred using a magnetic stirrer for 10 minutes and chronoamperometry was used to measure cholesterol.   Figure 4.8A shows the chronoamperometric signal of cholesterol in the range of 0.05 to 0.5 mM.
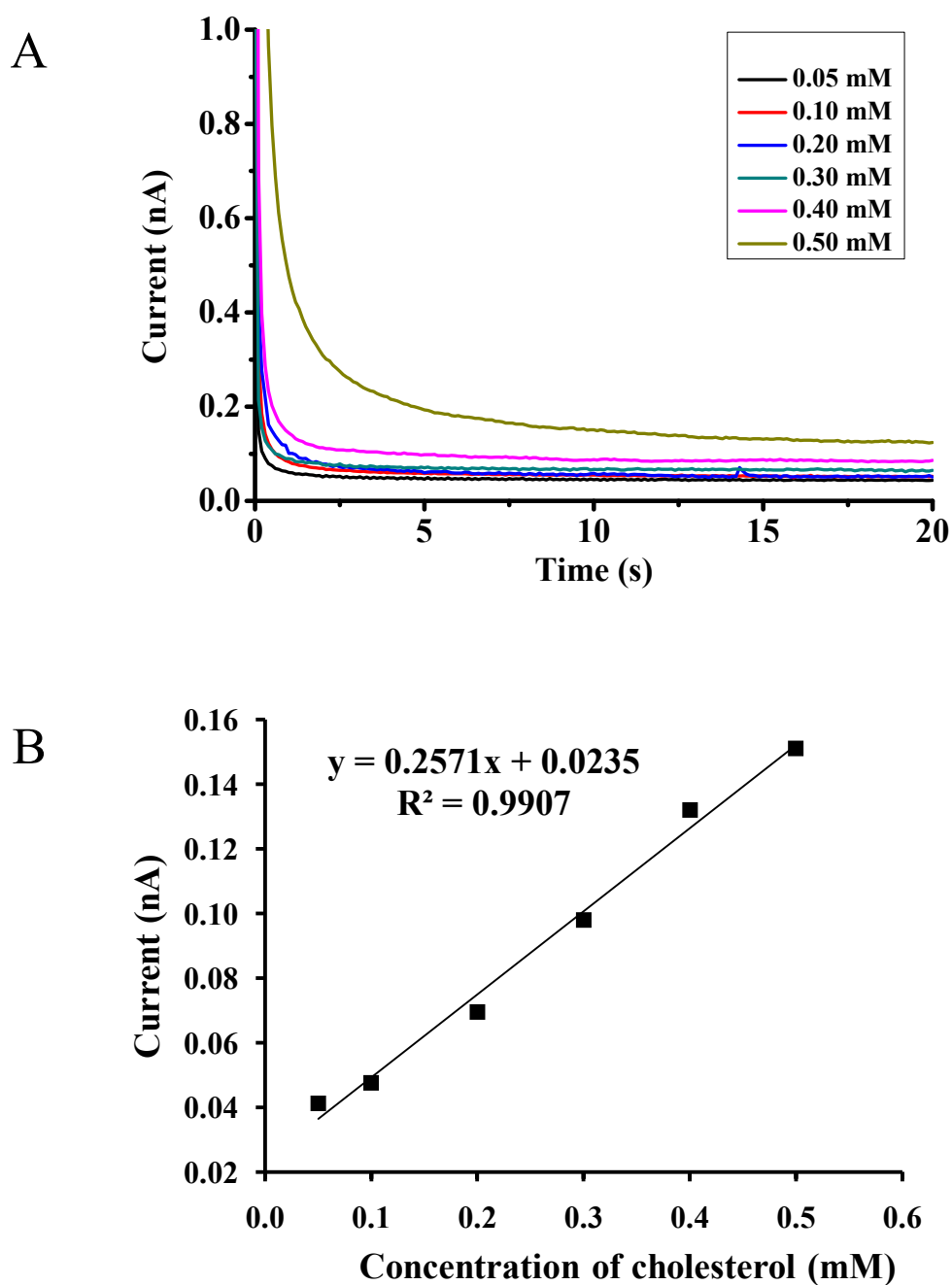
Figure 4.8 Chronoamperometric signals (A) and calibration curve (B) of cholesterol at concentration 0.05, 0.1, 0.2, 0.3, 0.4, and 0.5 mM in 0.05 M phosphate buffer solution, pH 7.4 at AuNPs/CF microelectrode.

The calibration curve of cholesterol for the range from 0.05 to 0.5 mM in 0.05 M phosphate buffer solution was obtained as shown in the figure 4.8B. The linear regression analysis yielded a R^2 value of 0.9907. The detection limit was obtained as 10 μM based on the criterion of a signal to background ratio of 3.

4.2 Electrochemical detection of cholesterol using microbiosensor

In this research, the cholesterol microbiosensor was prepared by electrodepositing AuNPs on the surface of platinum (Pt) microelectrode. ChOx was covalently immobilized on the AuNPs/Pt microelectrode surface using EDC/NHS crosslinker. The preparation of microbiosensor were studied in this section.

4.2.1 Electrochemical behavior of the platinum microelectrode

To study the electrochemical behavior of the microelectrode, cyclic voltammograms of $K_4[Fe(CN)_6]$ in 0.1 M phosphate buffer solution using Pt microelectrode were observed when compared to those at Pt macroelectrode, as shown in figure 4.9 and 4.10. The sensitivity of microelectrode (25 μm diameter) and macroelectrode (3 mm diameter) were calculated from the current density. It was found that the sensitivity of microelectrode (7.8 nA mM^{-1} μm^{-2}) was higher than the sensitivity of macroelectrode (0.9 nA mM^{-1} μm^{-2}).
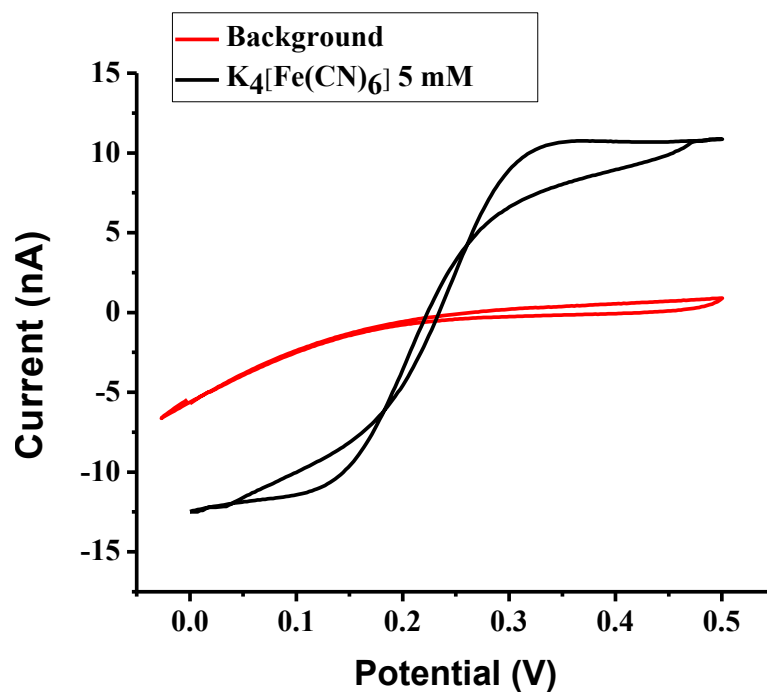
Figure 4.9 Cyclic voltammograms of 5 mM of $K_4[Fe(CN)_6]$ in 0.1 M phosphate buffer solution at the Pt microelectrode.
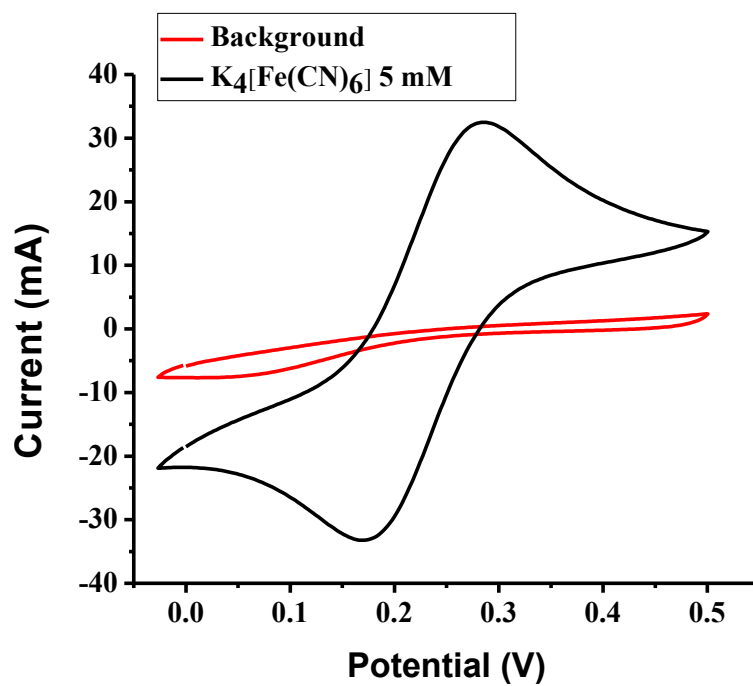
Figure 4.10 Cyclic voltammograms of 5 mM of $K_4[Fe(CN)_6]$ in 0.1 M phosphate buffer solution at the Pt macroelectrode.

4.2.2 Characterization of AuNPs on the platinum microelectrode

To investigate the AuNPs on the surface of Pt microelectrode, SEM was used for characterization. The SEM images of the microelectrode surface before and after electrodeposition of AuNPs are shown in figure 4.11. From the comparison between SEM images of a bare Pt microelectrode and that of AuNPs/Pt microelectrode, the results indicated that AuNPs were electrochemically deposited on the surface of Pt microelectrode. From SEM image, the electrodeposited AuNPs were well distributed on the surface with an average diameter in the range of 200 – 500 nm.
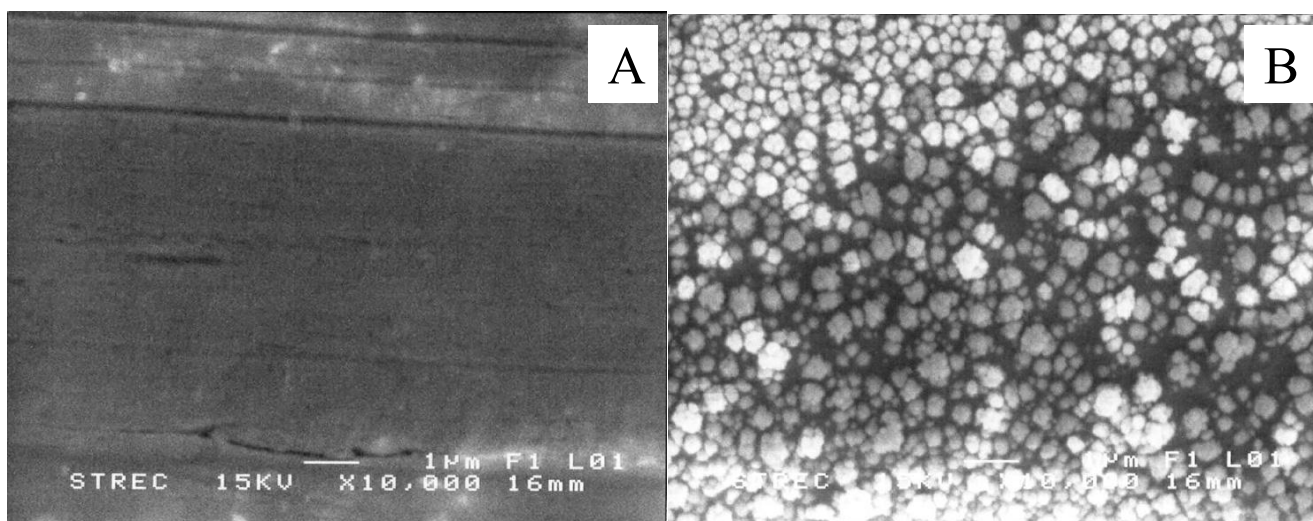
Figure 4.11 Scanning microscope images of the surface of platinum microelectrode before (A) and after the electrodeposited AuNPs (B).

As shown in figure 4.12, cyclic voltammograms Pt microelectrode and AuNPs/Pt microelectrode were investigated. It can be seen from voltammograms that AuNPs were electrochemically deposited on the microelectrode surface. The results of SEM images and cyclic voltammograms indicated that AuNPs were deposited on the microelectrode surface.
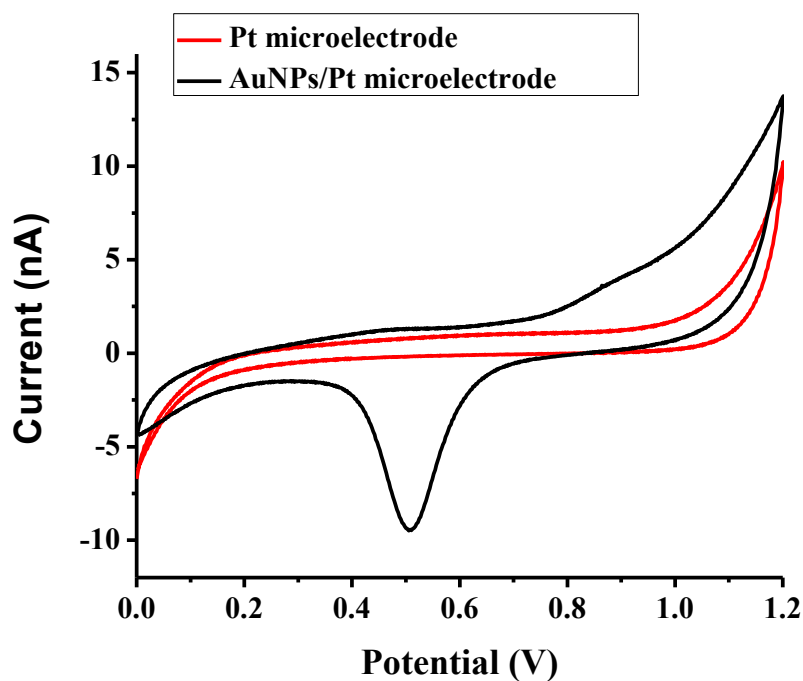
Figure 4.12 Cyclic voltammograms of 0.05 M phosphate buffer solution at a bare Pt microelectrode and an AuNPs/Pt microelectrode.

4.2.3 Optimization of immobilization conditions

In this research, the immobilization of ChOx on the surface of AuNPs/Pt microelectrode was schematically summarized in figure 4.13.

For the immobilization, microbiosensor was fabricated by immersing the microelectrode into an L-cysteine solution. The activated AuNPs/Pt microelectrode was rinse with Milli-Q water and was immersed in the mixture solution of EDC/NHS. Finally, the modified microelectrode was rinsed with Milli-Q water and was immersed in ChOx. The optimal condition was investigated in this part.
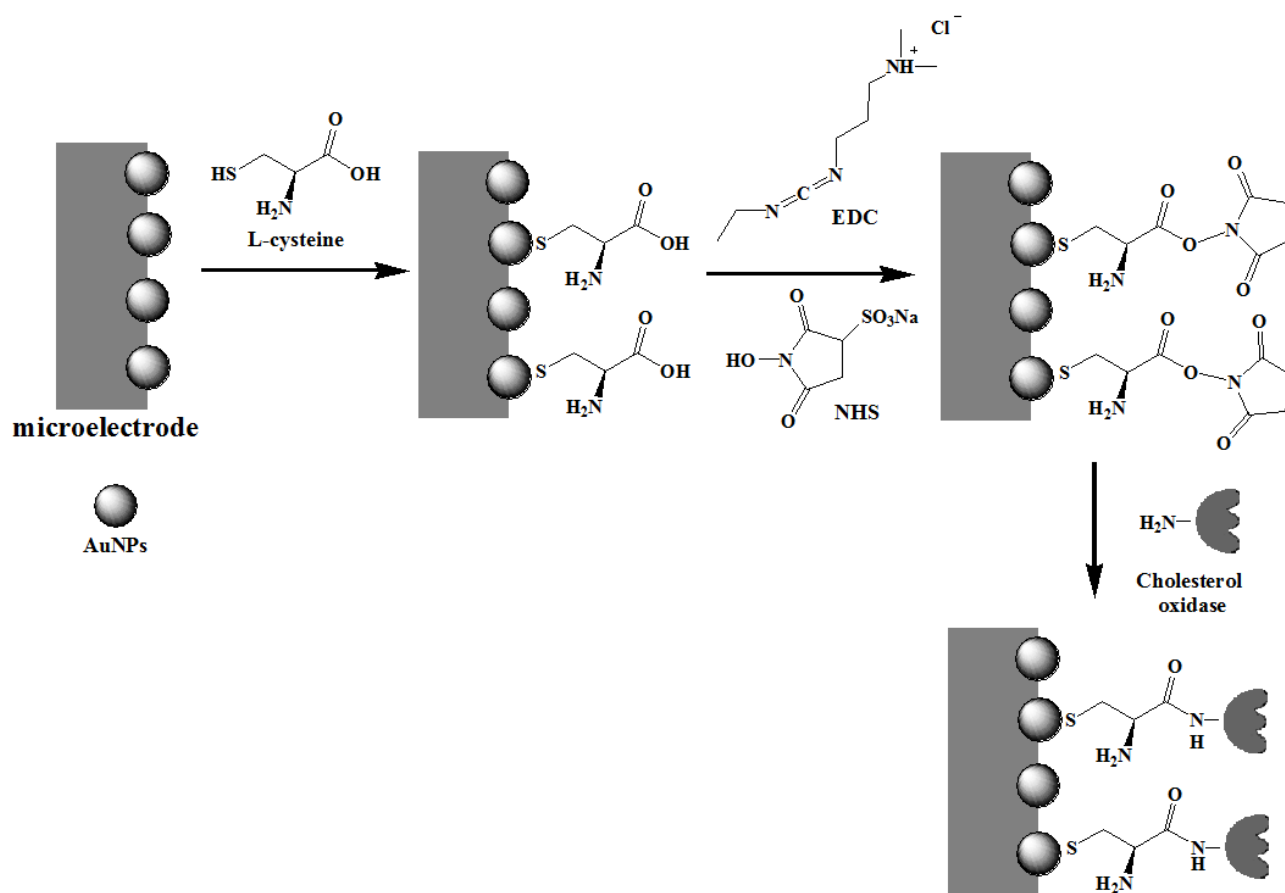
Figure 4.13 Schematic presentation of the immobilization of ChOx using EDC/NHS crosslinker.

4.2.3.1 The effect of incubation time for L-cysteine

In the first step of immobilization, the AuNPs/Pt microelectrode was immersed in 10 mM L-cysteine solution. L-cysteine contains a functional thiol group and this thiol group is easily adsorbed onto the AuNPs surface on Pt microelectrode. The incubation time of L-cysteine was investigated. It can be seen from figure 4.14 that the incubation time of 6 and 12 hours shows a high S/B ratio. To reduce immobilization time of L-cysteine, the incubation time of 6 hours was chosen.
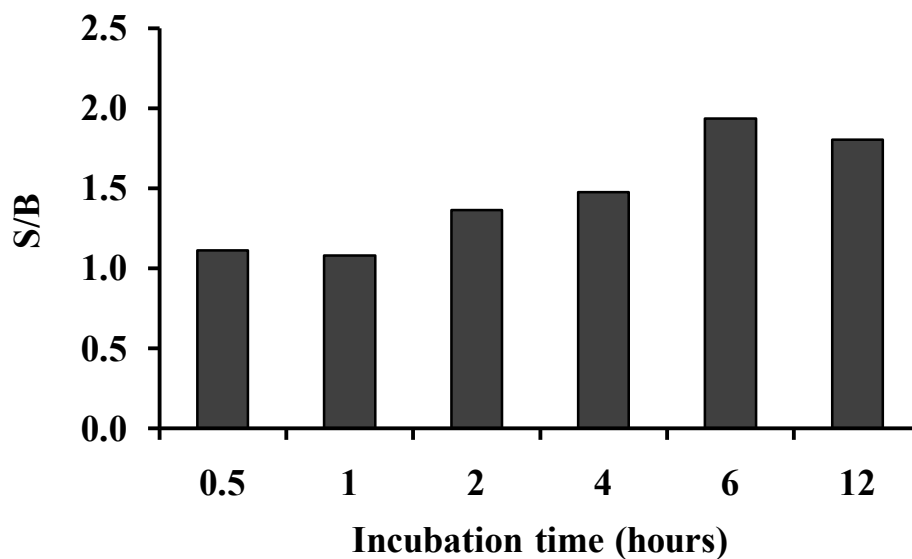
Figure 4.14 Schematic presentation of the effect of incubation time for L-cysteine.

4.2.3.2   The effect of incubation time for EDC/NHS

In this research, EDC/NHS was used as crosslinker for the immobilization of ChOx.   The carboxyl group of L-cysteine are reacted with EDC in the presence of NHS to obtain a semistable amine reactive NHS-ester. Therefore, the modified microelectrode was immersed in solution containing 50 mM of EDC and 20 mM of NHS.
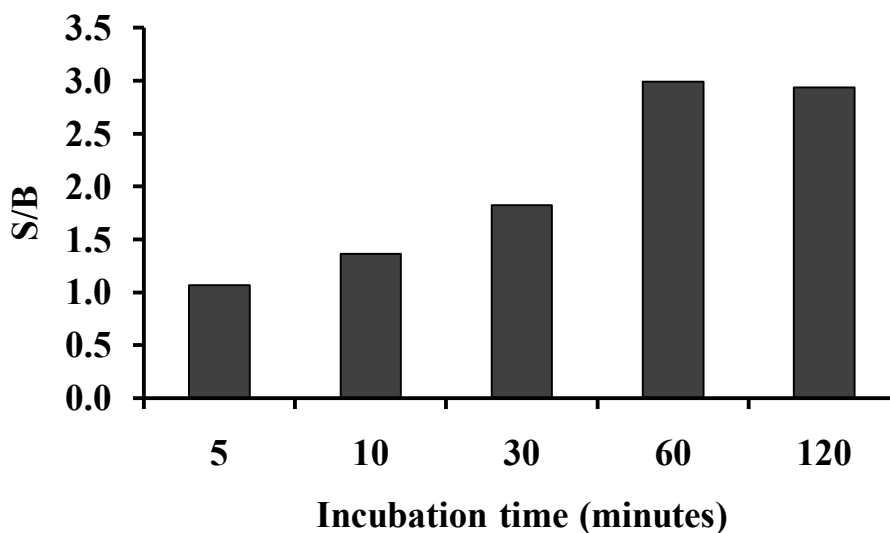
Figure 4.15 Schematic presentation of the effect of incubation time for EDC/NHS.

As shown in figure 4.15, the results indicated that 60 and 120 minutes of the incubation time for EDC/NHS show a high S/B ratio. For short immobilization time, the incubation time of 60 minutes was chosen in this step.

4.2.3.3 The effect of incubation time for cholesterol oxidase

For binding of ChOx onto the modified microelectrode, the last step of the immobilization was carried out using a 39 unit mL^{-1} of ChOx in 0.05 M phosphate buffer solution. ChOx was covalently conjugated to microelectrode using EDC/NHS crosslinker.
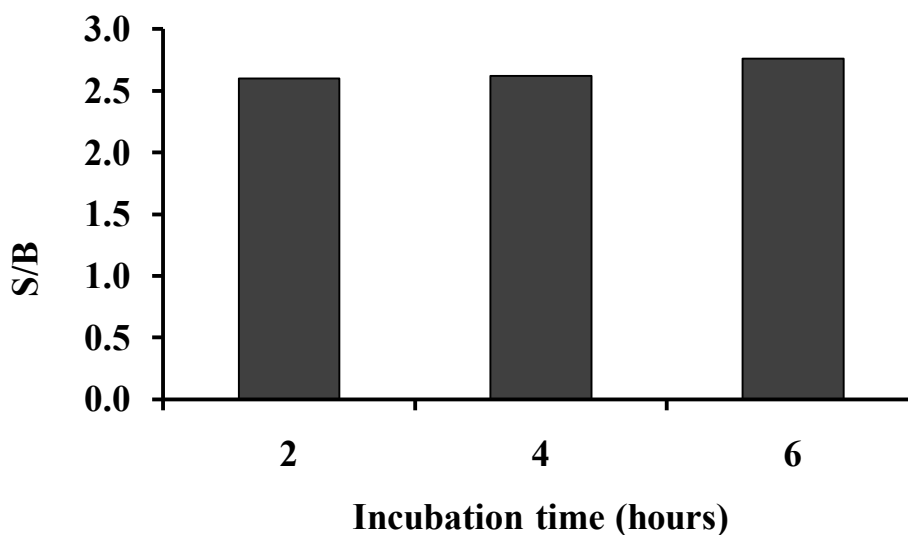
Figure 4.16 Schematic presentation of the effect of incubation time for cholesterol oxidase.

As shown in figure 4.16, it was found that the selected incubation time at 2 hours for immobilization of ChOx is the most suitable. Compared to the incubation times of 4 and 6 hours, the S/B ratios were slightly increased. Therefore, the incubation time of 2 hours was selected for the optimum immobilization time.

4.2.4 Electrochemical detection of cholesterol

4.2.4.1 The effect of the detection potential

The detection potential is important for selectivity and sensitivity of microbiosensor. For electrochemical detection of microbiosensor, the detection potential was investigated using chronoamperometry. To optimize the detection potential, 1 mM of H_2O_2 was examined in the range of 0.3 to 1.0 V. The results indicated that the chronoamperometric response of H_2O_2 increased as the detection potential increased. Nevertheless, the background response also increased when the detection potential increased. Therefore, the S/B ratios of chronoamperometric response between H_2O_2 and background were considered.

As shown in figure 4.17, the S/B ratio of detection potential of 0.4 V is higher than other S/B ratios. Therefore, the potential of 0.4 V was chosen as the detection potential in this work.
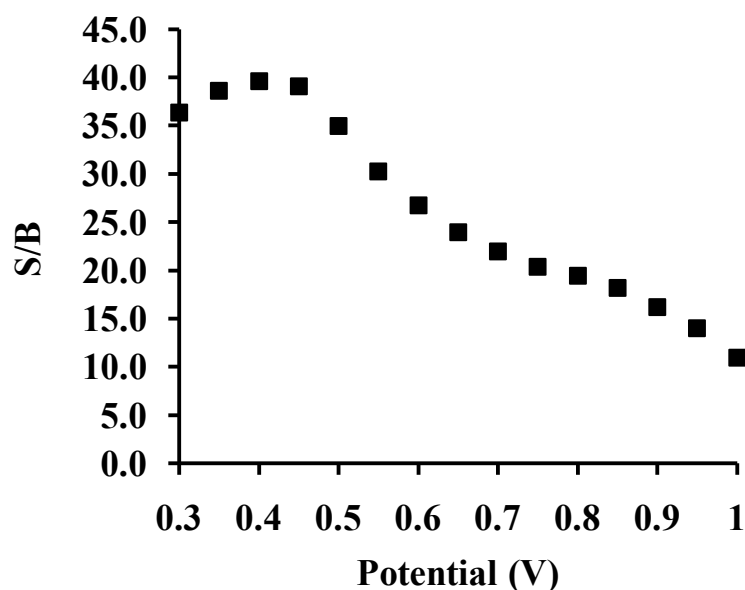
Figure 4.17 Schematic presentation of the effect of detection potential for microbiosensor.

4.2.4.2 The calibration curve of cholesterol using microbiosensor

For the detection of cholesterol using microbiosensor, the relationship between current (nA) and time (seconds) at the various concentrations of chlolesterol was obtained by chronoamperometry, as shown in figure 4.18. The concentration of cholesterol was studied in the range of 0.001 to 7 mM in 0.1 M phosphate buffer solution, pH 7.4. The results indicated the chronoamperometric response is proportional to the concentration of cholesterol.
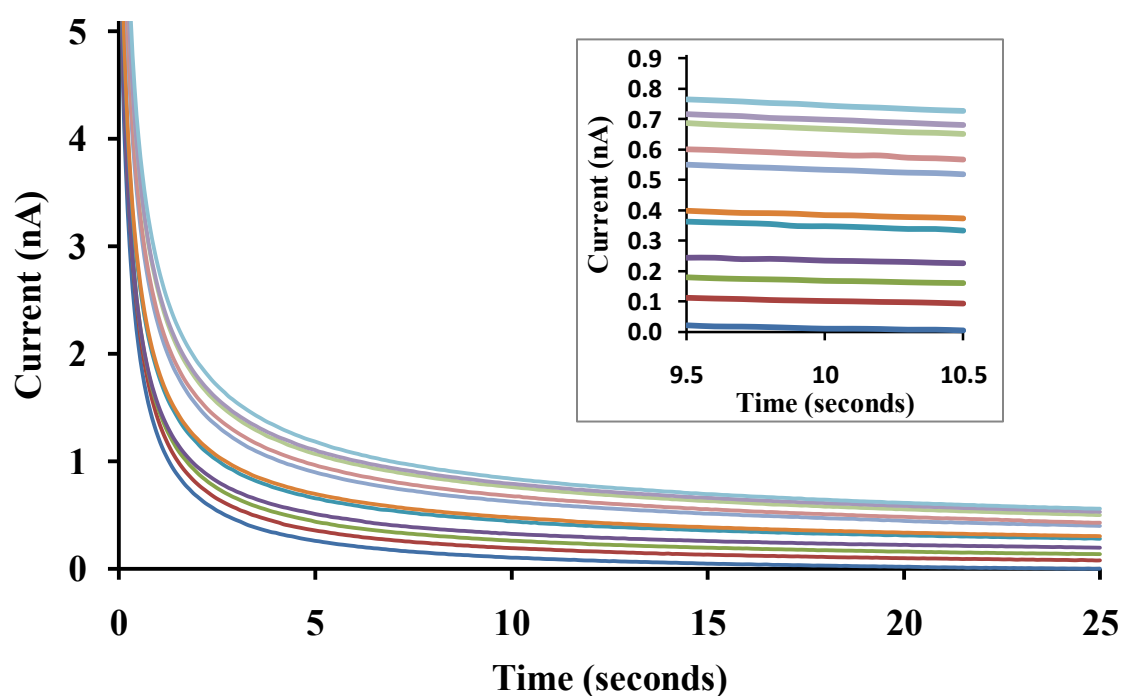
Figure 4.18 Chronoamperometric signals of cholesterol at concentration 0, 0.001, 0.005, 0.01, 0.05, 0.1, 0.5, 1, 3, 5, and 7 mM in 0.1 M phosphate buffer solution, pH 7.4 using microbiosensor. The inset is a zoom-in of chronoamperometric signal of cholesterol.

It can be seen from figure 4.19, the chronoamperometric responses linearly increase with the increase of the logarithm of cholesterol concentration in the range of 0.001 to 7 mM, with a correlation coefficient of 0.9943. The detection limit of this method was found to be 0.001 mM.
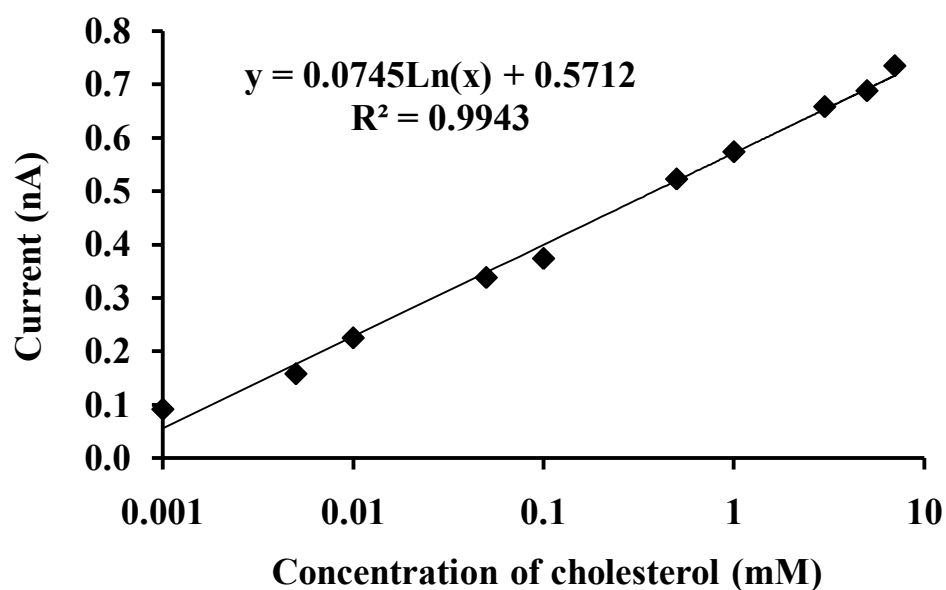
Figure 4.19 Calibration curve of cholesterol at concentration 0.001, 0.005, 0.01, 0.05, 0.1, 0.5, 1, 3, 5, and 7 mM in 0.1 M phosphate buffer solution, pH 7.4 using microbiosensor.

The cholesterol microbiosensor was used to detect 0.5 mM control level of cholesterol in bovine serum sample. The cholesterol serum was found to be 0.59 mM from the calibration curve. To study the precision of the microbiosensor, 0.5 mM control level of cholesterol spiked with 0.5 mM standard cholesterol was determined and then the percentage of relative standard deviation (%RSD) for 1 mM cholesterol was 4.13 (n=6) and the recovery of 92 – 118% were achieved for the microbiosensor.

4.3 Electrochemical immunoassay using QD labels for the detection of phosphorylated bovine serum albumin

4.3.1 Characterization of QD-anti-phosphoserine

In this research, the synthesis of QD-anti-phosphoserine conjugates was schematically summarized in figure 4.20.
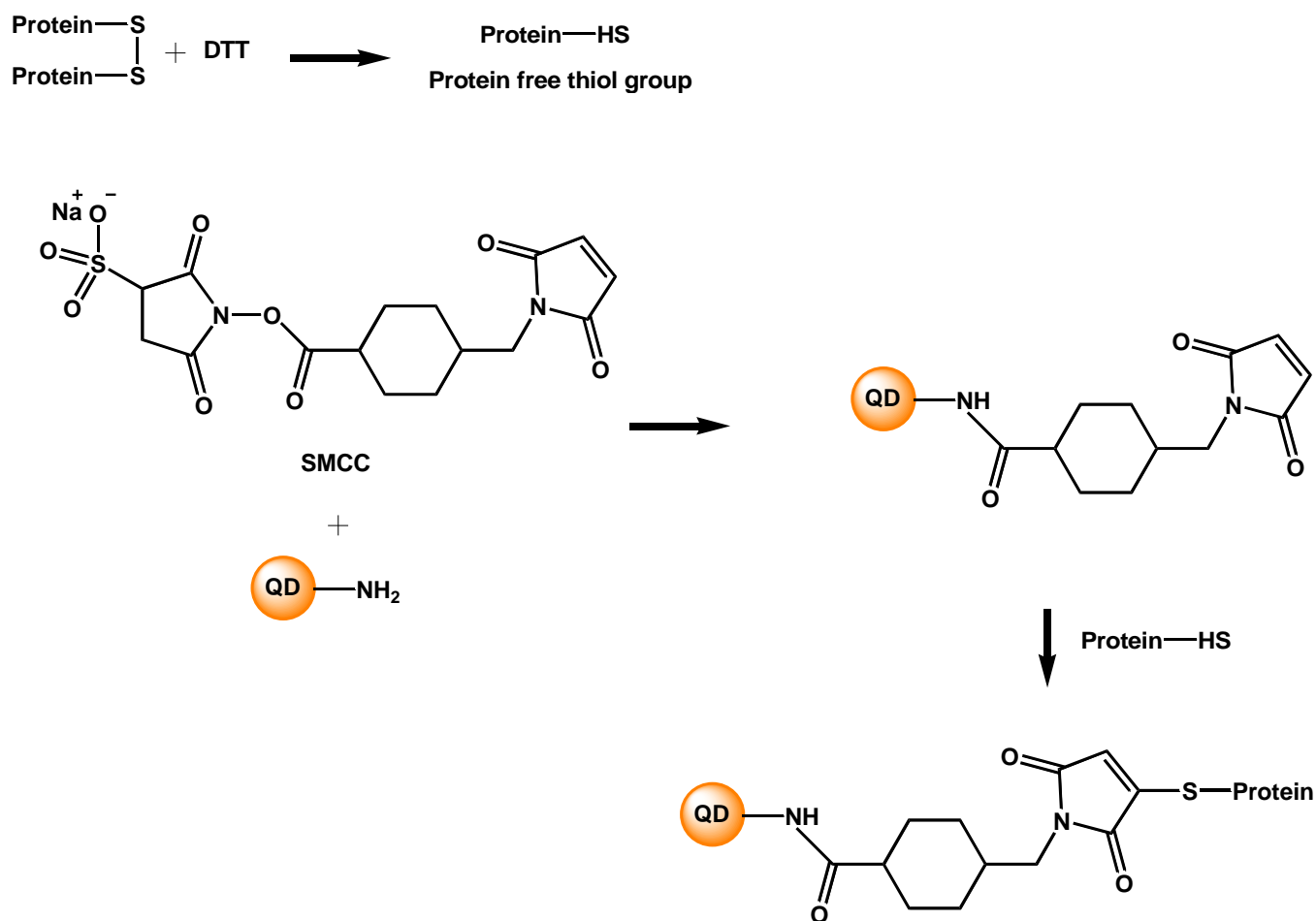
Figure 4.20 Schematic illustration of the synthetic procedure for preparation of the QD-anti-phosphoserine conjugates.

To facilitate the conjugation with biological molecules, the QD was coated with a polymer shell. The QD-anti-phosphoserine conjugates were characterized by transmission electron microscopy (TEM). As shown in figure 4.21, TEM image shows that the QD-anti-phosphoserine conjugates are uniform in size, without aggregation, and have an average diameter of approximately 10 nm, which is similar to other reports (Wang et al. 2008b; Wu et al. 2007).
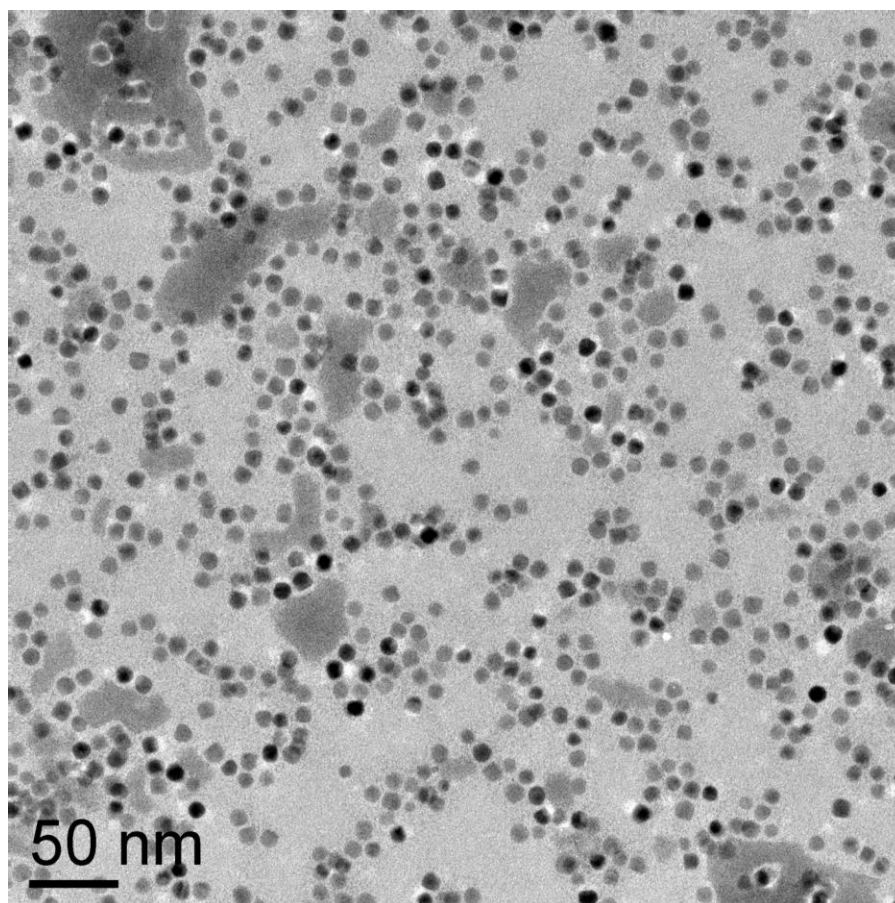
Figure 4.21 Transmission electron microscope image of the QD-anti-phosphoserine conjugates.

4.3.2   Square wave anodic stripping voltammetric analysis of cadmium

This technique consists of two steps.   First, cadmium ions are deposited onto an electrode, which is held at a suitable potential.

$$Cd^{2+} + 2e^- \rightarrow Cd°$$
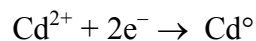
Second, cadmium deposits are stripped from the electrode by scanning the potential.

$$Cd° \rightarrow Cd^{2+} + 2e^-$$

Consequently, the deposition potential and time are two important parameters in the anodic stripping voltammetric determination of cadmium.

4.3.2.1   Effect of the deposition potential

To study the condition of square wave anodic stripping voltammetric analysis of cadmium, the influence of the variation of the deposition potential was examined in the range of -1.0 to -1.4 V, as shown in figure 4.22.   The results indicated that the current of the cadmium increased as the deposition potential increased.   However, the background current also increased when the deposition potential increased.

Therefore, the ratios between the current of cadmium and background (S/B) were considered.   The deposition potential of -1.2 V was selected, as shown in figure 4.23.
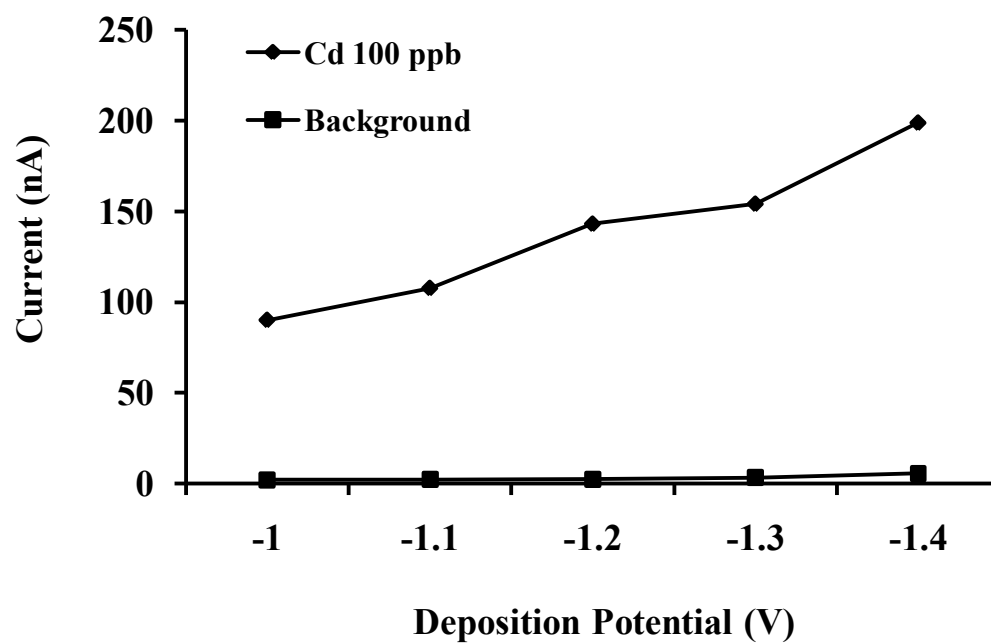
Figure 4.22 The effect of the varying deposition potential in the range of -1.0 to -1.4 V on the deposition step of 100 ppb of cadmium (II) and background.
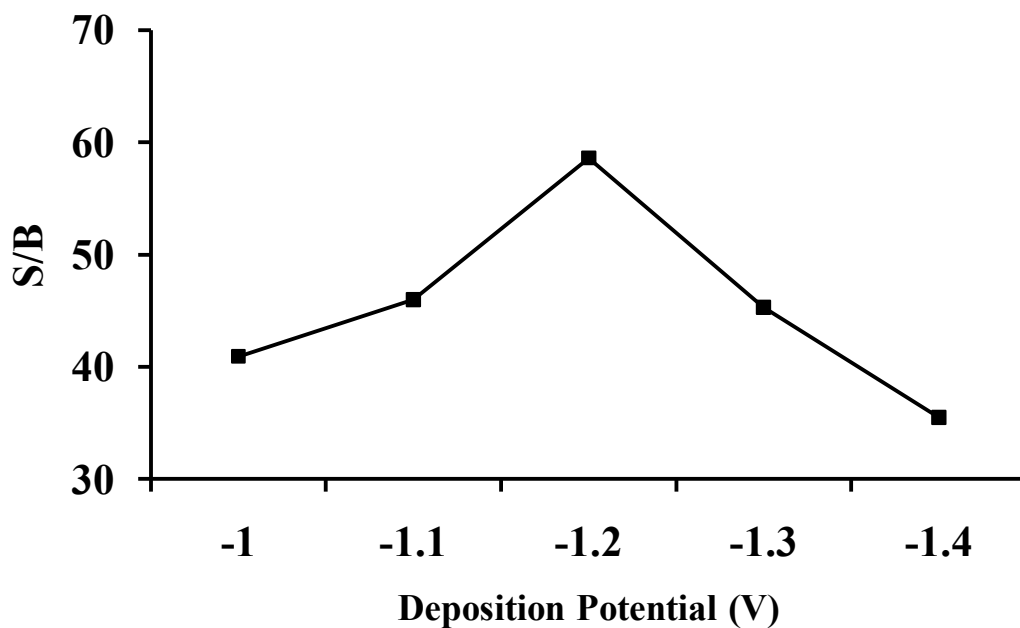
Figure 4.23 The effect of varying deposition potential on the signal to background ratio between the current of 100 ppb of cadmium (II) and background.

4.3.2.2   Effect of the deposition time

To obtain the high sensitivity of electrochemical detection, the deposition time was investigated in the range of 0.5 to 3 minutes. The signal to background ratio between the current of 100 ppb of cadmium (II) and background is shown in figure 4.24. The ratio between cadmium and background current for 2 and 3 minutes shows a high S/B ratio. However, the deposition time at 3 minutes showed a larger error bar than the deposition time at 2 minutes. For fast detection, the deposition time at 2 minutes was used as an optimal deposition time.
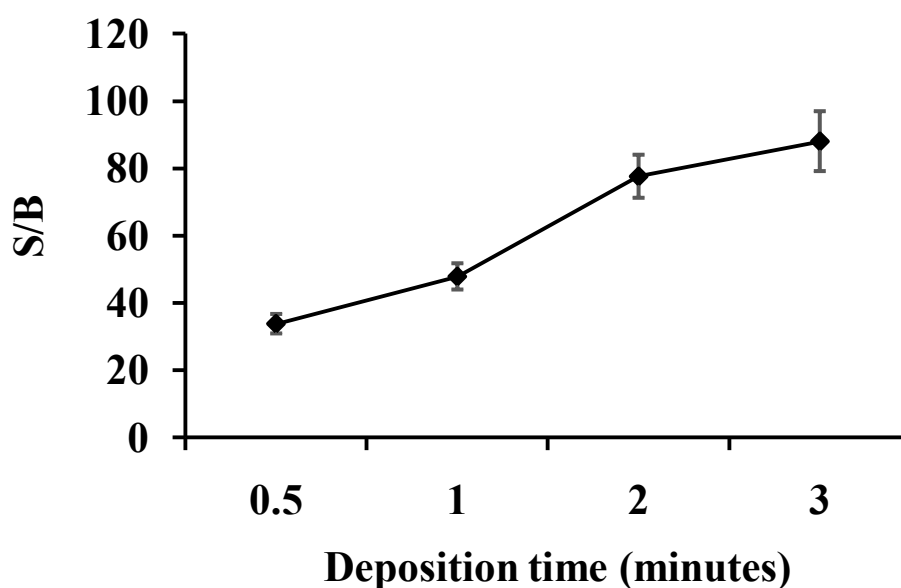
Figure 4.24 The effect of varying accumulation time in the range of 0.5 to 3 minutes on the deposition step of 100 ppb of cadmium (II) and background.

4.3.2.3 The calibration curve of cadmium by square wave anodic stripping voltammetry

The analytical performance of cadmium was investigated under the optimal deposition potential and time. The calibration curve was obtained with a SPE by adding cadmium standard solution to the supporting electrolyte. As shown in figure 4.25, a linear calibration curve between concentration of cadmium and the current was obtained over 0.1 to 1,000 ppb. The calibration curve shows a good linearity, with a correlation coefficient of 0.9997.
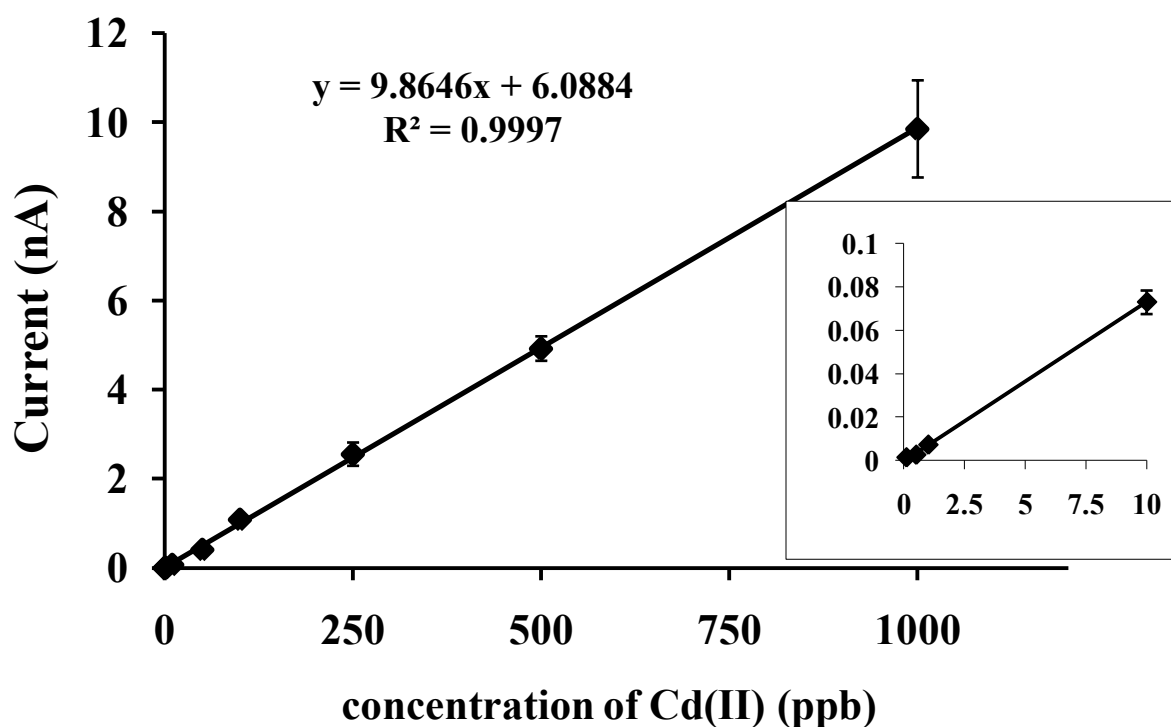
Figure 4.25 The plot of peak current versus the concentration of cadmium (II) in the range of 0.1 to 1,000 ppb.

4.3.3 Immunoassay procedure

Firstly, BSA-OP was captured with the primary anti-BSA on the well of the microplate and then the QD-anti-phosphoserine conjugates were added to form a sandwich immunoassay. By adding HCl, the QDs were dissolved and cadmium ions were released. These cadmium ions were measured with SWV using an *in situ* plated mercury film on the SPE. The concentration of cadmium ions was directly proportional to the amount of BSA-OP. It was found that both the stripping peak potential of standard cadmium ions and those obtained from the dissolved QDs were both at -0.75 V.

The specificity of the QD-anti-phosphoserine conjugates to BSA-OP was tested with the presence and absence of BSA-OP. It can be seen from figure 4.26 that the SWV response from BSA-OP is much higher than that from the control (without BSA-OP), indicating a pair of antibodies are specific to BSA-OP. However a high signal was observed in the control sample (figure 4.26), indicating that there was some non-specific adsorption of the QD-anti-phosphoserine conjugates.
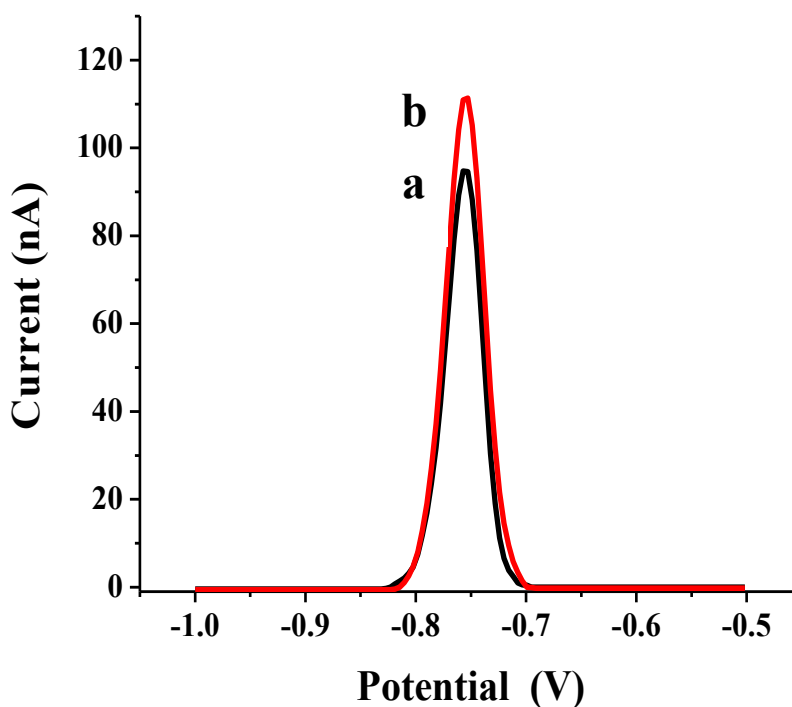
Figure 4.26 Square wave voltammograms of (a) 0 ng mL^{-1} BSA-OP and (b) 10 ng mL^{-1} BSA-OP.

For immunoassay procedure, any non-specific binding of the QD-anti-phosphoserine conjugates to the solid surface of 96-well microplate was an important factor, as shown in figure 4.27. The blocking buffer can protect the surface of microplate from any non-specific binding of QD-anti-phosphoserine conjugates.
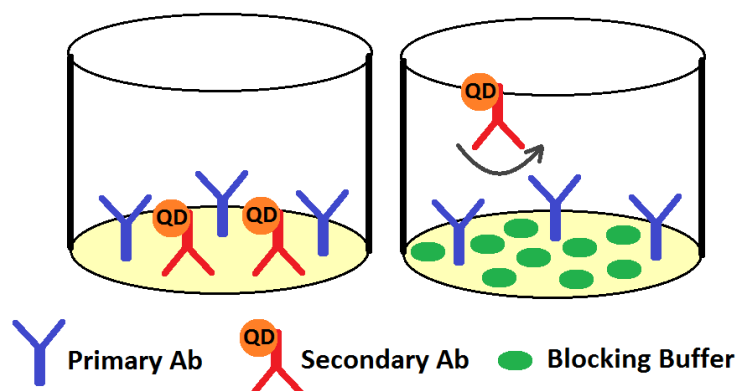
Figure 4.27 Schematic illustrations of the effect of blocking buffer.

4.3.3.1 The effect of the blocking buffer

To reduce the non-specific adsorption of the QD-anti-phosphoserine conjugates, the percentage of blocking buffers was investigated.
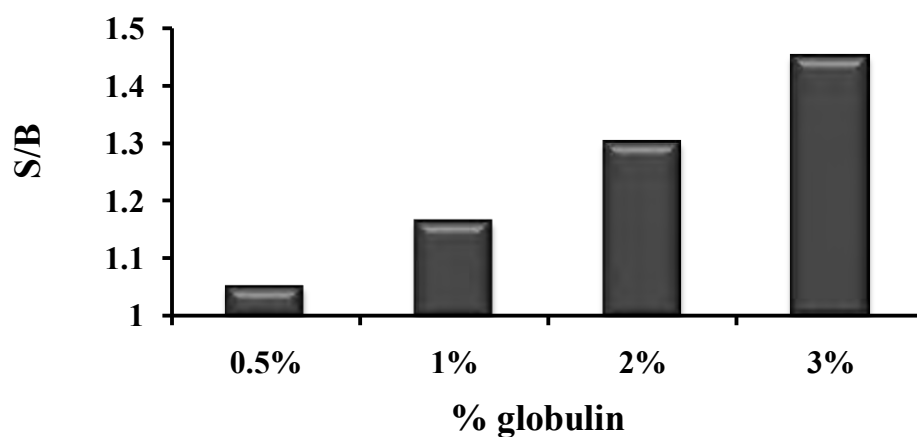
Figure 4.28 Schematic illustrations of the effect of blocking buffers on signal to background ratio between the current of 10 ng mL^{-1} BSA-OP and 0 ng mL^{-1} BSA-OP (control).

The variation of the percentage of globulin from 0.5 to 3% (w/v) in the presence of 0.01 M PBS was investigated. It can be seen from figure 4.28 that 3% globulin provides the best signal to background ratio and for 4% globulin in PBS, it could not be dissolved. Therefore, 3% globulin in PBS was chosen for a blocking buffer in the assay.

4.3.3.2 The effect of the additive reagent in blocking buffer

To further reduce the non-specific adsorption of the conjugates, different kinds of additive in blocking buffer were considered, as shown in figure 4.29. It was found that 1% (w/v) PEG as well as 3% (w/v) globulin added blocking buffer can lower background and achieve higher signal to background ratio (~1.72).
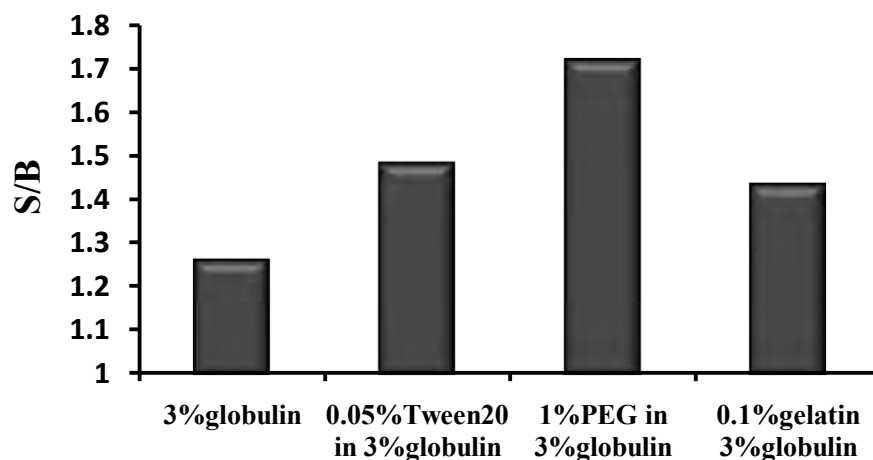
Figure 4.29 Schematic illustrations of the additive effect in blocking buffer on signal to background ratio between the current of 10 ng mL^{-1} BSA-OP and 0 ng mL^{-1} BSA-OP (control).

Moreover, the effect of changing the concentration of PEG from 0.5 to 3% (w/v) in the co-presence of 3% (w/v) globulin in PBS was studied and it can be seen from figure 4.30 that 2% (w/v) PEG works best in term of the blocking efficiency of the blocking buffer for this assay.
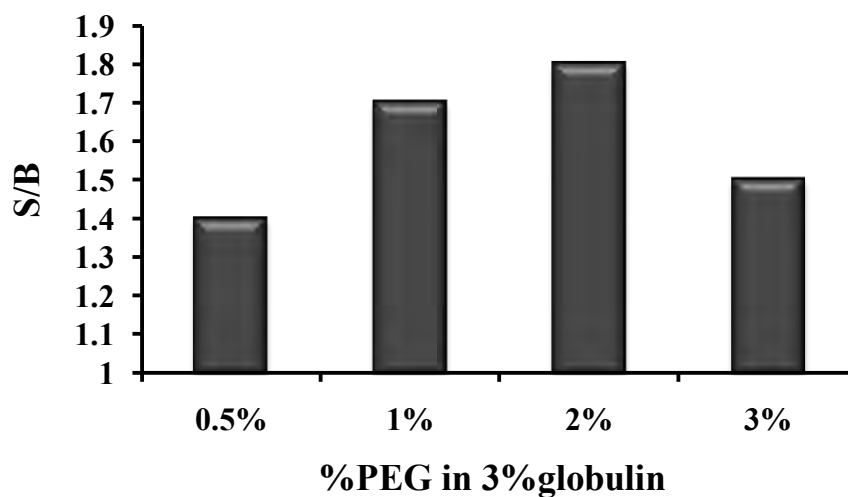
Figure 4.30 Schematic illustrations of the effect of additive percentage in blocking buffer on signal to background ratio between the current of 10 ng mL^{-1} BSA-OP and 0 ng mL^{-1} BSA-OP (control).

4.3.3.3   The effect of the blocking buffer for QD-anti-phosphoserine conjugates

For the blocking buffer of QD-anti-phosphoserine conjugates, the different percentages of globulin were investigated to dilute the conjugates, as shown in figure 4.31.
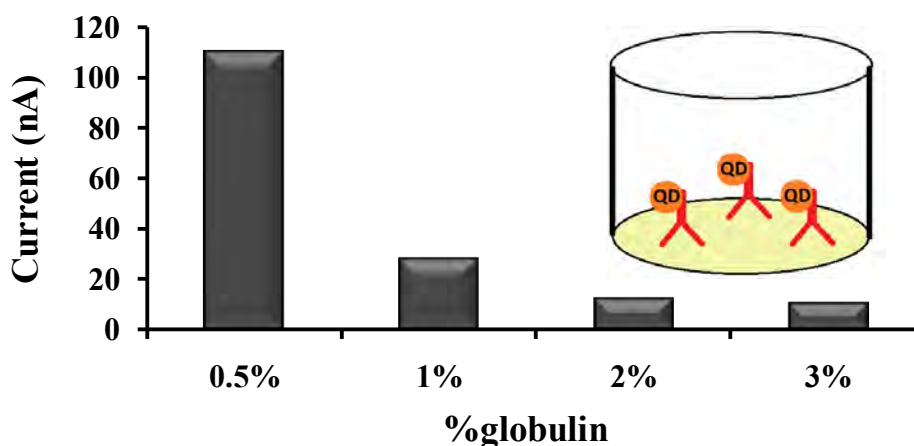
Figure 4.31 Schematic illustrations of the effect of blocking buffer for QD-anti-phosphoserine conjugates.

It was found that 3% globulin in PBS was chosen as a diluted solution to reduce any non-specific binding of the QD-anti-phosphoserine conjugates to the solid surface of microplate.

4.3.4 The calibration curve of BSA-OP using electrochemical immunoassay

Under these optimal conditions, the proposed method was used to detect BSA-OP based on the QD labels. As shown in figure 4.32, the square wave voltammogram (SWV) responses increased when the BSA-OP concentration was increased from 0.5 to 500 ng mL^{-1}. It can be seen that the SWV response in the absence of BSA-OP (curve a) was lower than that in the presence of 0.5 ng mL^{-1} BSA-OP (curve b), attributing to excellent blocking and washing of the assay.
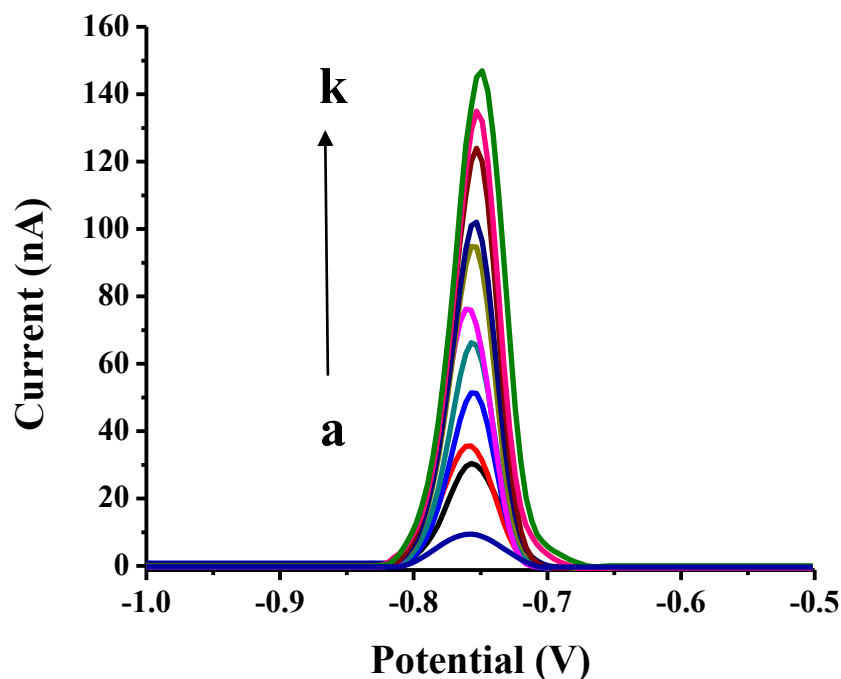
Figure 4.32 Square wave voltammograms acquired in 0, 0.5, 1, 2.5, 5, 10, 25, 50, 100, 250, and 500 ng mL^{-1} of BSA-OP (a-k, respectively) using the assay method under optimal conditions.

As shown in figure 4.33, the SWV responses linearly increase with the increase of the logarithm of BSA-OP concentration in the range of 0.5 to 500 ng mL^{-1}, with a correlation coefficient of 0.9961 (n = 3). The detection limit of this method was estimated to be 0.5 ng mL^{-1} (about 7.8 pM). To test the reproducibility of the method, a series of six wells repetitive measurements of 25 ng mL^{-1} BSA-OP was investigated and yielded reproducible electrochemical signals with a relative standard deviation of 8.6%.
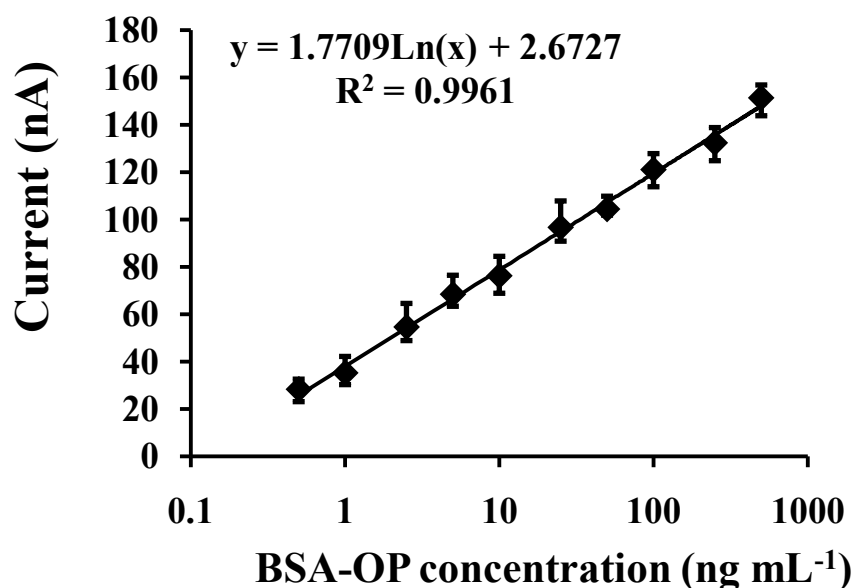
Figure 4.33 A plot of the peak current versus the logarithm of 0.5, 1, 2.5, 5, 10, 25, 50, 100, 250, and 500 ng mL^{-1} BSA-OP.

4.3.5 The selectivity of electrochemical immunoassay

The selectivity of the assay to BSA-OP is examined with the presence and absence of BSA-OP (figure 4.34). The results showed that the SWV response from BSA-OP is highest amongst BSA, AChE-OP, and BChE-OP, indicating the assay is specific to BSA-OP. The results demonstrated the good selectivity of this immunoassay.
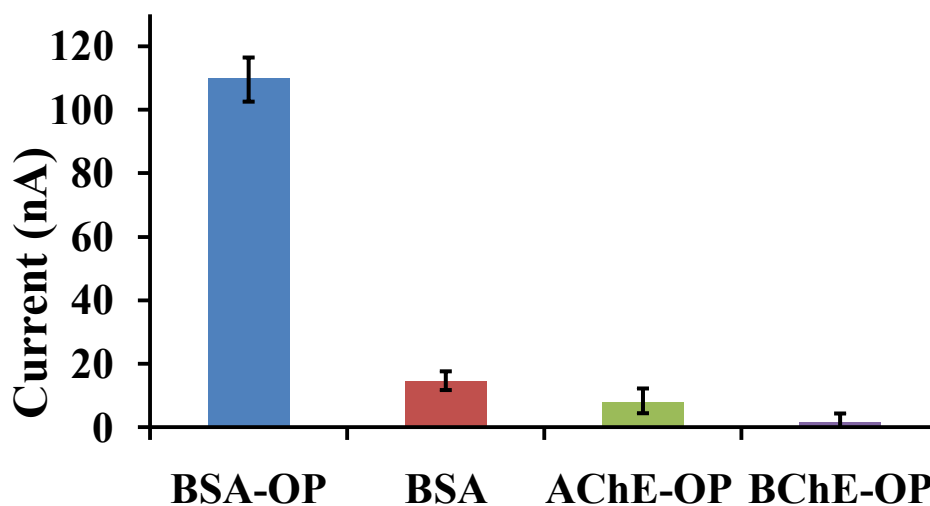
Figure 4.34 The electrochemical response of the assays in different protein solutions including BSA-OP, BSA, AChE-OP, and BChE-OP. The concentration of the four different proteins is 100 ng mL^{-1}.

4.3.6 Comparison with other method

Further comparison of this method with the conventional enzyme-linked immunosorbent assay (ELISA) using horseradish peroxidase (HRP)-anti-phosphoserine conjugates for analysis of BSA-OP was investigated, as shown in figure 4.35. The results demonstrated that the electrochemical immunoassay showed a lower detection limit compared with ELISA.
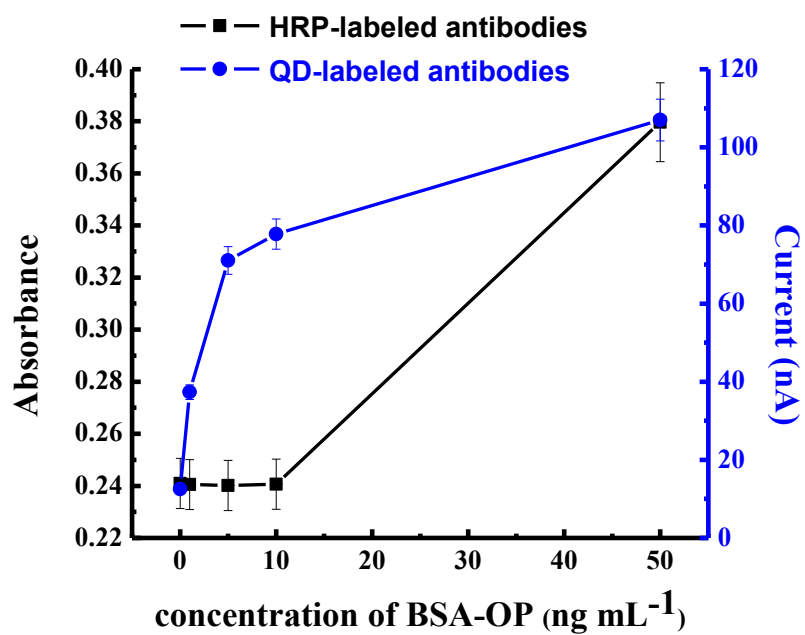
Figure 4.35 Comparison between the electrochemical immunoassay using QD labeled anti-phosphoserine conjugates and the conventional enzyme-linked immunosorbent assay (ELISA) using HRP labeled anti-phosphoserine.

CHAPTER V

CONCLUSIONS AND FUTURE PERSPECTIVE

5.1   Conclusions

In this work, microelectrodes were fabricated from carbon fiber (diameter of 7 μm) and platinum wire (diameter of 25 μm) for the determination of cholesterol. A highly sensitive cholesterol sensor was successfully fabricated by modifying a microelectrode with electrodeposited AuNPs and the modified electrode surface was characterized by SEM and cyclic voltammetry. For microsensor, the AuNPs/CF microelectrode showed effective catalytic activity towards the oxidation of H_2O_2. Comparison results were performed by using AuNPs/CF microelectrode and CF microelectrode for detection of H_2O_2. It was found that AuNPs/CF microelectrode provided the lower detection potential than bare CF microelectrode. The cholesterol was detected through the enzymatically generated H_2O_2. Chronoamperometric measurements of cholesterol showed the linear response in the range of $50 - 500$ μM with the detection limit of 10 μM. The current response of microsensor was very rapid (response time was 10 s). For microbiosensor, the AuNPs/Pt microelectrode was utilized for covalent immobilization of cholesterol oxidase using EDC/NHS as crosslinker.   The microbiosensor exhibited linearly over 0.001 to 7 mM of cholesterol with response time of 10 s. In addition, the microbiosensor was applied to measure cholesterol in a real sample of bovine serum.

For electrochemical immunoassay, this work demonstrated good performance using QD labels for the determination of BSA-OP, as a model analyte. To increase the analytical sensitivity of the assay, QD labels were conjugated to the secondary anti-phosphoserine antibody in a sandwich immunoassay format. Under optimal conditions, the obtained detection limit of the assay was 7.8 pM using a 60-min immunoreaction time. A comparison between the conventional enzyme-linked immunosorbent assay (ELISA) using horseradish peroxidase (HRP)-anti-phosphoserine conjugates and QD

labels-based electrochemical immunoassay for analysis of BSA-OP, the results indicated that the detection limit of this proposed method is lower than the conventional method. The proposed method provides a simple, sensitive, and reproducible assay for phosphorylated protein.

5.2   Future perspective

In the future, this microbiosensor can be applied for *in vivo* determination with a fast analysis.   Futhermore, microsensor and microbiosensor can be easily extended to other biomarkers.   For electrochemical immunoassay, this work may be extended to the simultaneous detection of multiple biomarkers using different QD labels, such as CdS, ZnS, and PbS.

REFERENCES

[1]   Kumar, A., R.R. Pandey, and Brantley, B. Tetraethylorthosilicate film modified with protein to fabricate cholesterol biosensor. *Talanta*, 69, (2006): 700-705.

[2]   Li, G., et al. Study of carbon nanotube modified biosensor for monitoring total cholesterol in blood. *Biosensors and Bioelectronics*, 20, (2005): 2140-2144.

[3]   Hooda, V., et al. Biosensor based on enzyme coupled PVC reaction cell for electrochemical measurement of serum total cholesterol. *Sensors and Actuators B: Chemical*, 136, (2009): 235-241.

[4]   Pemberton, R.M., et al. A screen-printed microband glucose biosensor system for real-time monitoring of toxicity in cell culture. *Biosensors and Bioelectronics*, 26, (2011): 2448-2453.

[5]   Salazar, P., et al. Prussian Blue-modified microelectrodes for selective transduction in enzyme-based amperometric microbiosensors for in vivo neurochemical monitoring. *Electrochimica Acta*, 55, (2010): 6476-6484.

[6]   Biloivan, O.A., et al. Protein detection based on microelectrodes with the PPy[3,3-Co(1,2-C2B9H11)]2 solid contact and immobilized proteinases: Preliminary investigations. *Materials Science and Engineering: C*, 26, (2006): 574-577.

[7]   Crumbliss, A.L., et al. A carrageenan hydrogel stabilized colloidal gold multi-
       enzyme biosensor electrode utilizing immobilized horseradish peroxidase
       and cholesterol oxidase/cholesterol esterase to detect cholesterol in serum
       and whole blood. *Biosensors and Bioelectronics*, 8, (1993): 331-337.

[8]   Martin, S.P., et al. Enzyme-based determination of cholesterol using the quartz
       crystal acoustic wave sensor. *Analytica Chimica Acta*, 487, (2003): 91-
       100.

[9]   Chen, X., Hu, Y., and Wilson, G.S. Glucose microbiosensor based on alumina sol-
       gel matrix/electropolymerized composite membrane. *Biosensors and
       Bioelectronics*, 17, (2002): 1005-1013.

[10] Dungchai, W., et al. Salmonella typhi determination using voltammetric
       amplification of nanoparticles: A highly sensitive strategy for
       metalloimmunoassay based on a copper-enhanced gold label. *Talanta*, 77**,
       (**2008): 727-732.

[11] Tang, H., et al. A label-free electrochemical immunoassay for carcinoembryonic
       antigen (CEA) based on gold nanoparticles (AuNPs) and nonconductive
       polymer film. *Biosensors and Bioelectronics*, 22, (2007): 1061-1067.

[12] Prabhakar, N., et al. Polypyrrole-polyvinyl sulphonate film based disposable
       nucleic acid biosensor. *Analytica Chimica Acta*, 589, (2007): 6-13.

[13] Nugen, S.R., et al. PMMA biosensor for nucleic acids with integrated mixer and
       electrochemical detection. *Biosensors and Bioelectronics*, 24, (2009):
       2428-2433.

[14] Prabhakar, N., et al. Improved electrochemical nucleic acid biosensor based on polyaniline-polyvinyl sulphonate. *Electrochimica Acta*, 53, (2008): 4344-4350.

[15] Bentley, A., et al. Whole cell biosensors - electrochemical and optical approaches to ecotoxicity testing. *Toxicology in Vitro.* **15**(4-5): p. 469-475.

[16] Biloivan, O.A., et al. Development of bi-enzyme microbiosensor based on solid-contact ion-selective microelectrodes for protein detection. *Sensors and Actuators B: Chemical*, 123, (2007): 1096-1100.

[17] Arya, S.K., Datta, M., and Malhotra, B.D. Recent advances in cholesterol biosensor. *Biosensors and Bioelectronics*, 23, (2008): 1083-1100.

[18] Arya, S.K., et al. Poly-(3-hexylthiophene) self-assembled monolayer based cholesterol biosensor using surface plasmon resonance technique. *Biosensors and Bioelectronics*, 22, (2007): 2516-2524.

[19] Marazuela, M.D., et al. Free cholesterol fiber-optic biosensor for serum samples with simplex optimization. *Biosensors and Bioelectronics*, 12, (1997): 233-240.

[20] Hnaien, M., et al. Integrity characterization of myoglobin released from poly([epsilon]-caprolactone) microspheres using two analytical methods: UV/Vis spectrometry and conductometric bi-enzymatic biosensor. *European Journal of Pharmaceutics and Biopharmaceutics*. In Press, Corrected Proof.

[21] Thompson, C.S., et al. Effective monitoring for ractopamine residues in samples of animal origin by SPR biosensor and mass spectrometry. *Analytica Chimica Acta*, 608, 2008: 217-225.

[22] Ashwin, H.M., et al. Development and validation of screening and confirmatory methods for the detection of chloramphenicol and chloramphenicol glucuronide using SPR biosensor and liquid chromatography-tandem mass spectrometry. *Analytica Chimica Acta*, 529, (2005): 103-108.

[23] Parra, A., et al. Cholesterol oxidase modified gold electrodes as bioanalytical devices. *Sensors and Actuators B: Chemical*, 124, (2007): 30-37.

[24] Masson, J.F., et al. Improved sensitivity and stability of amperometric enzyme microbiosensors by covalent attachment to gold electrodes. *Biosensors and Bioelectronics*, 23, (2007): 355-361.

[25] Israr, M.Q., et al. Potentiometric cholesterol biosensor based on ZnO nanorods chemically grown on Ag wire. *Thin Solid Films*, 519, (2010): 1106-1109.

[26] Tsai, Y.C., Chen, S.Y., and Lee, C.A. Amperometric cholesterol biosensors based on carbon nanotube-chitosan-platinum-cholesterol oxidase nanobiocomposite. *Sensors and Actuators B: Chemical*, 135, 2008: 96-101.

[27] Salazar, P., et al. Amperometric glucose microbiosensor based on a Prussian Blue modified carbon fiber electrode for physiological applications. *Sensors and Actuators B: Chemical*, 152, (2011): 137-143.

[28] Tang, D., Yuan, R., and Chai, Y. Ultrasensitive Electrochemical Immunosensor for Clinical Immunoassay Using Thionine-Doped Magnetic Gold Nanospheres as Labels and Horseradish Peroxidase as Enhancer. *Analytical Chemistry*, 80, (2008): 1582-1588.

[29] Kuramitz, H., et al. Application of an automated fluidic system using electrochemical bead-based immunoassay to detect the bacteriophage MS2 and ovalbumin. *Analytica Chimica Acta*, 561, (2006): 69-77.

[30] Li, Y., et al. A nonenzymatic cholesterol sensor constructed by using porous tubular silver nanoparticles. *Biosensors and Bioelectronics*, 25, (2010): 2356-2360.

[31] Kerman, K., et al. Gold nanoparticle-based electrochemical detection of protein phosphorylation. *Analytica Chimica Acta*, 588, (2007): 26-33.

[32] Saxena, U., Chakraborty, M., and Goswami, P. Covalent immobilization of cholesterol oxidase on self-assembled gold nanoparticles for highly sensitive amperometric detection of cholesterol in real samples. *Biosensors and Bioelectronics*, 26, (2011): 3037-3043.

[33] Kerman, K., and Kraatz, H.-B. Electrochemical detection of protein tyrosine kinase-catalysed phosphorylation using gold nanoparticles. *Biosensors and Bioelectronics*, 24, (2009): 1484-1489.

[34] Khan, R., et al. Zinc oxide nanoparticles-chitosan composite film for cholesterol biosensor. *Analytica Chimica Acta*, 616, (2008): 207-213.

[35] Kaushik, A., et al. Iron oxide nanoparticles-chitosan composite based glucose biosensor. *Biosensors and Bioelectronics*, 24, (2008): 676-683.

[36] Gao, F., et al. Amperometric third-generation hydrogen peroxide biosensor based on immobilization of Hb on gold nanoparticles/cysteine/poly(p-aminobenzene sulfonic acid)-modified platinum disk electrode. *Colloids and Surfaces A: Physicochemical and Engineering Aspects*, 295, (2007): 223-227.

[37] Andreescu, S., and Luck, L.A. Studies of the binding and signaling of surface-immobilized periplasmic glucose receptors on gold nanoparticles: A glucose biosensor application. *Analytical Biochemistry*, 375, (2008): 282-290.

[38] Aravamudhan, S., et al. Sensitive estimation of total cholesterol in blood using Au nanowires based micro-fluidic platform. *Biosensors and Bioelectronics*, 22, (2007): 2289-2294.

[39] Oliveira B., A.M.C.F., Gil, M.H., and Piedade, A.P. An electrochemical bienzyme membrane sensor for free cholesterol. *Bioelectrochemistry and Bioenergetics*, 28, (1992): 105-115.

[40] Shih, W.-C., Yang, M.-C. and Lin, M.S. Development of disposable lipid biosensor for the determination of total cholesterol. *Biosensors and Bioelectronics*, 24, (2009): 1679-1684.

[41] Basu, A.K., et al. Development of cholesterol biosensor based on immobilized cholesterol esterase and cholesterol oxidase on oxygen electrode for the determination of total cholesterol in food samples. *Bioelectrochemistry*, 70, (2007): 375-379.

[42] Srisawasdi, P., et al. Application of Streptomyces and Brevibacterium cholesterol oxidase for total serum cholesterol assay by the enzymatic kinetic method. *Clinica Chimica Acta*, 372, (2006): 103-111.

[43] Strike, D.J., de Rooij, N.F., and Koudelka-Hep, M. Electrochemical techniques for the modification of microelectrodes. *Biosensors and Bioelectronics*, 10, (1995): 61-66.

[44] Alvin Koh, W.C., et al. A cytochrome c modified-conducting polymer microelectrode for monitoring in vivo changes in nitric oxide. *Biosensors and Bioelectronics*, 23, (2008): 1374-1381.

[45] Wang, J., et al. Quantum-dot-based electrochemical immunoassay for high-throughput screening of the prostate-specific antigen. *Small*, 4, (2008): 82-86.

[46] Wu, H., et al. Quantum-dots based electrochemical immunoassay of interleukin-1α. *Electrochemistry Communications*, 9, (2007): 1573-1577.

[47] D'Ambrosio, C., et al. Analytical methodologies for the detection and structural characterization of phosphorylated proteins. *Journal of Chromatography B*, 849, (2007): 163-180.

[48] Mann, M., et al. Analysis of protein phosphorylation using mass spectrometry: deciphering the phosphoproteome. *Trends in Biotechnology*, 20, (2002): 261-268.

[49] McLachlin, D.T., and Chait, B.T. Analysis of phosphorylated proteins and peptides by mass spectrometry. *Current Opinion in Chemical Biology*, 5, (2001): 591-602.

[50] Paradela, A., and Albar, J.P. Advances in the Analysis of Protein Phosphorylation. *Journal of Proteome Research,* 7, (2008): 1809-1818.

[51] Yan, J.X., et al., Protein phosphorylation: technologies for the identification of phosphoamino acids. *Journal of Chromatography A*, 808, (1998): 23-41.

[52] Liu, G., and Lin, Y. Nanomaterial labels in electrochemical immunosensors and immunoassays. *Talanta*, 74, (2007): 308-317.

[53] Song, H., Kerman, K., and Kraatz, H.-B. Electrochemical detection of kinase-catalyzed phosphorylation using ferrocene-conjugated ATP. *Chemical Communications*, 4, (2008): 502-504.

[54] Yang, H., et al. An aptamer-based biosensor for sensitive thrombin detection. *Electrochemistry Communications*, 11, (2009): 38-40.

[55] Farré, M., and Barceló, D. Sensor, biosensors and MIP based sensors, *Food Toxicants Analysis*, Elsevier: Amsterdam, 2007.

[56] Kandimalla, V.B., Tripathi, V.S., and Ju, H. Biosensors based on immobilization of biomolecules in sol-gel matrices, *Electrochemical Sensors, Biosensors and their Biomedical Applications*, Academic Press: San Diego, 2008.

[57] Ju, H. and V.B. Kandimalla, Biosensors for pesticides, *Electrochemical Sensors, Biosensors and their Biomedical Applications*., Academic Press: San Diego, 2008.

[58] Andreescu, S., Njagi, J., and Ispas, C. Nanostructured materials for enzyme immobilization and biosensors, *The New Frontiers of Organic and Composite Nanotechnology*, Elsevier: Amsterdam, 2008.

[59] Fang, Y., Ferrie, A.M. and Li, G. Cellular functions of cholesterol probed with optical biosensors. *Biochimica et Biophysica Acta (BBA) - Molecular Cell Research*, 1763, (2006): 254-261.

[60] Salazar, P., et al. Amperometric glucose microbiosensor based on a Prussian Blue modified carbon fiber electrode for physiological applications. *Sensors and Actuators B: Chemical*, 152, (2011): 137-143.

[61] Shumyantseva, V., et al. Cholesterol amperometric biosensor based on cytochrome P450*scc. Biosensors and Bioelectronics,* 19, (2004): 971-976.

[62] Ghindilis, A.L., et al. Immunosensors: electrochemical sensing and other engineering approaches. *Biosensors and Bioelectronics*, 13, (1998): 113-131.

[63] Parra, A., et al. Cholesterol oxidase modified gold electrodes as bioanalytical devices. *Sensors and Actuators B: Chemical*, 124, (2007): 30-37.

[64] Martin, S.P., et al. Enzyme-based determination of cholesterol using the quartz crystal acoustic wave sensor. *Analytica Chimica Acta*, 487, (2003): 91-100.

[65] Thévenot, D.R., et al. Electrochemical biosensors: recommended definitions and classification. *Biosensors and Bioelectronics,* 16, (2001): 121-131.

[66] Peteu, S.F., Emerson, D. and Mark Worden, R. A Clark-type oxidase enzyme-based amperometric microbiosensor for sensing glucose, galactose, or choline. *Biosensors and Bioelectronics*, 11, (1996): 1059-1071.

[67] Scheller, F.W., et al. Research and development in biosensors. *Current Opinion in Biotechnology*, 12, (2001): 35-40.

[68] Andreescu, S., Njagi, J., and Ispas, C. Nanostructured materials for enzyme immobilization and biosensors, *The New Frontiers of Organic and Composite Nanotechnology*, Elsevier: Amsterdam, 2008.

[69] Fowler, J.M., et al. Recent developments in electrochemical immunoassays and immunosensors, *Electrochemical Sensors, Biosensors and their Biomedical Applications*, Academic Press: San Diego, 2008.

[70] Ballou, B. Quantum Dot Surfaces for Use In Vivo and In Vitro, *Current Topics in Developmental Biology*, Academic Press, 2005.

[71] Shin, S.K., et al. Nanoscale controlled self-assembled monolayers and quantum dots. *Current Opinion in Chemical Biology*, 10, (2006): 423-429.

[72] Tothill, I.E. Biosensors for cancer markers diagnosis. *Seminars in Cell & Developmental Biology*, 20, (2009): 55-62.

[73] Wang, J. *Analytical Electrochemiatry*. 1st ed. United States of America: Wiley-VCH, 1994.

[74] Douglas, S. A., James, H. F., and Nieman, T. A. *Principles of Instrumental Analysis.* 5th ed. United States of America: Saunders Collage, 1998.

[75] Wang, J. *Stripping Analysis*. United States of America: VCH, 1948.

[76] Devadoss, A., et al. Enzyme Modification of Platinum Microelectrodes for Detection of Cholesterol in Vesicle Lipid Bilayer Membranes. *Analytical Chemistry*, 77, (2005): 7393-7398.

[77] Usman Ali, S.M., et al. A fast and sensitive potentiometric glucose microsensor based on glucose oxidase coated ZnO nanowires grown on a thin silver wire. *Sensors and Actuators B: Chemical*, 145, (2010): 869-874.

[78] Luo, Y., et al. A new strategy for electrochemical immunoassay based on enzymatic silver deposition on agarose beads. *Talanta*, 74, (2008): 1642-1648.

VITA

Name   :   Miss Kulwadee Pinwattana

Date of Birth :   October 11, 1978

Place of Birth :   Nakhonsawan, Thailand

Education   :

Period	College/University	Qualification
Jun 1997 – Apr 2000	Naresuan University, Phitsanulok	Bachelor of Science
Jun 2000 – Apr 2004	Naresuan University, Phitsanulok	Master Degree of Science (Chemistry)
Jun 2006 – Apr 2011	Chulalongkorn University, Bangkok	Doctoral of Philosophy (Analytical Chemistry)

Research Grants: The Higher Education Commission, Thailand

Home Address :   615/40 Moo 9 Tambol Nakhonsawan Tok, Amphur Muang, Nakhonsawan 60000, Thailand

Publications   :

Pinwattana, K.; Wang, J.; Lin, CT.; Wu, H.; Du, D.; Lin, Y.; and Chailapakul, O. CdSe/ZnS quantum dots based electrochemical immunoassay for the detection of phosphorylated bovine serum albumin. *Biosensor and Bioelectronics*. 26 (2010): 1109-1113.